QUANTITATIVE ANALYSIS OF NEW KEY FACTORS OF IMMUNE CELLS IN AUTOIMMUNE DISEASES

By

Demarcus Bunn

A DISSERTATION

Submitted to
Michigan State University
in partial fulfillment of requirements
for the degree of

Comparative Medicine and Integrative Biology – Doctor of Philosophy

2022

ABSTRACT

QUANTITATIVE ANALYSIS OF NEW KEY FACTORS OF IMMUNE CELLS IN AUTOIMMUNE DISEASES

By

Demarcus Bunn

The work presented in this dissertation demonstrates an emerging role of immune cells in type one diabetes (T1D) and multiple sclerosis (MS). The immune cells that will be presented are neutrophils and T-cells. Presented work shows an altered cell metabolism in both disease states that leads to further secondary complications. An overview of the immunology, as well as each autoimmune disease, will be presented. Experimental efforts to increase or decrease cell metabolism in order to alleviate secondary complications will be shown. Furthermore, the use of 3D printed devices for in vitro models mimicking these disease states properties will be presented.

Individuals T1D have a history of being more susceptible to infection. This section of the dissertation will demonstrate how a once forgotten pancreatic peptide, C-peptide, has a positive effect on raising immunity through improving immune cell energetics. Previous studies in the Spence lab have shown that C-peptide only binds to red blood cells (RBC) in the presence of albumin, but for the biological changes, Zn^{2+} is needed. Spence lab research has shown that the combination of C-peptide/Zn^{2+}/albumin increases the metabolism of RBCs. This work shows novel data showing that C-peptide binds specifically to other cell types. Additionally, changes in cell metabolism will be investigated. This portion of the dissertation is important for alleviating reoccurring and persistent infections.

MS is characterized by the destruction of the myelin sheath around the nerves. The cell type that does the damage is T lymphocytes. However, little research has been done investigating what makes the permeability of the blood-brain barrier increase. Here, we will introduce the potential role of NETosis, a form of programmed cell death, has on blood brain barrier permeability. There have been recent reports that exogenous adenosine triphosphate (ATP) increases the rate of NETosis production in vitro. Previous work in the Spence lab has shown that RBCs from individuals with MS secrete significantly more ATP than control red blood cells. Presented work will show that ATP derived directly from RBCs causes dysregulation of NETosis.

The concluding section of the dissertation will be dedicated to 3D printing. An overview of the current state and future advancements of 3D printing will be presented. Presented work will show the use of 3D printing to provide more relevant conditions for in vitro experiments. Here, 3D printed models were used to investigate immune cell behaviors and changes in cell bioenergetics.

ACKNOWLEDGMENTS

I would like to first thank Michigan State University for blessing me with this opportunity to further my education. Additionally, the National Institute of Health for providing financial assistance to make this research possible. I would like to thank Memorial hospital for providing MS blood samples essential for my research.

With that being said, I would like to thank the department of Veterinary Medicine, specifically the Comparative Medicine and Integrative Biology program for being a supporting program professionally and personally. This program fosters growth, collaboration, individuality, and offered space to decompress during the rigors of graduate school. I am grateful for MSUs graduate school, specifically Steven Thomas, who has helped untap my potential as a summer intern at MSU in 2016, and allowing me to give back as an MSU summer research opportunities program mentor for graduate school pursuing minority undergraduates. Further, I would like to thank the Alliance for Graduate School and the Professoriate (AGEP), for providing a space for underrepresented graduate students to conglomerate, network, and share research in a great environment.

I would like to acknowledge my PI Dr. Dana Spence as he has been a critical part in my professional development since I was a summer intern in his lab in 2016. He has provided strong guidance while also giving me leeway to make and learn from my own mistakes. I would like to thank the members of the Spence Lab during my tenure for being so helpful and supportive in and out of the lab.

I want to thank my teachers from earlier in my education through my professors in graduate school. Teaching is a selfless job, and I am appreciative for the time spent and

knowledge gained. I would like to thank my undergraduate academic advisor Dr. Anderson, for guiding me on finding my passion and helping me achieve opportunities that I thought were out of reach for me.

Conquering milestones is something that everyone lives for. Completion of a doctoral degree is something that I never saw in my future as a child. Growing up, I was blessed to have such a dedicated support system that helped me tap into my potential. I want to thank my parents for instilling in me that anything is possible with hard work and dedication. Without their guidance, I do not know where I would have landed in life, and I am forever grateful for them. My family is small, but the love we have for each other is unlike any other, and I am thankful to be surrounded by such a beautiful family inside and out. Thank you for collectively allowing me to grow as a faith filled, and humbled individual.

Lastly, I would like to thank all the current and post members of the Spence lab who have not only been essential in research, but also a friendly group of people who made the graduate school experience more enjoyable. I would specifically like to thank Cody Pinger and Andre Castiaux for their help producing 3D printing data, and Monica Jacobs for her help with ATP secretions. To the current Spence lab members: Suzanne Summers, Lauren Skrajewski, Logan Soule, Morgan Geiger, Nathan Redman, Monica Jacobs, Amalie Moyna Lobel, Stephen Branch, I would like to thank you as the connections gained are both professional and friendly, bringing me peace in times of uncertainty.

TABLE OF CONTENTS

LIST OF TABLES

LIST OF FIGURES

Chapter 1 - Introduction into Immunology and Autoimmunity

1.1 Introduction into Immunology

Immunology is the study of the body's defense against foreign antigens such as viruses, microbes, and toxins.[1] The immune system is composed of effector cells, functions and molecules that aim to protect the body from pathogens and microbes.[2] As shown in table 1.1, there are two main proponents of immunity, namely adaptive and innate. While both systems aim to provide protection in vivo, the mechanisms by which protection is elicited varies. For example, adaptive immunity is an immune response that is acquired over a lifetime and is specific due to the production of antibodies for a specific foreign antigen. Differing from adaptive immunity, innate immunity is a nonspecific response to pathogens, and the protective mechanisms encompasses humans at birth. Due to the differences in specificity associated with adaptive and innate immunity, each response has different response times, innate being much faster than adaptive.[3, 4] Although the roles of the two immunities are functionally different, many functions are dependent on each other in an act known as "cross-talk" between the two branches.[2] in the next few sections, details associated with immunity are discussed, beginning with innate immunity.

Table 1.1: Characteristics of the two branches of the immune system.

	Innate Immunity	**Adaptive Immunity**
Response time	Minutes to hours	Several days
Key components	Antimicrobial peptides, and phagocytosis, complement	Antibody production, cell mediated immunity
Specificity	Nonspecific	Highly specific
Cell type	Neutrophil, macrophage, basophil, eosinophil, NK cell	T cell, B cell
Immunological memory	None	Yes, heightened memory leads to faster clearance
Self-identification	Strong self-identification components	Normal self-identification, miscommunication leads to autoimmune diseases

1.1.1 Innate Immunity

Innate immunity is the first line of cellular defense against pathogens. Being the first to recognize pathogens, cells of innate immunity have a nonspecific response allowing rapid recognition of antigens.[5] Some cell types of this branch includes phagocytes, leukocytes, and dendritic cells. Their main functions are to eradicate pathogens, specifically bacteria, by the recognition of pathogen-associated molecular proteins (PAMPS) through pattern-recognition receptors (PRRs).[6] This receptor ligand interaction allows for phagocytic cells of innate immunity to engulf microbes, digest and secrete bacterial lysates, and ultimately recruit adaptive immunity.[2]

Innate response can be segmented into four parts including anatomical barriers, physiological, cell mediated, and inflammation (see Table 1.2.).[3, 7] Anatomical is the first line of defense against pathogens and includes such barriers as skin and the mucosal

membranes. Skin provides a physical barrier as well as a high acidic surface to deter microbial growth. The mucosal membranes have several mechanisms to reflect microbes. Normal flora, or human microbiome, competes with microbes for binding sites, simultaneously while mucous traps microbes and cilia ejects the microbes. Examples of physiological defense includes simple yet effective clearance tactics to interrupt pathogens growth environment. Alternating body temperature, stomach pH, and chemical mediators (lysozymes, interferons, complement proteins), all create undesirable environments reducing bacterial growth and are excellent examples of physiological defense. Cell mediated forms of innate immunity include the introduction of phagocytic cells, or cells that engulf bacteria. Neutrophils, macrophages, and monocytes will internalize bacteria and kill them. Phagocytosis and the cells that perform this process will be discussed more further below beginning in section 1.1.3. Lastly, inflammation is a process that follows tissue damage. Vascular fluid leaks to the sight of damage or infection, bringing serum antimicrobial factors leading to rapid influx of phagocytic cells to the site.[2, 3, 5]

Table 1.2: Overview of the mechanisms involved in the innate immune response.

Anatomical barriers	
Skin	– Physical barrier – Surface is pH 3-4 for microbe deterrent
Mucus	– Mucosal membranes traps microbes – Normal flora can compete for binding sites – Cilia can eject microbes out of the body
Physiological barriers	
pH	– Ingested microbes can be destroyed by lowering the pH in the stomach
Temperature	– Increasing body temperature causes fever like conditions halting microbe proliferation
Chemical mediators	– Pattern recognizing receptors react to microbes eliciting proinflammatory cytokine production – Compliment system opsonizes microbes to induce phagocytic activity – Lysozymes degrade microbe cell wall
Cell mediated	– Specific immune cells are capable of Phagocytosis (Endocytosis), the ingestion and digestion of microbes
Inflammation	– Circulatory serum protein from vasculature fluid leakage recruit phagocytic cells to the site of tissue damage

1.1.2 Innate Cell Types

Cells that are categorized under innate immunity are derived from common myeloid progenitor cells. As mentioned earlier, innate immune cells operate in a somewhat non-specific manner, having little to no immunological memory, no recombinant antigen receptors, and typically combat microbial infections leaving viral infections for the adaptive immune system. The cells identified are growing as new cell types and derivatives are discovered frequently. Examples of innate immune cells include macrophages, natural killer cells, monocytes, dendritic cells, and granulocytes.

Granulocytes are a family of granulocyte containing immune cells that consist of basophils, eosinophils, and neutrophils. A large portion of the cell-based research discussed in this dissertation was conducted utilizing neutrophils, therefore, the proceeding section will be dedicated to neutrophil biology.

1.1.3 Neutrophil Introduction

Peripheral neutrophils, the most abundant member of the granulocyte family of cells (and the most abundant immune cell overall), are an innate immune cell typically regarded as the first to respond to foreign antigens. Neutrophils have a have a diameter of 8-12 μm,[8] while differentiation and maturation process for a neutrophil spans up to 14 days. However, once the neutrophil is matured and leaves the bone marrow to the bloodstream it survives only 6-8 hours before entering the tissues to die.[9] A healthy human has between 2 and 7 million neutrophils per milliliter of whole blood.[10] There are many mechanisms by which neutrophils migrate to sites of infection or foreign pathogen in vivo. This migration is mostly driven by a process known as chemotaxis, which is largely a movement of the neutrophil towards a concentration gradient of molecules. Key components of the chemotaxis and defense mechanisms include reactive oxygen species (ROS) generation, antigen presentation, secretion of chemokines/cytokines, degranulation, and formation of neutrophil extracellular traps are all functions that are necessary for migration to, and destruction of, the site of an infection or foreign pathogen.[11-13]

Since neutrophils are typically the first to respond to infection, they have several mechanisms to not only clear infection, but also to recruit other immune cells. In the blood vessel, neutrophils respond to chemokines, complement proteins, and other chemoattractants (seen in figure 1.1).(*14*) Neutrophils eradicate pathogens, specifically bacteria, by the recognition of pathogen-associated molecular proteins (PAMPS) through pattern-recognition receptors (PRRs).(*5, 15*) This receptor ligand interaction allows for phagocytic cells of innate immunity to engulf microbes, digest and secrete bacterial lysates, and ultimately recruit adaptive immunity.(*6*)

Neutrophils will move across these chemotactic gradients to reach the site of infection. To leave the blood vessel, neutrophils will attach to endothelial cells through actin/selectin interactions depicted in figure 1.1. Vascular endothelium will dilate, slowing blood flow while simultaneously increasing the surface expression of adhesion molecules. Rolling along the endothelium is mediated by the weak binding affinity of P and E Selectins on the endothelium surface and P-selectin glycoprotein ligand-1 (PSGL-1) on activated neutrophils. As the neutrophil closes in on the site of infection, stronger binding affinity of ICAM-1 on endothelium surface and LFA-1 causes complete adhesion between the two cells.(*16, 17*)

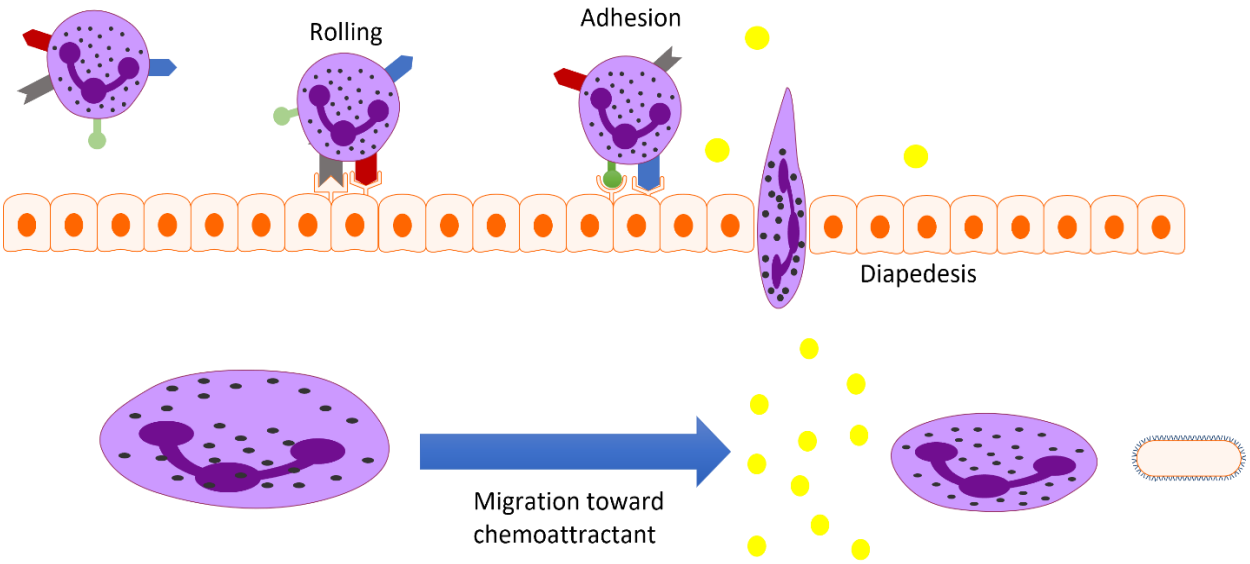

Figure 1.1: Schematic of neutrophil migration to a sight of infection. Upon stimulation a series of cell-to-cell interactions recruit neutrophils out of circulation and into the tissues. Once in the tissues, neutrophils then aid in the eradication of the infection using phagocytosis and cytokine release for recruitment of other immune cell types

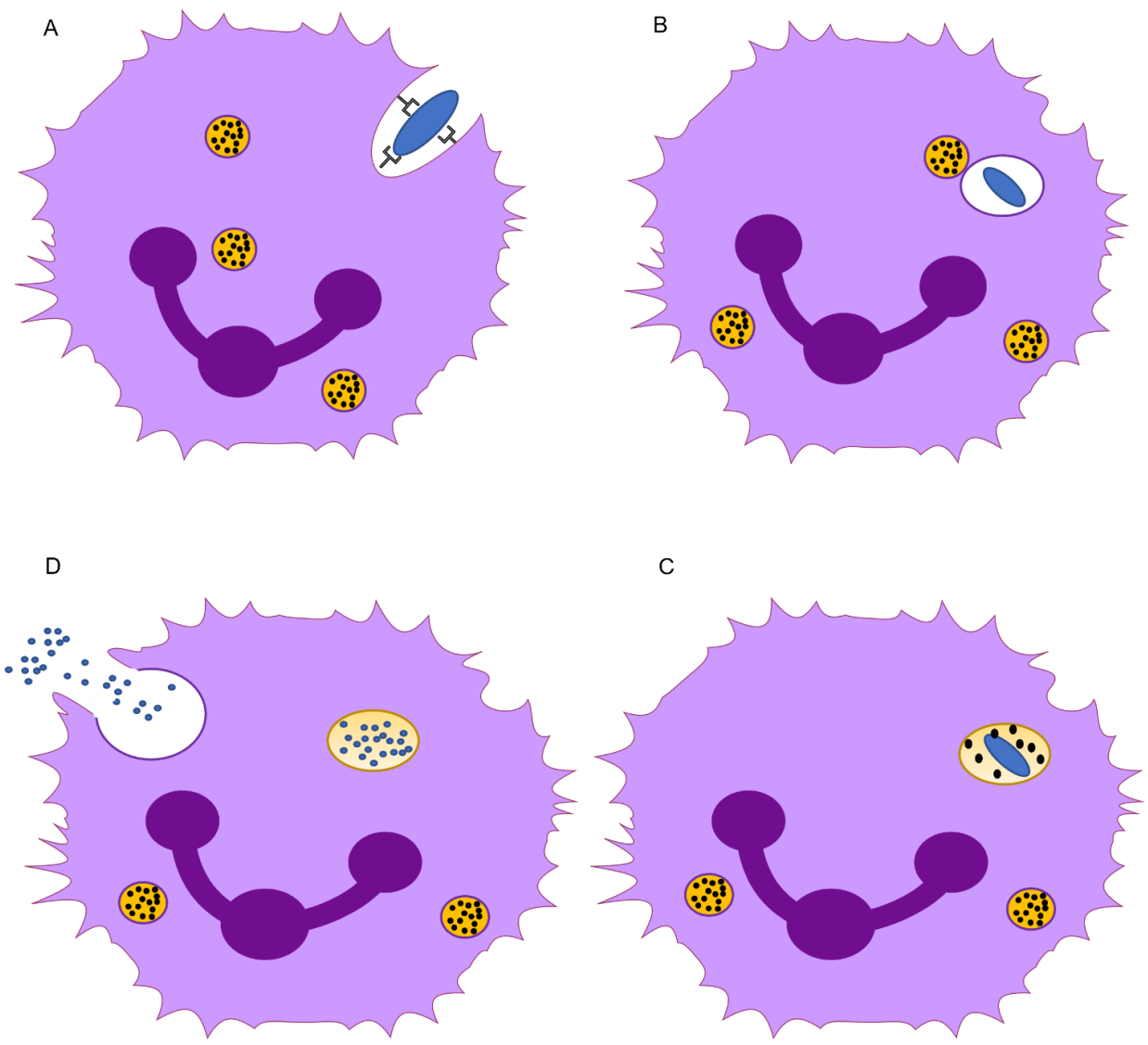

Figure 1.2: Phagocytosis in neutrophils. A. Phagocytosis is initiated by the recognition of an opsonized or antibody covered foreign antigen by phagocytic receptors. **B.** Internalization of an antigen into a phagosome. **C.** Phagosome fuses with a lysosome creating a phagolysosome. **D.** The degradation of the antigen through pH modifications and degradative enzyme activity.

Once the neutrophil arrives to the site of infection phagocytosis occurs. Phagocytosis is the process of engulfing a bacterium and destroying them inside intracellular vesicles.(*18, 19*) Once the antigen is recognized by phagocytic receptors, the antigen is ingested into a phagosome. A lysosome or intracellular vesicles contain degradative enzymes and other antimicrobial substances will fuse with the phagosome creating a phagolysosome.(*2*) The phagolysosome will digest the antigen using a series of mechanism that raise pH through phagolysosome membrane bound proton-pumping V-ATPases.(*20*) Also present on the phagolysosome is the NADPH complex which controls the production of such reactive oxygen species (ROS) such as super oxide.(*21*) Finally, through the combative effort of hypochlorous acid and hydrolytic enzymes, the antigen is degraded and expelled into the extracellular space.(*22, 23*) Figure 1.2 outlines the process of phagocytosis.

1.1.4 Adaptive Immunity

Acquired immunity is a specific response to an antigen, much stronger and effective than innate immunity. However, it takes time for adaptive immunity to generate immunological memory and develop specificity through clonal selection of lymphocyte antigen specific receptors. Cell types of this branch include numerous subsets of T and B lymphocytes which are critical in viral defense and antibody production.(*3, 24*)

Although the innate response is effective, the specific nature of adaptive immunity provides a more powerful response. The adaptive immune response occurs between 12

and 24 hours post infection. This response relies on two cell types to develop specific antigens and immunological memory to clear infection.(*25*) T and B cells are immune cells derived from multipotent hematopoietic stem cells in the bone marrow. These naïve cells contain several membrane bound antibodies that will recognize specific antigens that cause activation. Once activated, immunological memory is formed, meaning a second encounter of the same foreign antigen elicits a rapid immune response.

1.1.5 Adaptive Cell Types

Similar to the innate response, the adaptive response has multiple cell types to achieve eradication of an infection. Cell types of this branch include numerous subsets of T and B cells that are critical in viral defense and antibody production. Both T and B cells have a variety of subsets that include memory, regulatory and cytotoxic. The main role of T-cells is to kill infected host cells through apoptosis.(*26*) The role of the B-cells is antibody production.(*27*) Since cells of the adaptive immune system have a specific response to an antigen, it takes time to develop specificity through clonal selection of lymphocyte antigen specific receptors.(*27, 28*) Once a strong antigen response is achieved, clones are produced. The specific phenotype will be regular expressed allowing for rapid clearance of an antigen if encountered again, this describes immunological memory.(*29, 30*) Immunological memory is the basis of vaccination.(*31*) Out of the two adaptive immune cell types, this dissertation contains studies involving T-cells and therefore this cell type is discussed in more detail in the following section.

1.1.6 T-cell Introduction

T-cells are derived from stem cells in the bone marrow and mature until they become thymocytes. The thymocytes will then migrate to the thymus and lymph nodes where they further mature and go through a process called clonal selection. Clonal selection is a process where the T-cell develops their T-cell receptors. They will be presented to self-antigens, causing an outcome of positive or negative selection. During this process a pool of pre-existing antigens, including self-antigens, are presented to T-cells expressing unique antigen receptors. The T-cells that prove strong binding affinity to non-self-antigens are selected and cloned creating mature naïve T-cells.(*2, 26*) The selection process is illustrated in figure 1.3.

There are several subsets of T-cells in the body. Here, we will only discuss subsets CD4 and CD8 T-cells. CD, or cluster of differentiation, is a way to recognize and categorize surface antigen receptors on lymphocytes.(*32*) In terms of T-cells there are cytotoxic T-cells (CD8) and helper T-cells (CD4).(*33*) CD8 T-cells have the ability to kill infected cells by co-stimulation of peptide-MHC class 1 receptors. Cytotoxic T-cells kill infected cells using two different mechanisms. This mechanism can be direct or indirect. Inside the cytotoxic T-cells cytosol are un-synthesized forms of granzyme B and perforin.(*34*) Binding of the T-cell receptor to MHC class 1 initiates the synthesis and release of the two granules to the infected cell. Perforin will bind to the membrane of the target cell allowing the granzymes to enter. Granzymes are a series of serine proteases that induce caspase activity, leading to apoptosis.(*35*) Cytotoxic T-cells can also induce

apoptosis through a more cell-cell binding pathway. This pathway is facilitated through Fas-FasL binding between the cytotoxic T-cell and infected cell.(*36*) Lastly, the cytotoxic T-cell can kill infected cells indirectly. When activated though litigation of T-cell receptor MHC class 1 complex, a cytotoxic T-cell will release of pro-inflammatory cytokines effecting nearby infected cells.(*37*) Cytokines such as TNFα, INFγ, and lymphotoxin-α are released which work together to increase MHC class 1 expression and inhibit viral replication on nearby infected cells. These cytokines also work to recruit both innate and adaptive immune cells to the site.(*2, 38*)

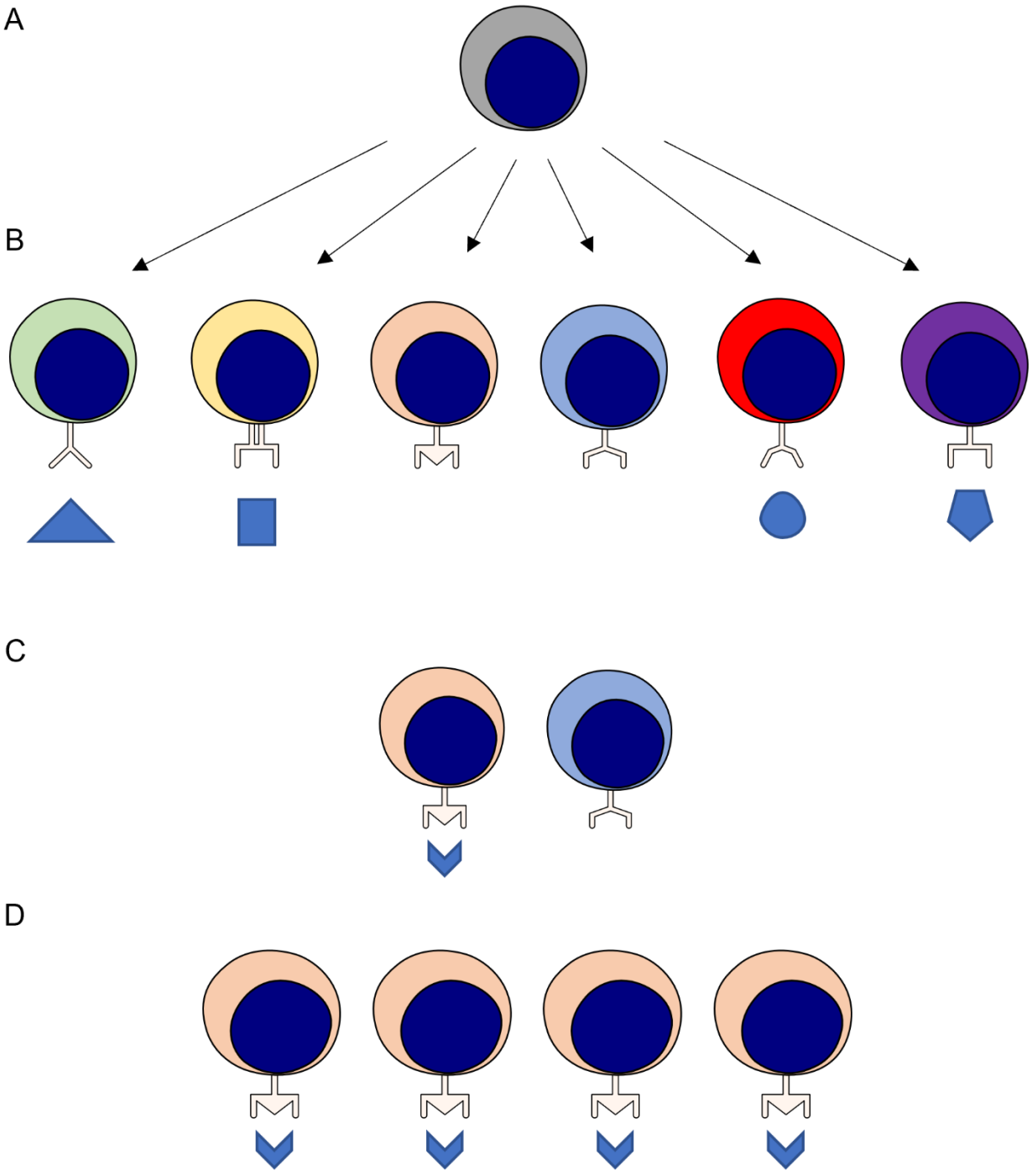

Figure 1.3: Clonal selection of T-cells. A. Hematopoietic cell goes through TCR differentiation. **B.** A pool of T-cells exposed to self-antigens. Subsets that do not interact with self-antigens are selected to move on to the next phase. **C.** A pool of non-self-reacting T-cells are exposed to foreign antigens. The subset that shows strong affinity will move on to the next phase. **D.** The subset that has a strong reaction to a foreign antigen are cloned and sent into the circulation.

CD4 T-cells or helper T-cells have a more indirect cytotoxic effect compared to their cytotoxic counterparts. Helper T-cells recognize peptides presented through MHC class II molecules from antigen presenting cells (APC). Like cytotoxic T-cells, this presentation causes activation and differentiation into different subsets of helper T-cells. The cytokines secreted from the APC during this exchange influences the subset of helper T-cell that is produced. Briefly, an introduction to these subsets follows.

A naïve CD4 T-cell is differentiated into a T helper 1 (Th1) subset by downstream signaling due to cytokines interleukin 12 (IL12) and INFγ. The role of Th1 is aiding in the elimination of intracellular pathogens and mediating organ specific autoimmunity.(*39*) Since CD4 T-cells do not kill directly, their mode of action involves secretion of cytokines for recruitment of other immune cells. In the case of the Th1, this subset recruits phagocytic cells through the secretion of cytokines such as INFγ, IL2, and lymphotoxin α. T helper 2 (Th2) aid in the elimination of extracellular parasites. Th2 cells are differentiated through APCs release of cytokines IL2 and IL4. Dysfunction of Th2 have been linked to the pathology and persistence of allergy related conditions.

T helper 9 (Th9) have been categorized as a derivative of the Th2. TGF-β and IL4 has been shown to further push the Th2 into a special phenotype of a IL9 secreting cell.(*40*) TH9 has been linked to the pathogenesis of asthma.(*41*) T helper 17 (Th17) are responsible for eradicating extracellular bacteria and fungi. Th17 are differentiated though IL6, IL21, IL23, and TGF-β cytokine signaling.(*42*) The master regulator is retinoic acid receptor-related orphan receptor gamma-T (RORγt).(*43*) T regulatory cells are formed in

the thymus and have high expression of forkhead transcription factor FOXP3. This gene is key in the regulation of the immune system.(*44*) After clearance of infection, Tregs act to decrease the activity of activated immune cells to decrease the chances of an autoimmune reaction.(*45, 46*) Lastly, T follicular helper (Tfh) cells are key in the regulation of humoral immunity. Thf cells interact directly with B-cells in the pregerminal and germinal center. In the pregerminal center Thf will induce antigen primed B-cells differentiation into Ig producing plasma cells. In the germinal center, Thf cells aid in the development of memory B-cells. Tfh use cytokines IL10, TGF-β, and INFγ to alter B-cell phenotype.(*2, 47, 48*)

1.2 Introduction into Autoimmunity

Autoimmune disease is broadly defined as dysregulated damage to self-tissues which lead to various chronic syndromes.(*2, 49*) These diverse diseases affects nearly 3-5% of the world's population and continues to grow.(*50*) In 2001, Dr. Anthony Fauci estimated that the estimated annual total cost of autoimmune disease treatment reaches $100 billion, which some argue is underestimated. However, in 2009 the allotted budget for research funding provided by the National institute of Health amounts to $898 million.(*51*) Figure 1.4 shows a map of world prevalence of the most common autoimmune diseases.(*55*)

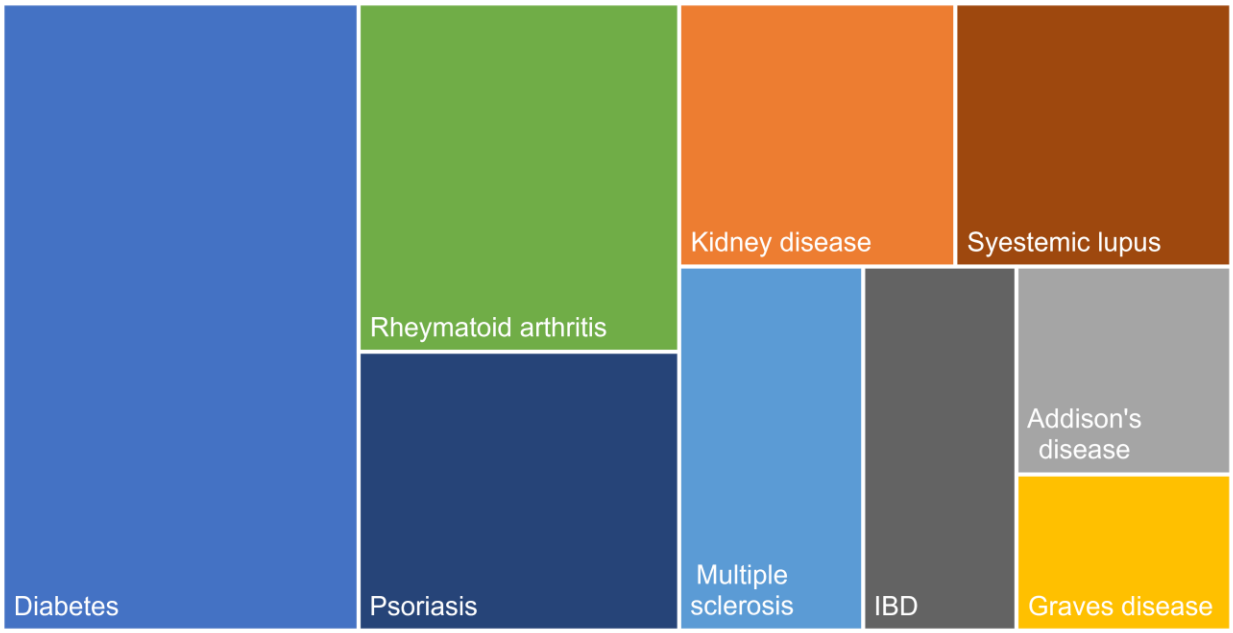

Figure 1.4: Tree map showing the prevalence of the most common autoimmune disease.

This umbrella of a term can be further defined in two ways, immune deficiency syndromes(primary) and secondary immune disease. Immune deficiency syndrome is the inability of the immune system to react efficiently to a pathogen, which can be either genetic or acquired. Secondary immune disease can be a result of factors such as an environmental or disease, such as medical treatment or malnutrition.(*49, 52*)

1.3 Immunodeficiency

Immunodeficiency is defined as a state in which an individual's immune system has a decreased ability or are entirely absent in fighting infections. There are two forms of

immunodeficiency, primary and secondary. Primary is categorized by a single gene mutation causing a defect in immunity. Primary immunodeficiency is typically diagnosed in infants and late adulthood. Secondary is categorized by genetic defects in immune cells typically caused by extrinsic factors (disease, drug, infectious agents, environmental factors).(*49, 53*) In most cases, immunodeficiency is acquired due to extrinsic factors that disrupt he efficiency of the immune system.(*49, 54*) Here, this dissertation will further look to identify diabetes as a secondary cause of immunodeficiency, while investigating a potential therapeutic mediator.

REFERENCES

REFERENCES

1. A. C. Villani, S. Sarkizova, N. Hacohen, Systems Immunology: Learning the Rules of the Immune System. *Annu Rev Immunol* **36**, 813-842 (2018).
2. K. Murphy *et al.*, *Janeway's immunobiology*. (Garland Science, New York, ed. Eighth edition., 2012), pp. xix, 868 pages.
3. J. S. Marshall, R. Warrington, W. Watson, H. L. Kim, An introduction to immunology and immunopathology. *Allergy Asthma Clin Immunol* **14**, 49 (2018).
4. R. R. Rich, D. D. Chaplin, *Clinical Immunology*. (ed. Fifth Edition, 2019).
5. S. Akira, S. Uematsu, O. Takeuchi, Pathogen recognition and innate immunity. *Cell* **124**, 783-801 (2006).
6. A. Iwasaki, R. Medzhitov, Control of adaptive immunity by the innate immune system. *Nat Immunol* **16**, 343-353 (2015).
7. S. E. Turvey, D. H. Broide, Innate immunity. *J Allergy Clin Immunol* **125**, S24-32 (2010).
8. G. P. Downey *et al.*, Retention of leukocytes in capillaries: role of cell size and deformability. *J Appl Physiol (1985)* **69**, 1767-1778 (1990).
9. R. Omman, A. Kini, *Rodak's Hematology*. (Elsevier, ed. 6, 2020).
10. J. Scher, S. Abramson, M. Pillinger, *Kelly's Textbook of Rheumatology*. (Elsevier, 2013), vol. 1.
11. P. Kubes, The enigmatic neutrophil: what we do not know. *Cell Tissue Res* **371**, 399-406 (2018).
12. B. Petri, M. J. Sanz, Neutrophil chemotaxis. *Cell Tissue Res*, (2018).
13. V. Kumar, A. Sharma, Neutrophils: Cinderella of innate immune system. *Int Immunopharmacol* **10**, 1325-1334 (2010).
14. J. Gane, R. Stockley, Mechanisms of neutrophil transmigration across the vascular endothelium in COPD. *Thorax* **67**, 553-561 (2012).
15. K. Newton, V. M. Dixit, Signaling in innate immunity and inflammation. *Cold Spring Harb Perspect Biol* **4**, (2012).
16. K. Futosi, S. Fodor, A. Mócsai, Neutrophil cell surface receptors and their intracellular signal transduction pathways. *Int Immunopharmacol* **17**, 638-650 (2013).

17. R. Sumagin, H. Prizant, E. Lomakina, R. E. Waugh, I. H. Sarelius, LFA-1 and Mac-1 define characteristically different intralumenal crawling and emigration patterns for monocytes and neutrophils in situ. *J Immunol* **185**, 7057-7066 (2010).

18. C. C. Daniels *et al.*, Modified opsonization, phagocytosis, and killing assays to measure potentially protective antibodies against pneumococcal surface protein A. *Clin Vaccine Immunol* **20**, 1549-1558 (2013).

19. J. A. Smith, Neutrophils, host defense, and inflammation: a double-edged sword. *J Leukoc Biol* **56**, 672-686 (1994).

20. V. Marshansky, M. Futai, The V-type H+-ATPase in vesicular trafficking: targeting, regulation and function. *Curr Opin Cell Biol* **20**, 415-426 (2008).

21. R. Minakami, H. Sumimotoa, Phagocytosis-coupled activation of the superoxide-producing phagocyte oxidase, a member of the NADPH oxidase (nox) family. *Int J Hematol* **84**, 193-198 (2006).

22. E. Uribe-Querol, C. Rosales, Phagocytosis: Our Current Understanding of a Universal Biological Process. *Front Immunol* **11**, 1066 (2020).

23. J. M. Kinchen, K. S. Ravichandran, Phagosome maturation: going through the acid test. *Nat Rev Mol Cell Biol* **9**, 781-795 (2008).

24. F. A. Bonilla, H. C. Oettgen, Adaptive immunity. *J Allergy Clin Immunol* **125**, S33-40 (2010).

25. Adaptive Immunity in *Immune Response*. Khan Academy.

26. N. Zhang, M. J. Bevan, CD8(+) T cells: foot soldiers of the immune system. *Immunity* **35**, 161-168 (2011).

27. B. Alberts, A. Johnson, J. Lewis, *Molecular Biology of the Cell*. (Garland Science, New York, NY, ed. 4th, 2002).

28. D. G. Schatz, Y. Ji, Recombination centres and the orchestration of V(D)J recombination. *Nat Rev Immunol* **11**, 251-263 (2011).

29. R. Ahmed, D. Gray, Immunological memory and protective immunity: understanding their relation. *Science* **272**, 54-60 (1996).

30. D. Gray, Immunological memory. *Annu Rev Immunol* **11**, 49-77 (1993).

31. J. I. Gray, L. M. Westerhof, M. K. L. MacLeod, The roles of resident, central and effector memory CD4 T-cells in protective immunity following infection or vaccination. *Immunology*, (2018).

32. J. K. Chan, C. S. Ng, P. K. Hui, A simple guide to the terminology and application of leucocyte monoclonal antibodies. *Histopathology* **12**, 461-480 (1988).

33. R. K. Srivastava, H. Y. Dar, P. K. Mishra, Immunoporosis: Immunology of Osteoporosis-Role of T Cells. *Front Immunol* **9**, 657 (2018).

34. I. S. Afonina, S. P. Cullen, S. J. Martin, Cytotoxic and non-cytotoxic roles of the CTL/NK protease granzyme B. *Immunol Rev* **235**, 105-116 (2010).

35. M. E. Pipkin *et al.*, Interleukin-2 and inflammation induce distinct transcriptional programs that promote the differentiation of effector cytolytic T cells. *Immunity* **32**, 79-90 (2010).

36. C. Gerner *et al.*, The Fas-induced apoptosis analyzed by high throughput proteome analysis. *J Biol Chem* **275**, 39018-39026 (2000).

37. F. Castellino *et al.*, Chemokines enhance immunity by guiding naive CD8+ T cells to sites of CD4+ T cell-dendritic cell interaction. *Nature* **440**, 890-895 (2006).

38. J. Reiser, A. Banerjee, Effector, Memory, and Dysfunctional CD8(+) T Cell Fates in the Antitumor Immune Response. *J Immunol Res* **2016**, 8941260 (2016).

39. G. Del Prete, Human Th1 and Th2 lymphocytes: their role in the pathophysiology of atopy. *Allergy* **47**, 450-455 (1992).

40. M. Veldhoen *et al.*, Transforming growth factor-beta 'reprograms' the differentiation of T helper 2 cells and promotes an interleukin 9-producing subset. *Nat Immunol* **9**, 1341-1346 (2008).

41. J. Xing, Y. Wu, B. Ni, Th9: a new player in asthma pathogenesis? *J Asthma* **48**, 115-125 (2011).

42. E. Bettelli *et al.*, Reciprocal developmental pathways for the generation of pathogenic effector TH17 and regulatory T cells. *Nature* **441**, 235-238 (2006).

43. N. Manel, D. Unutmaz, D. R. Littman, The differentiation of human T(H)-17 cells requires transforming growth factor-beta and induction of the nuclear receptor RORgammat. *Nat Immunol* **9**, 641-649 (2008).

44. M. Jutel, C. Akdis, T-cell regulatory mechanisms in specific immunotherapy. *Chem Immunol Allergy* **94**, 158-177 (2008).

45. K. J. Maloy, F. Powrie, Regulatory T cells in the control of immune pathology. *Nat Immunol* **2**, 816-822 (2001).

46. K. J. Maloy *et al.*, CD4+CD25+ T(R) cells suppress innate immune pathology through cytokine-dependent mechanisms. *J Exp Med* **197**, 111-119 (2003).

47. N. Fazilleau, L. Mark, L. J. McHeyzer-Williams, M. G. McHeyzer-Williams, Follicular helper T cells: lineage and location. *Immunity* **30**, 324-335 (2009).

48. R. V. Luckheeram, R. Zhou, A. D. Verma, B. Xia, $CD4^+$T cells: differentiation and functions. *Clin Dev Immunol* **2012**, 925135 (2012).

49. J. Chinen, W. T. Shearer, Secondary immunodeficiencies, including HIV infection. *J Allergy Clin Immunol* **125**, S195-203 (2010).

50. G. E. Dinse *et al.*, Increasing Prevalence of Antinuclear Antibodies in the United States. *Arthritis Rheumatol* **72**, 1026-1035 (2020).

51. American Autoimmune Related Diseases Association. The Cost Burden of Autoimmune Disease: The Latest Front in the War on Healthcare Spending. http://www.diabetesed.net/page/_files/autoimmune-diseases.pdf

52. L. Wang, F. S. Wang, M. E. Gershwin, Human autoimmune diseases: a comprehensive update. *J Intern Med* **278**, 369-395 (2015).

53. K. S. Tuano, N. Seth, J. Chinen, Secondary immunodeficiencies. An overview. *Ann Allergy Asthma Immunol*, (2021).

54. C. McCusker, J. Upton, R. Warrington, Primary immunodeficiency. *Allergy Asthma Clin Immunol* **14**, 61 (2018).

55. G. Cooper, B. Stroehla, The epidemiology of autoimmune diseases, *Autoimmunity Reviews*, Volume 2, Issue 3, 2003, Pages 119-125, ISSN 1568-9972,

Chapter 2 - The Emerging role of C-peptide on Immune Cells

2.1 Introduction into Diabetes

In 2015, the Centers for Disease Control and Prevention (CDC) reported that 9.3% of the total United States U.S. population, or 23 million individuals, have diabetes. Additionally, it was reported that 7.2 million individuals go undiagnosed, and over 80 million individuals have pre-diabetes.(*1*) In U.S. adults, 5% of the diagnosed have Type 1 diabetes (T1D).(*1, 2*) The American Diabetes Association reported annual costs of $327 billion in diabetic treatment in 2017.(*2, 3*) Although diabetes has different forms and pathologies, it can be characterized as chronic hyperglycemia following insulin depletion or sensitivity.(*4*)

Insulin is a hormone that is produced in the pancreas.(*5*) Specifically, it is made inside the islets of Langerhans in the pancreatic β-cells. Insulin's role in the body is to regulate blood glucose levels by activating glucose transporter 4 (GLUT4).(*6, 7*) Skeletal, muscle, liver, and fat cells directly bind insulin resulting in translocation of GLUT4 to the cell membrane.(*8*) Once GLUT4 is in the membrane, glucose is transported across a concentration gradient.(*9*) Inability of the body to clear glucose properly leads to hyperglycemic conditions. Left untreated, long term exposure to hyperglycemic conditions can result in several secondary complications such as retinopathy, neuropathy, nephropathy, and cardiovascular disease.(*10*) In this chapter, we will be investigating immune dysfunction, an additional regularly reported complication of diabetes.

2.1.1 Classifications of Diabetes

Individuals with diabetes are typically asymptomatic. For this reason, on yearly checkups with a healthcare provider, specific vitals are checked that correlate with an individual having with diabetes. Examples of key yearly vitals that are measured are age, high body mass index, high blood pressure, high cholesterol, and family history.(*11, 12*) If an individual is suspected of having diabetes based on predisposition or higher than normal values on the aforementioned measurements, there are a few determining tests that can be ran performed to confirm the presence of diabetes.

The main test to determine if an individual has a form of diabetes is a hemoglobin A1C test, which quantifies in a percentage, the amount of hemoglobin proteins that are coated with glucose or glycated. If the percentage is less than 5.7%, the hemoglobin glycation is considered normal. However, values between 5.7% and 6.4% are considered “prediabetic” and anything over 6.5% is considered diabetic.(*13*) As with any diagnostic, there are inconsistencies due to certain conditions such as pregnancy or genetic hemoglobin variances. Under those circumstances, a secondary test to determine if a patient has diabetes is a blood glucose test, of which there are several types of this test.

A random blood sugar test is taken without eating or drinking restrictions. If the test comes back with a concentration of 11.1 mmol/L or higher, that individual is considered to have diabetes. A fasting blood sugar test is taken after an overnight fast. In a fasting blood glucose test, a concentration of 7 mmol/L or higher is diagnosed as diabetes.(*12,*

13) While both of these are tests are used to help determine if a person has diabetes, neither test determines the type (I or II) of diabetes that person has. Table 2.1 illustrates the possible types of diabetes that could be diagnosed.

Table 2.1: Classifications of diabetes variations.

Forms	Cause	Treatment
Type 1 Diabetes	Destruction of β-cell from autoreactive T-cells	Insulin injections
Type 2 Diabetes	Insulin resistance due to genetics and lifestyle factors	Medication for glucose control, and lifestyle changes
Gestational Diabetes	Glucose buildup in the bloodstream during a pregnancy	Monitoring lifestyle choices
Other forms of diabetes	Damage to pancreas	Medication for insulin sensitivity and glucose control, insulin injections

Type 2 diabetes (T2D) results from insulin-dependent cells become increasingly resistant to the hormone. T2D is the most common form of diabetes, affecting approximately 90% of people who have diabetes.(*1*) T2D disproportionately affects specific ethnicity groups including African Americans, Native Americans, Latinx, and Native Hawaiians.(*14*) T2D is often characterized as insulin resistance. Individuals with T2D still have the capability to produce insulin. However, the insulin is less effective in stimulating glucose transport compared to a control patient.(*14, 15*) The cause of this inefficacy is linked to genetic factors and unhealthy lifestyle choices. Examples of lifestyle factors include obesity, stress, poor diet, and physical inactivity, which have all been linked to development of T2D.(*4, 16*)

Therapies for T2D include a controlled diet, regular exercise or therapeutic intervention, such as metformin.(*1, 17*) Typically, insulin is not used as a therapeutic for T2D because, as mentioned above, a possible cause of T2D is insulin resistance. However, there are cases where a long-acting insulin analog is used for treatment.(*18*) Metformin treatment decreases the production of glucose in the liver, decreasing circulating glucose, and subsequent hyperglycemia.(*19*) However, the side effects of Metformin have been shown to increase clotting factors, subsequently accelerating microvascular complications associated with diabetes.(*20*)

In contrast to the origins of T2D, T1D is an autoimmune disorder in which insulin producing β-cells of the pancreas are destroyed. While not confirmed, many researchers agree that the β-cells are destroyed by autoreactive cytotoxic T lymphocytes.(*21, 22*) While the pathophysiology may seem straight forward, studies have shown that collectively, many factors need to occur prior to the onset of T1D figure 2.1.(*23*)

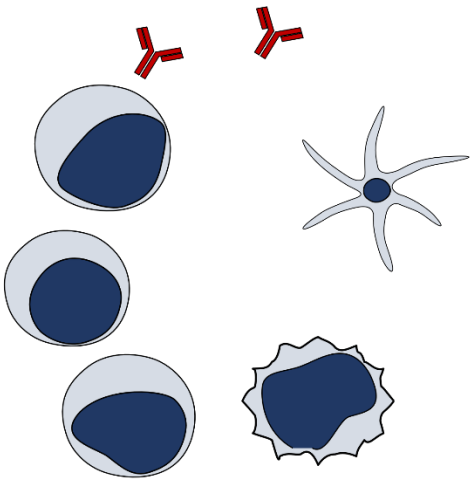

Immune System
Immune regulation dysfunction
Autoantibody production
High cytokine production
Adhesion defects
Self antigen reaction
Antigen presenting cell activation

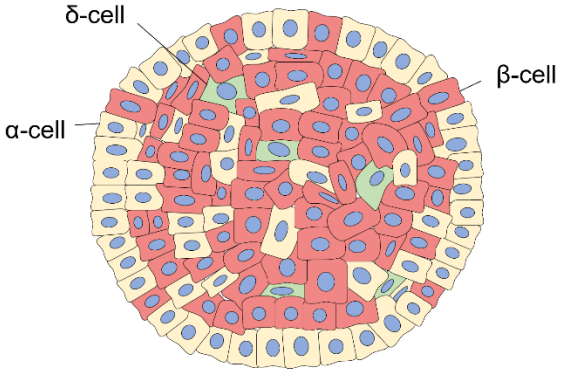

β-cells
Expression of class I MHC
Increased free radical sensitivity
Abnormal expression of cytokines and chemokines
Self antigen presentation through class II MHC
Inability to clear inflammation

Figure 2.1: Proposed homeostatic disruptions in the immune system and islets of Langerhans. Left. Malfunctions in immune cells lead to abnormal activation and reaction to self-tissue. **Right.** Abnormal surface receptor presentation and secretion of pro-inflammatory cytokines recruit and activate immune cells. Due to the autoreactive nature of the recruited immune cells, self-damage to the islets occurs.

The decrease in β-cell mass results in minimal to no production of insulin. In T1D, with the absence of insulin, exogenous administration of insulin is essential as a therapeutic intervention.(*24*) Insulin injections help regulate blood glucose concentrations and thereby decrease advanced glycation end products, which have been correlated to pathologies of several complications.(*25*)

Lastly, there is gestational diabetes, which affects pregnant women. Similar to T2D, there is glucose build up in the bloodstream not caused by insulin deficiency. The treatment for this form of diabetes is also similar to T2D with options being lifestyle changes such as monitoring nutrition, or becoming less sedentary.(*26*) In contrast to other forms of diabetes, gestational diabetes often subsides after pregnancy.

2.1.2 Diabetic Complications

Insulin treatment and lifestyle changes are the gold standard in diabetes treatment. However, insulin administration does not help mediate the several diabetic complications including cardiovascular diseases, nephropathy, neuropathy, and retinopathy. Hyperglycemia induces metabolic pathways that leads to cellular dysfunction, altered osmosis and redox potentials, and toxic metabolite production. These metabolic alterations lead to irregular blood flow in the vasculature, a common denominator in these secondary complications.(*27-29*)

Retinopathy is the most common complication of diabetes and the leading cause of vision loss in adults.(*30*) Diabetic retinopathy results from damage to the retina that leads to vision impairment or blindness.(*31*) Early indications of diabetic retinopathy include visible retinal microaneurysms, or small leaking of blood from a retinal artery or vein.(*32*) Damage to the retina brings recruitment of growth factors, vasculature endothelial growth factor (VEGF) in particular, to promote angiogenesis. Due to improper blood flow in the retina leading to lack of oxygen, the new vessels formed are typically

weakened. The body's normal response to progressing diabetic retinopathy is to promote occlusion or blocking off the vessel. However, the process of occlusion in the retina leads to ischemia, beginning the drastic drop in vision loss.(*32*)

Diabetic nephropathy affects 1 out of 3 individuals with diabetes.(*33*) This complication of diabetes also has the highest mortality rate in individuals with diabetes.(*34*) Nephropathy is a condition in which the kidney malfunctions, affecting its normal function of removing waste and excess fluid from the body. Microvasculature complications lead to irregular pressure systems in the kidney, which can lead to key characteristics or pathologies being observed, specifically high quantities of albumin in urine (albuminuria), glomerular lesions, and the loss of the glomerular filtration rate.(*35, 36*)

Diabetic neuropathy is defined as damage to nerves that create irregular neuronal signals, and is estimated to affect one half of the diabetic population.(*37*) In peripheral diabetic neuropathy, irregular signals tend to affect the arms and legs. Individuals with diabetic neuropathy experience loss of sensation, burning, and/or sharp pain. Similar to the previously described complications, hyperglycemia in the blood stream of individuals with diabetes leads to hindered blood flow.(*38*)

Along with the microvascular complications of diabetes, individuals with diabetes have characteristics related to immune deficiency. Some of the proposed extrinsic factors contributing to diabetic immune deficiency are shown in figure 2.2. A hyperglycemic

environment is known to negatively affect several immune functions, resulting in an ideal environment for opportunistic pathogens.(*39*) Circulating innate immune cells such as neutrophils, have shown a decreased ability to perform key functions such as chemotaxis, phagocytosis, participate in the formation of reactive oxygen species, and display decreased release of pro-inflammatory cytokines.(*40-42*) Additively, circulating adaptive immune cells such as T lymphocytes, have decreased functions as well including: decreased cell surface expression of major histocompatibility complex (MHC), decreased pro-inflammatory cytokines, glycation of immunoglobulins, and overall decreased activation to primary promoting antigens.(*43-45*)

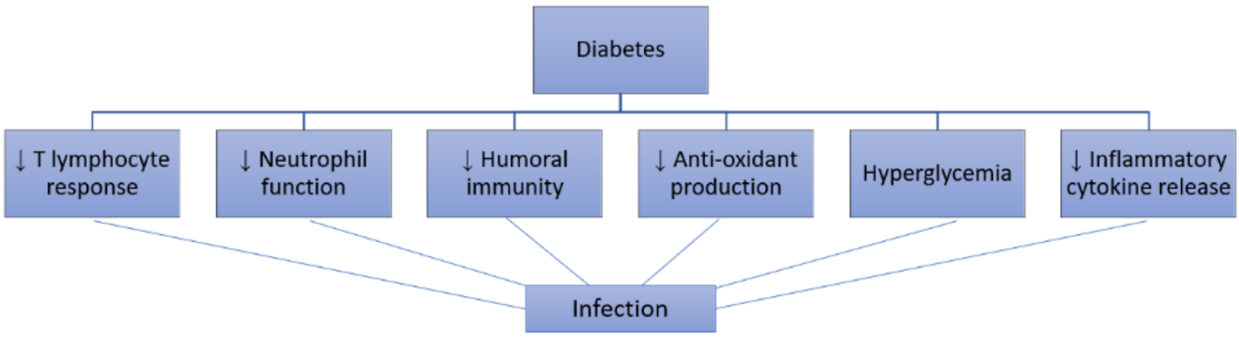

Figure 2.2: Proposed diabetic factors contributing to an increased rate of infection. An overall decrease in immune cell activity coupled with hyperglycemia provides forein pathogens with an ideal enviornment to replicate and infect.

A recent study by Han et al. showed that individuals with diabetes T2D had a higher mortality rate from COVID-19 than non-diabetic patients. Han's findings showed that diabetics with a fasting plasma glucose > 7.0 mmol/L or random plasma glucose have a significantly decreased chance of survival. This indicates that hyperglycemia may play a

role dysregulating the immune system. The diabetic serum cytokine levels were significantly elevated compared to non-diabetic as well. A key cytokine imbalance of IL-6/IL-2 was indicated in non-survivor diabetics. This cytokine imbalance has been shown to overpromote Th2 and downregulate Th1 cells. These two subsets play opposing roles as Th1 is important for promoting an antiviral defense, and Th2 is important for deactivating antiviral action.(*46, 47*) This study shows a link between how hyperglycemia, a result of diabetes, can alter immune cell homeostasis and further complicate health conditions in the current pandemic.

2.2 Immune Cell Metabolism

Immune cells are dynamic cells of the immune system that require rapid transitioning from quiescent to an active state in response to infection. This transition requires acquisitions of specific mediators (molecules and/or nutrients), activation of pathways, and most importantly availability of energy.(*48*) Availability of ATP is essential for the activation of immune cells.(*49*) In immune cells, there are few ways in which ATP, through glucose conversion, is used as fuel for immune cells.(*48, 50*) The most common pathway is through glycolysis, which is a process where glucose is converted through enzymatic reactions into pyruvate, producing ATP molecules as a byproduct.(*51*) Pyruvate can be transported into the mitochondria and is further metabolized to carbon dioxide (CO_2) through the Krebs cycle. The Krebs cycle drives oxidative phosphorylation, resulting in the translocation of protons across the mitochondrial membrane. Due to the

ensuing proton gradient change, the enzyme ATP synthase converts ADP to ATP.(*52*) The tricarboxylic acid (TCA) pathway is a second method of ATP production in immune cells.(*53*) The process of TCA involves the reduction of nicotinamide adenine dinucleotide (NADH) and flavin adenine dinucleotide ($FADH_2$).(*54*) During the reduction, electrons are donated to the electron transport chain that fuels oxidative phosphorylation, as mentioned previously, and produces ATP in the mitochondria.(*48*) Glycolysis and TCA can work cooperatively if pyruvate is converted to acetyl-CoA and the tricarboxylic acid (TSA) pathway becomes active.(*50*) Lastly, immune cells can metabolize lipids (fatty acid β-oxidation) and glutamine (gluataminolysis).(*54, 55*) Metabolites of these pathways are acetyl-CoA and a-ketoglutarate respectfully. The metabolites enter and start the Krebs cycle, which fuels oxidation phosphorylation, and subsequent ATP production.(*54, 55*)

The neutrophils primary source of ATP is through glycolysis. However, neutrophils have a decreased number of mitochondria and consume little oxygen.(*56*) When a neutrophil becomes active through TLR antagonist binding, or phagocytosis of an antigen, the immune cell increases its consumption of oxygen and glucose.(*57*) It would be simple to assume that mitochondria activity increases, however due to the sparse number of mitochondria in neutrophils, the increased consumption is a result of the Warburg effect and the pentose phosphate pathway.(*58*) The Warburg effect is an oxidative phosphorylation independent alternate of glycolysis where the cell rapidly uptakes glucose and is converted into lactate through fermentation.(*59*) NADPH is a byproduct of this altered metabolism. NADPH is particularly important in neutrophils because NADPH is a cofactor for NADPH oxidase that consumes oxygen to produce H_20_2, an important

microbicidal substance.(*58, 60, 61*) Interestingly, when researchers, induced nonfunctional mitochondria in neutrophils, neutrophils undergo cytochrome C dependent apoptosis, providing evidence for glycolysis as a key mechanism for neutrophil survival.(*62*)

Along with going from a quiescent to active state, activated T-cells must undergo rapid proliferation that requires massive amounts of energy.(*63*) T-cells utilize glycolysis and oxidative phosphorylation as their main source of energy production.(*64*) Post glycolysis, glucose is converted into pyruvate which either is converted into lactate or enters the TCA cycle.(*65*) Additionally, glutaminolysis plays an important role due to the production of glutamine that can replenish the TCA cycle intermediates.(*59, 65*) The pentose phosphate pathway metabolizes glucose to yield nucleotides and NADPH, important for lipid synthesis.(*48*) Overall, the metabolic hallmark of a T-cell going from an inactive to active state is metabolic switching from catabolic metabolism to anabolic metabolism.(*66*) However, for long lasting immune cells such as memory T-cells and subsets of macrophages, the metabolism stays in a catabolic state.(*48*) Memory T-cells rely on mitochondrial fatty acid oxidation to maintain longevity.(*67, 68*)

2.3 Pancreatic Secretions

2.3.1 Proinsulin

Inside the pancreas, resides the hormone producing islets of Langerhans cell clusters. The hormones released are involved in glucose regulation. The three different

cell types in the clusters are α, β, and δ cells. β cells are responsible for the secretion of insulin.(*6, 69*) However, prior to secretion, there are key steps in the insulin biosynthesis. Preproinsulin is the first form, a 110 ammino acid molecule that contains a hydrophobic N-terminus and a 35 amino acid connecting peptide signaling sequence. The connecting peptide links the C-terminus of the B chain to the N-terminus of the A-chain. The signaling peptide directs the protein to the secretory pathway through targeting the protein to the lumen of the endoplasmic reticulum. The signaling peptide is cleaved at the C-terminus through peptidase activity forming proinsulin, which is comprised of insulin bound to C-peptide. C-peptide mediates proper folding of insulin though disulfide bonds between the A and B chains of insulin.(*69*) As shown in figure 2.3, C-peptide connects the N-terminus of insulin A chain and the C-terminus of the insulin B chain.

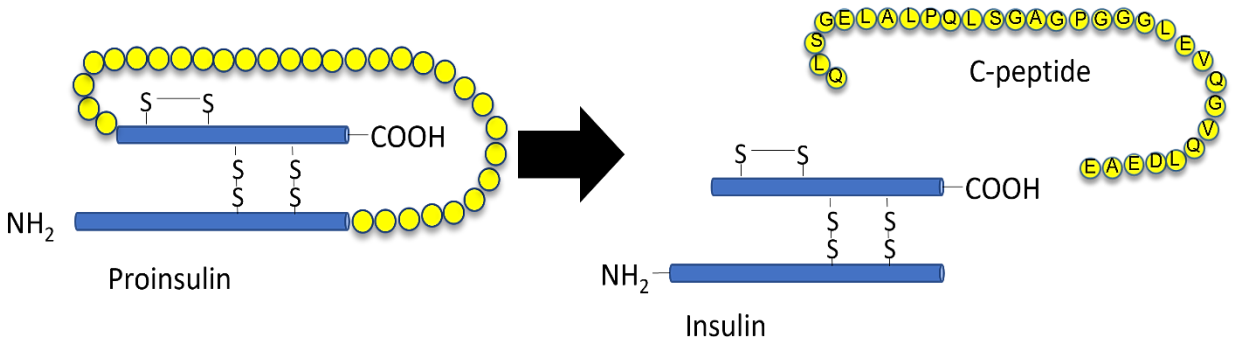

Figure 2.3: Proinsulin to insulin path. This diagram depicts the process of C-peptide (yellow) interact with insulin (blue). C-peptide links the A and B chain of insulin through disulfide bonds. Through enzymatic activity, C-peptide is cleaved leaving an intact functional insulin hormone.

The proinsulin molecule is moved to the Golgi to be cleaved by endopeptidases in a Ca^{2+} dependent manner.(*70*) At a resting state inside the βcell, there are low

concentrations of adenosine triphosphate (ATP). The low concentrations cause K_{ATP} channels to remain open and Ca^{2+} channels to remain closed due to the cell membranes hyperpolarized state. This voltage gated relationship switches as more glucose enters the body, for example after a meal. As more glucose enters the pancreas, glucose enters the β-cell through glucose transporter 2. As a result of glycolysis, more ATP is formed causing a shift in the ratio of ATP to ADP. The K_{ATP} channel closes and results in the depolarization of the β-cell, opening the voltage gated Ca^{2+} channel.(*69, 71, 72*) The influx of Ca^{2+} allows for the activation of the endopeptidase activity and the subsequent exocytosis of insulin, C-peptide, and Zn^{2+} figure 2.4.(*69, 70*)

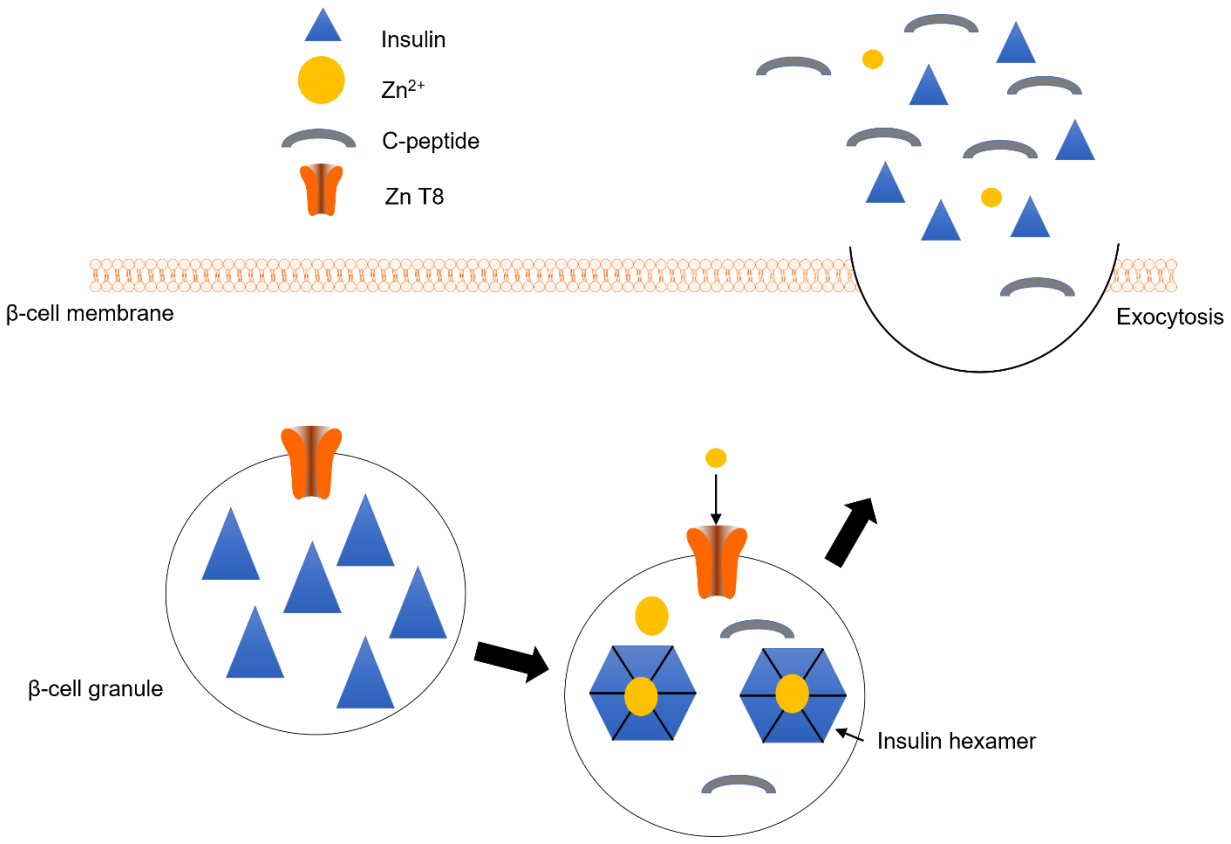

Figure 2.4: Insulin formation and exocytosis. In the Golgi apparatus, an insulin hexamer is formed which is composed of insulin, C-peptide and Zn^{2+}. When C-peptide is cleaved the hexamer loses its stability and dissociates, and insulin is stored in a

crystalized state in vesicles. As blood glucose levels increase, insulin, C-peptide and Zn^{2+} are released.

2.3.2 Insulin

Insulin, a pancreatic hormone, contains 51 amino acids and has a molecular mass of 5,802 Da.(*73*) The hormone, discovered in 1921, facilitates glucose uptake by cells containing glucose transporter 4.(*5*) Fredrick G. Banting and Charles Best were the first successful researchers in extracting insulin in John McLeod's research laboratory at the University of Toronto.(*74*) Within months the researchers observed that in felines, when the pancreas is removed, the animal develops diabetes. Intravenous injections of their pancreatic extract called isletin, lowered blood glucose. Isletin was then purified and in 1922, was injected into the first human subject.(*74*) The subject, who had T1D, experienced no reduction in ketosis and a mild reduction in blood glucose levels. However, after periodic injections the patient had a significant reduction in blood glucose levels, glucosuria, and ketonuria. Collectively, this work granted Banting, and Mcleod a Nobel Prize in 1923. Insulin was then purified, mass produced and distributed by the pharmaceutical company Elli Lilly.(*5, 74*)

Insulin works by facilitating glucose uptake through stimulating translocation of glucose transporter 4(GLUT4).(*75*) GLUT4 is highly expressed in adipose tissue, skeletal and cardiac muscles.(*76*) The hormone binds to a specific tyrosine kinase receptor initiating intracellular signaling shown in figure 2.5.(*77*) There are two pathways in which insulin signaling acts upon. One pathway is the phosphatidylinositol 3-kinase

(PI3K)/protein kinase B(AKT), which initiates the metabolic effects of insulin.(*78*) Second is the Ras/Raf/MAPK pathway. MAPK or mitogen activated protein kinase is involved in the regulation of gene expression.(*77, 79*) In addition to the regulation of glucose metabolism, insulin has been shown to serve other functions. Insulin is involved in lipid metabolism, fatty acids synthesis, increasing protein synthesis, decreasing apoptosis, and triglyceride uptake.(*80, 81*)

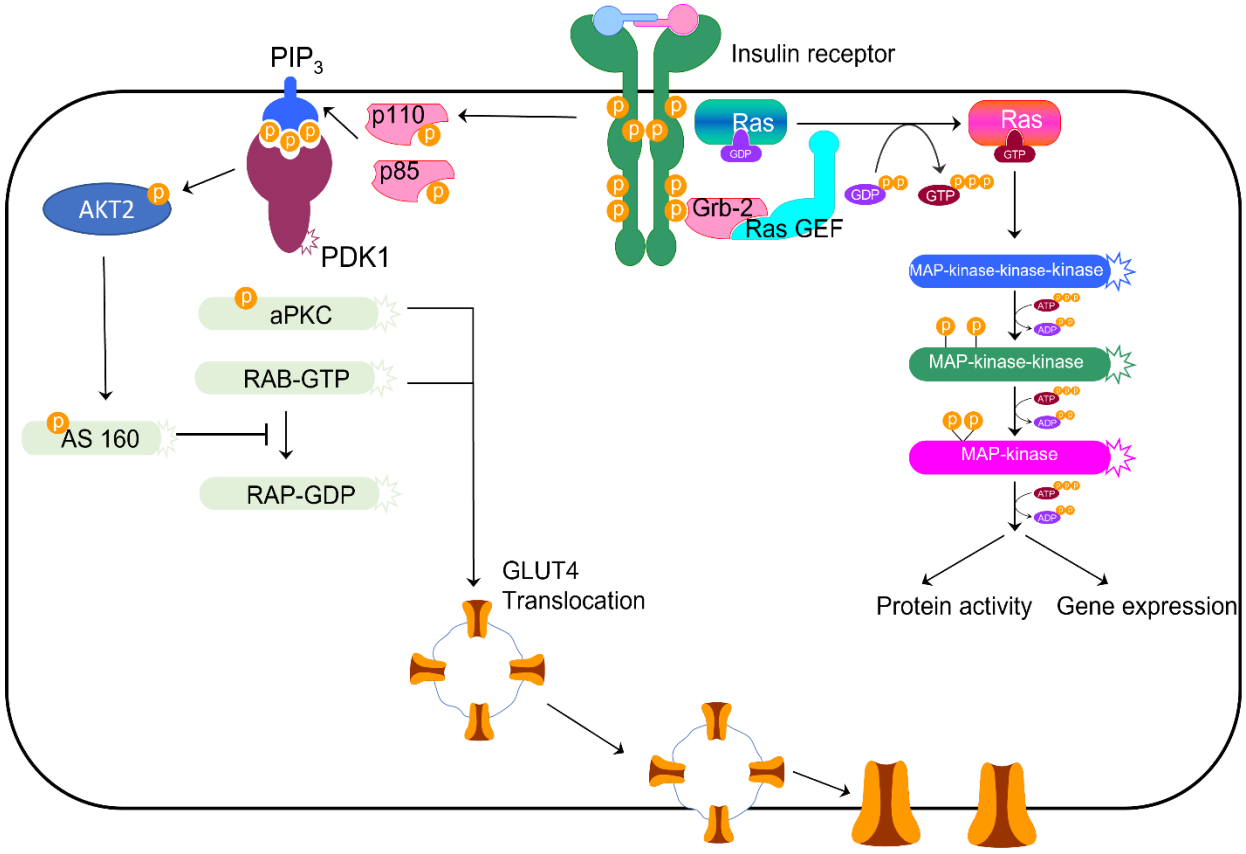

Figure 2.5: Simplified insulin signaling pathway. Insulin binding to its respected receptor tyrosine kinase initiates several intracellular signaling pathways. The intricate pathways lead to protein synthesis and GLUT4 translocation. Additional abbreviations PIP: phosphatidylinositol 3,4,5-trisphosphate: PDK phosphoinositide-dependent protein kinase: PKC protein kinase C: Growth factor receptor-bound protein 2.

2.3.3 C-peptide

C-peptide, discovered in 1967 by Steiner, is a 3,020 Da, 31 amino acid peptide that assists in the proper folding of insulin.(*82*) As stated previously, C-peptide is co-secreted from the pancreatic β-cells in an equimolar ratio with insulin. Besides assisting in the folding of insulin, C-peptide has been thought to be biologically irrelevant.(*83*) However, C-peptide has a half-life of 30 minutes in the blood stream, allowing the peptide to be used as a biomarker for β-cell function.(*84*) In the 1980s, researchers were able to detect residual B-cell activity in individuals with T1D through measuring of plasma C-peptide levels. The individuals who had this residual β-cell activity reported experiencing fewer diabetic complications than individuals with no detectable plasma C-peptide. This discovery prompted a surge of C-peptide research throughout the 1990s and early 2000s.(*6, 83, 85*)

Researchers have investigated other biological contributions of C-peptide since the early 90's(*86*) and several reports show the potential therapeutic possibilities of C-peptide. Researchers have reported the biological relevance of C-peptide in both humans and mice using in vivo and in vitro methods.(*85, 87-92*) These early studies showed the relevancy of C-peptide in decreasing diabetic complications which are associated with improper blood flow. The researchers investigated aspects such as RBC deformability, glomerular filtration, Na-K-ATPase activity, retinopathy, and neuropathy.

Researchers have also shown that C-peptide binds to GLUT1 containing cells such as, venues endothelium, renal tubular cells, and fibroblast.(*93, 94*) The Spence lab has added to these findings proving specific binding between C-peptide and RBCs.(*95*) In 2006, the Spence Lab found through in vitro studies that RBCs from individuals with T2D secreted significantly less ATP compared to controls.(*96*) This finding is important due to the indirect ability of ATP to regulate vasculature resistance through the stimulation of a known vasodilator nitric oxide (NO) synthesis in endothelial cells.(*97, 98*) This finding was further enhanced through breakthrough findings(*99, 100*) from Sprague et al who reported that rabbit lung vasculature resistance could be decreased with increased availability of extracellular ATP.(*99*) It was then hypothesized by the Spence lab that the microvasculature related complications of diabetes may stem from a lack of available ATP, which in control settings, is produced by RBCs.

These interesting findings led to new field of C-peptide studies. However, when investigating C-peptide stimulated ATP release from RBCs, researchers had reproducibility issues.(*83, 86*) The Spence Lab was able to make two important breakthroughs to push C-peptide research further. Mass spectrometry analysis showed that commercially purchased C-peptide is contaminated with a transition metal.(*101*) It was concluded that further purification of the purchased C-peptide through high performance liquid chromatography (HPLC) was necessary.(*102*) In addition to purity, it was also found that for C-peptide to elicit ATP release, a particular transition metal was needed. Knowing that the β-cell granule has a high concentration of Zn^{2+}, future

experiments used a combination of C-peptide and Zn^{2+}.(*70*) The combination of C-peptide and Zn^{2+} was able to provide reproducible ATP release data.

In all the C-peptide experiments performed by the Spence Lab, all RBC samples were prepared in a physiological salt solution buffer (PSS). This buffer contains a series of salts, sugar, and varying percentages of bovine serum albumin. It was found that when albumin was excluded from the buffer, the group indicated no C-peptide binding to RBCs and a subsequent lack of ATP release.(*95*) Utilizing isothermal titration calorimetry (ITC), it was reported that albumin is capable of carrying C-peptide and Zn^{2+} with high affinities (K_a = 2.66 ± 0.25 × 10^5 M^{-1}, K_a = 5.08 ± 0.98 × 107 M^{-1}).(*95*) Since albumin has a high affinity for acidic peptides, the glutamic acid residue at site 27 was mutated to an alanine.(*95, 103*) This mutation abolished the binding of C-peptide to albumin.(*95*) These findings indicate that albumin may be acting as a carrier protein for C-peptide and Zn^{2+} to an undescribed receptor on GLUT1 containing cells i.e., RBCs. Evidence for the biological relevancy of C-peptide has been produced on a few cells, however, evidence has not been shown on immune cells. The following sections will establish the binding relationship between C-peptide, T-cells and neutrophils, in addition, functional downstream effects of C-peptide uptake.

2.4 Experimental

2.4.1 Isolation of Human Immune Cells

All protocols were approved by the Institutional Review Board at Michigan State University (IRBs 14-892 and 17-1541). Both T-cells and neutrophils were isolated using their respected human whole blood isolation kits (EasySep Direct, STEMCELL Technologies, Vancouver, BC, Canada). The isolation method utilized negative magnetic separation of T-cells and neutrophils from whole blood shown in figure 2.6. Both cell types were resuspended in ~2 mL of phosphate buffer saline (PBS) and used during experiments within 6 hours of isolation. Cell counts were determined using an automatic cell counter (Thermo Scientific, San Jose, CA, USA). The concentrated neutrophil suspension typically contained ~8 million cells/mL. The concentrated T-cell suspension contained ~2 million T-cells/mL. In all cases, samples used during an analysis contained ~1 million neutrophils/mL.

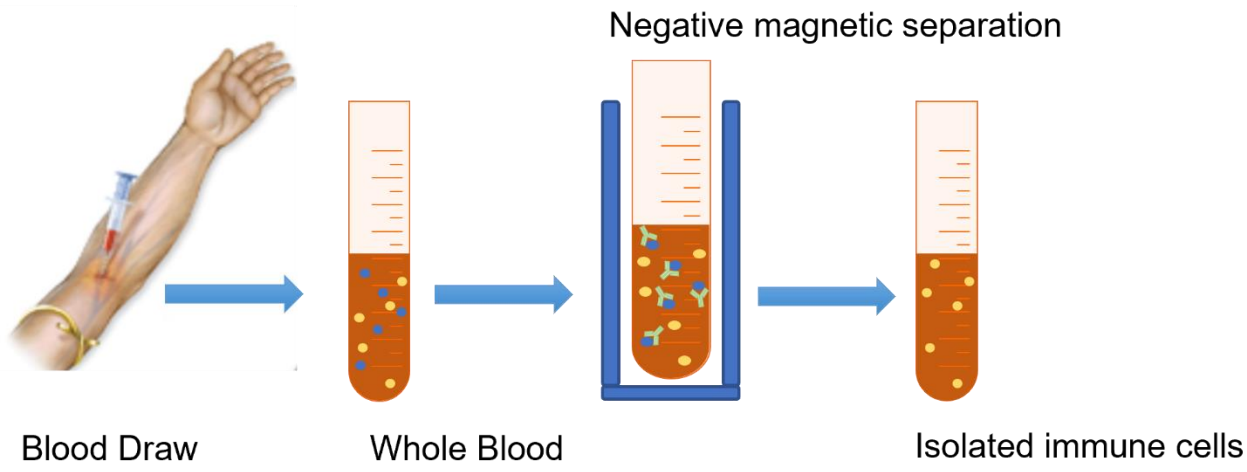

Figure 2.6: Immune cell isolation workflow. Whole blood is collected via venipuncture into heparinized blood tubes. Blood is slowly pipetted to a 45 mL Eppendorf tube where the primary and secondary antibodies are introduced. Since the secondary antibody is conjugated with magnetic beads, unwanted cells are pulled to the bottom and sides of the tube. An off-white-colored supernatant is pipetted off. The process is then repeated two times to achieve purity.

2.4.2 Purification of C-peptide

Synthesized human C-peptide (~85 % pure) was purchased from Peptide 2.0 (Chantilly, VA, USA), and purified using reverse phase high performance liquid chromatography (RP-HPLC, Shimadzu, Columbia, MD, USA). The system was comprised of an LC-20AB solvent delivery system and an SPD-20AV UV-Vis absorbance detection system coupled to an Atlantis T3 OBD Prep Column (10 mm x 150 mm; Waters, Milford, MA). Fractionated and collected C-peptide was lyophilized overnight and stored at -20 °C. C-peptide purity was verified by mass spectrometry (Thermo Scientific LTQ Orbitrap) equipped with a NanoMate electrospray source (Advion, Ithaca, NY, USA).

2.4.3 C-peptide Binding to Immune cells

Both T-cells and neutrophils were isolated by the neutrophil isolation methods described and added to a known concentration of C-peptide in a buffered physiological salt solution (PSS; in mM: 4.7 KCl, 2.0 $CaCl_2$, 140.5 NaCl, 12 $MgSO_4$, 21.0 tris(hydroxymethyl) aminomethane (Invitrogen, Carlsbad, CA), 5.5 mM dextrose (Sigma Aldrich), and 0.5% bovine serum albumin (Sigma Aldrich), final pH 7.40). C-peptide binding was investigated in the PSS buffer and a second version of PSS that was albumin-free. For studies involving C-peptide binding to immune cells in the presence of Zn^{2+}, the Zn^{2+} was mixed with C-peptide in a 1:1 molar ratio in 25 µL of distilled and deionized water (DDW, 18.0 MΩ). After 3 minutes, ~375 mL of PSS or albumin-free PSS were added to the C-peptide/Zn^{2+} mixture, followed immediately by the addition of 100 µL of the concentrated/purified immune cells and incubation at 37 °C for 2 hours. Following incubation, samples were centrifuged and the amount of C-peptide remaining in the supernatant was determined using a commercially available C-peptide enzyme linked immunosorbent assay (ELISA) kit (Alpco, Salem, NH). Shown in figure 2.7, the absolute amount of C-peptide bound to immune cells was determined by subtracting the moles of C-peptide measured in the supernatant from the number of moles initially added to the cell sample.

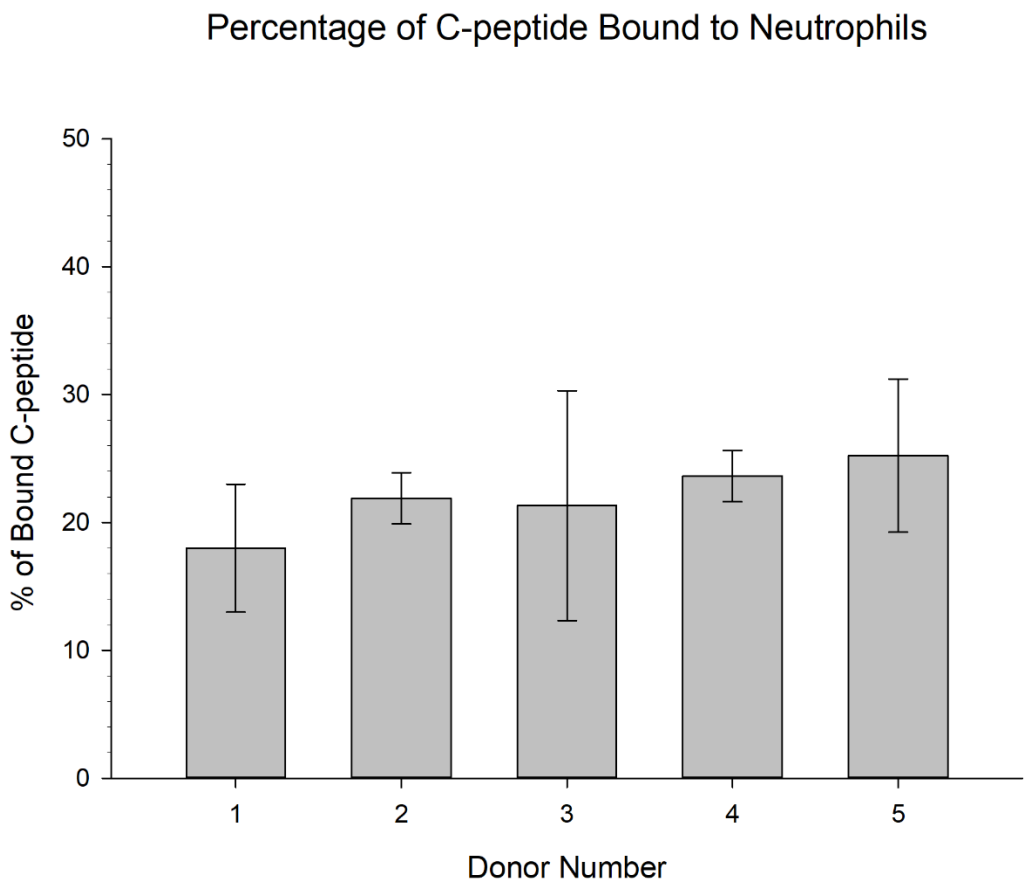

Figure 2.7: Percentage of C-peptide binding per donor. Percentage of 200 pM C-peptide binding neutrophils per donor. (n=5, error=Standard deviation)

C-peptide binding to neutrophils was analyzed to further investigate the interaction of C-peptide with immune cells. C-peptide bound to neutrophils only in the presence of albumin (Figure 1). Per donor, approximately 20% of the total amount of C-peptide added bound to the cells. This percentage equated to approximately 9,000 molecules/cell. In the absence of albumin, there is little to no C-peptide binding, seen in figure 2.8.

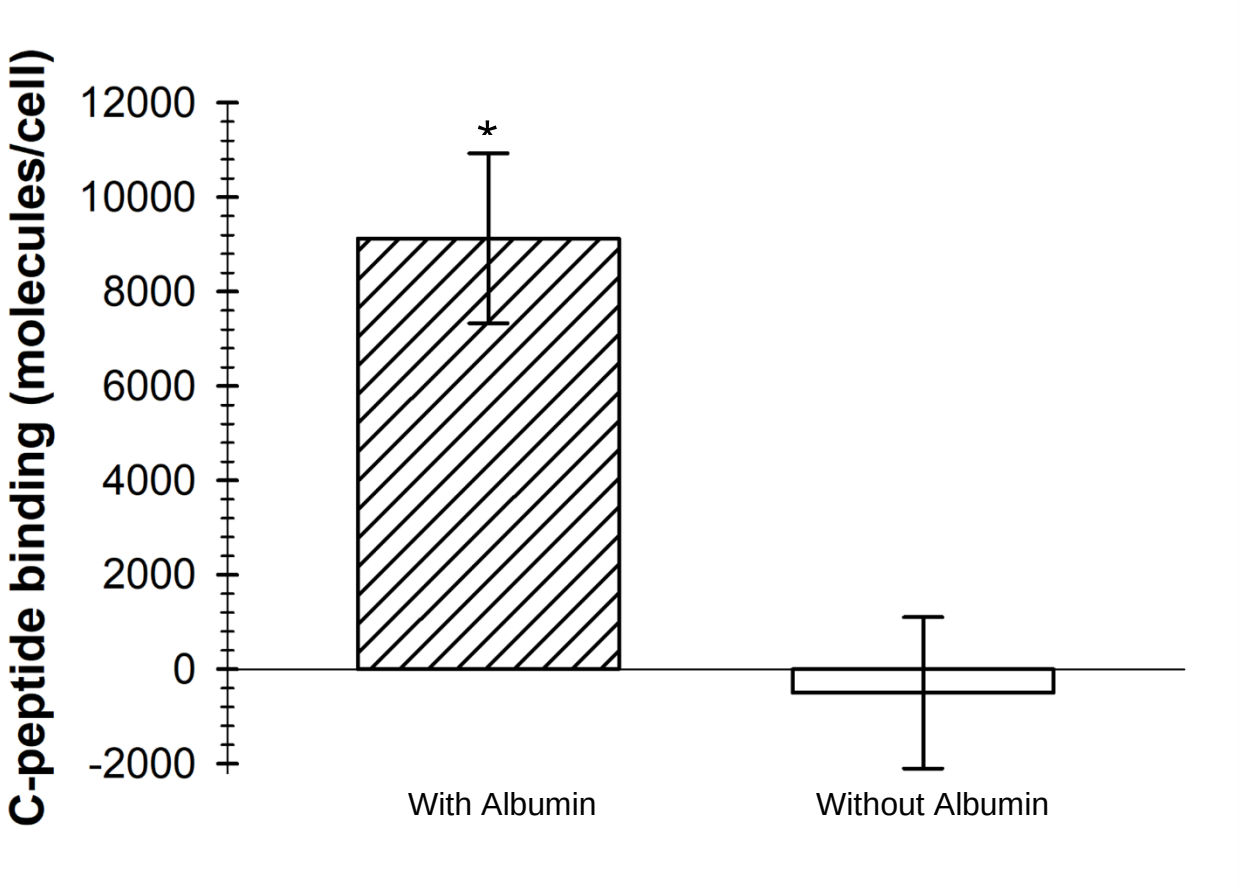

Figure 2.8: Percentage of C-peptide binding in the presence or absence of albumin. Percentage of 200 pM C-peptide binding neutrophils with (n=6) or without albumin (n≥3, error=SEM $p<0.05$).

Interestingly, when investigating C-peptide binding to T-cells an opposite trend was observed figure 2.9. C-peptide binds to T-cells in the presence and absence of albumin. When 200pM of c-peptide is added, 9,000 molecules per cell. In the absence of albumin, negligible binding of c-peptide to neutrophils was observed. Without the presence of albumin, C-peptide binding is more specific compared to the presence of albumin.

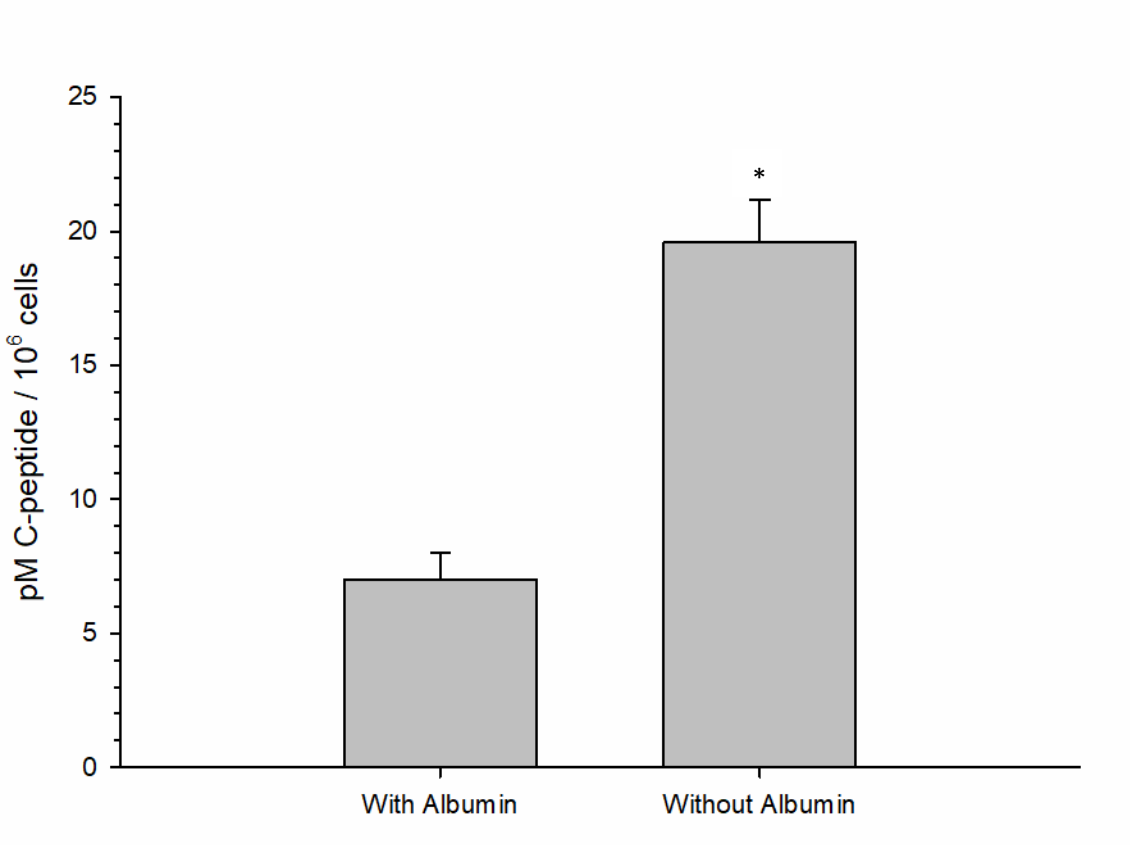

Figure 2.9: C-peptide binding T-cells. C-peptide binding occurred in both samples regardless of the presence or absence of albumin. Significant C-peptide binding was observed without albumin when compared to albumin containing conditions. (N=3, error=SEM $p<0.05$).

2.4.4 Radioisotopic Determination of Zn^{2+} Delivery to Immune Cells

Immune cells were isolated by negative separation as described above. Radioisotopic Zn^{2+}($^{65}Zn^{2+}$) was utilized to determine Zn^{2+} delivery to the immune cells. A known concentration of $^{65}Zn^{2+}$ was added to a known cell density in PSS containing a concentration of C-peptide in a 1:1 ratio with $^{65}Zn^{2+}$. Samples were incubated at 37°C for 2 hours. After incubation, samples were centrifuged at 250 *g* for 10 minutes, and the

amount of Zn^{2+} remaining in the supernatant was determined using gamma radiation emission counting (PerkinElmer Inc., Waltham, MA, USA). The centrifuged pellet was kept verifying amount of $^{65}Zn^{2+}$ was not lost during the process. The moles of $^{65}Zn^{2+}$ bound to the immune cells were determined by subtracting the moles of $^{65}Zn^{2+}$ left in the supernatant from the moles originally added to the sample.

Zn^{2+} is a known contributor to improving immune function. Zn^{2+} binding to neutrophils in both the presence and absence of C-peptide figure 2.10. Zn binds to neutrophils in the absence (~1.5 pM/10^6 cells) and presence (~2.9 pM/10^6 cells) of C-peptide, however Zn binding is more significant in the presence of C-peptide.

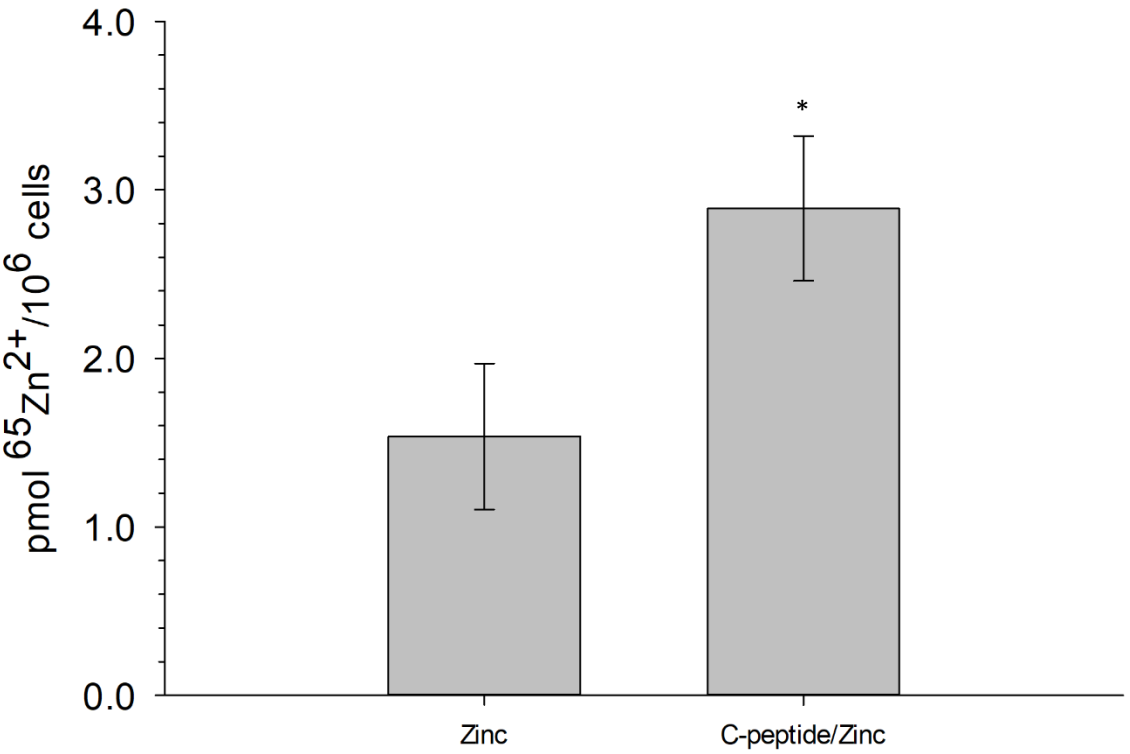

Figure 2.10: Radioisotopic Zn^{2+} binding to neutrophils. 20 nM Zn^{2+} binding to human peripheral neutrophils in the presence and absence of C-peptide. (n≥3, error=S.E.M. $p<0.05$)

When investigating the role of C-peptide on Zn^{2+} binding, no significant difference was observed. In the presence of C-peptide, ~ 1.5 pM Zn^{2+}/ million cells was observed. In the absence of C-peptide, the binding data shows ~ 3 pM Zn^{2+}/ million cells. Verification through analysis of the supernatant, shows 20 nM of $65Zn^{2+}$ was added, adding validity to the experimental methods choice, however, there was no statistical significance in Zn^{2+} binding to T-cells in the presence or absence of C-peptide as seen in figure 2.11.

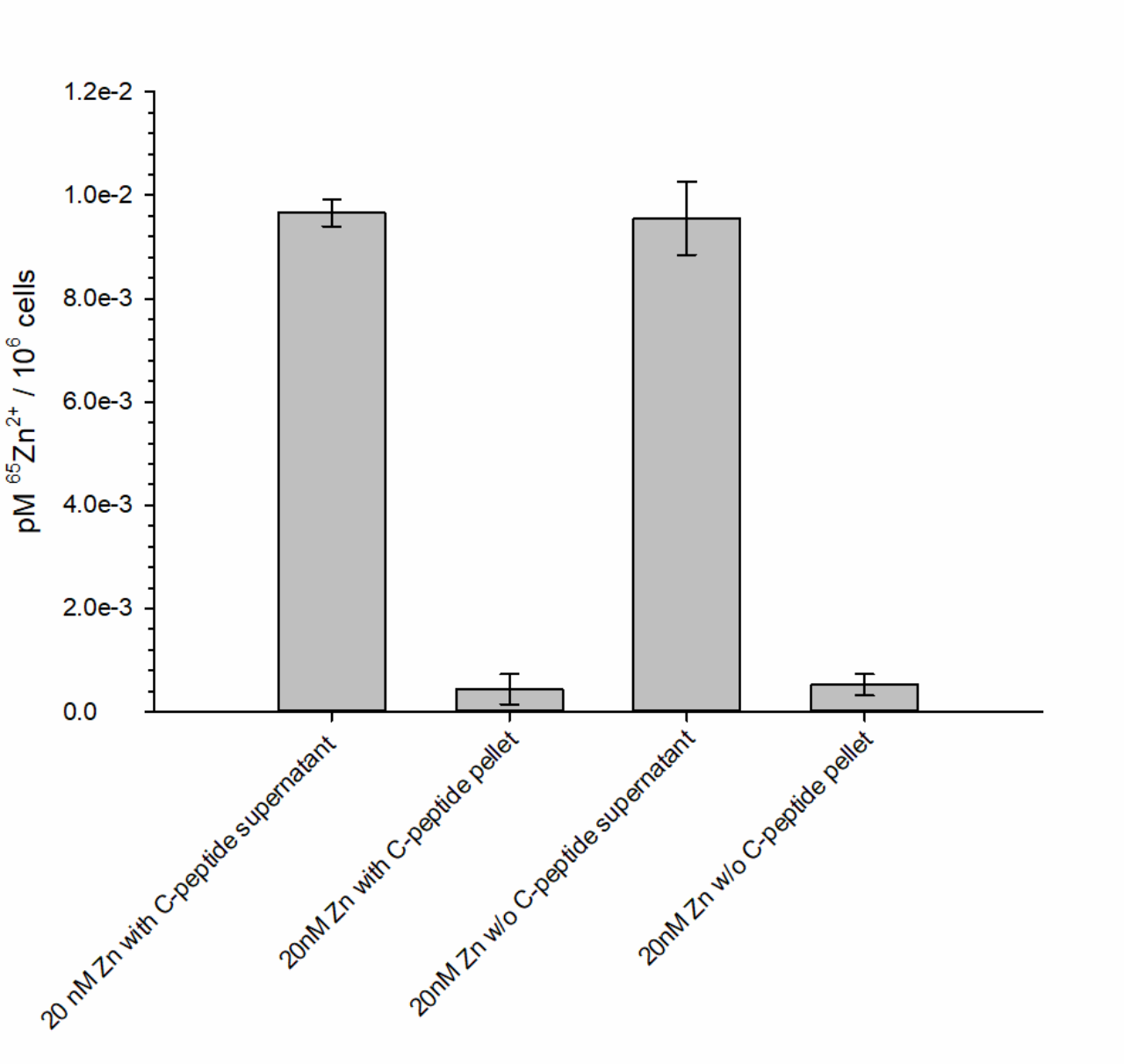

Figure 2.11: Radioisotopic Zn^{2+} binding to T-cells. Zn^{2+} binds to T-cells in the presence or absence of C-peptide. Both the supernatant and cell pellet were measured to ensure concentrations added were accurate. There is no statistical difference between the two groups. (N=3, error=SEM)

2.4.5 Reactive Oxygen Species Production

Human neutrophils were isolated as previously described. ROS activity was measured using the ROS-Glo H_2O_2 Assay (Promega, Madison, WI), reaction shown in figure 2.12. 70 µL of a 10^4 cell suspension, 10 µL of a 2 nM Zn/C-peptide/water solution, and 20 µL of H_2O_2 substrate solution were added to an opaque 96 well plate. The plate was placed in an incubator at 37 °C for 3 hours. Post incubation, the detection solution (Luciferin, D-cysteine, signal enhancer) was immediately added to the wells and allowed to incubate for 20 minutes. Quantification of H_2O_2 was determined recording relative luminescence on a plate reader.

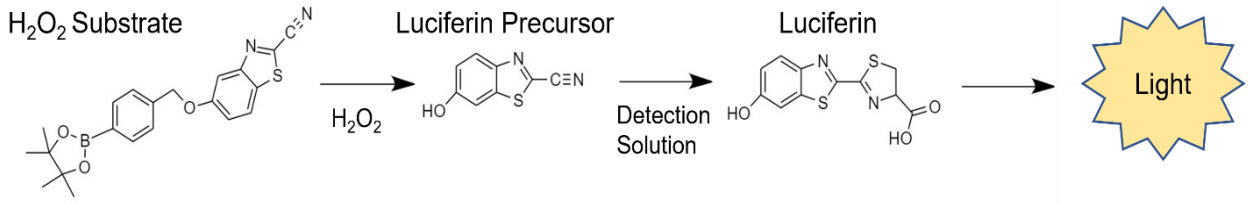

Figure 2.12: ROS-Glo H_2O_2 Assay chemistry. H_2O_2 substrate reacts directly to produce a luciferin precursor. Detection solution contains luciferase and D cysteine reacts directly with the luciferin precursor. D-cysteine converts the precursor to luciferin, and the luciferin reacts with the luciferase. The luciferin luciferase reaction generates a luminescence signal proportional to the H_2O_2 concentration.

ROS is a known as a collection of highly reactive molecules that can function as both signaling molecules and antimicrobial effector. In excess, ROS can cause be destructive to homeostasis. H_2O_2 has the longest half-life of all known ROS. Many ROS are also converted to H_2O_2 within cells.(*104*) With this information, H_2O_2 was established as a prime candidate to measure ROS production figure 2.13. Observation of ROS

production showed that between experimental groups there was no statistical difference in ROS production. However, when compared to the control, both the 2 nM C-peptide/Zn^{2+} and the 80 pM Zn^{2+} groups showed a significant increase in ROS production.

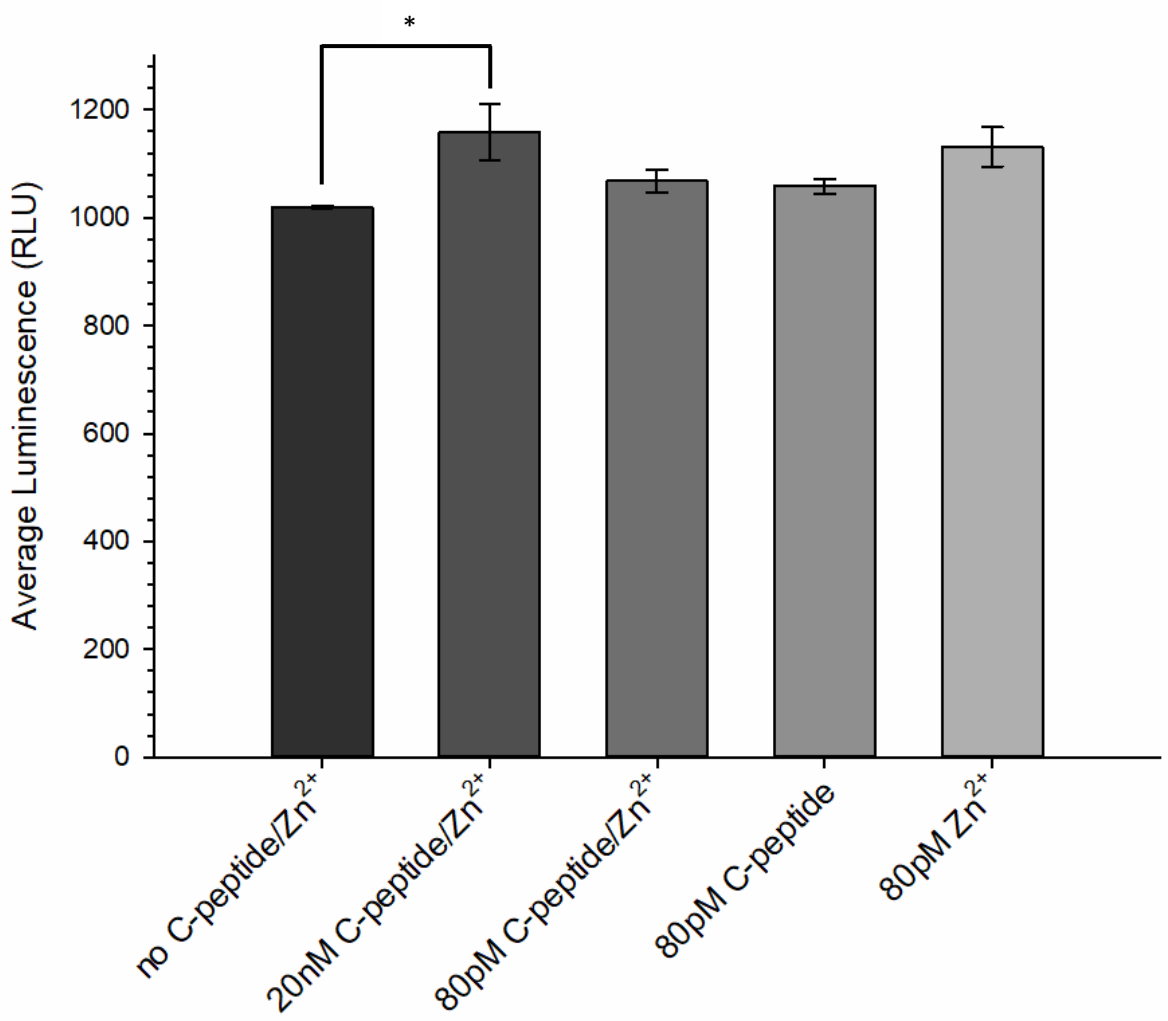

Figure 2.13: ROS production from samples with varying concentrations of C-peptide and Zn^{2+}. Human neutrophils only when exposed to 2nM C-peptide/Zn^{2+} and 80 pM Zn^{2+} showed a significant increase in ROS production when compared to the control. (n=3, error=SEM $p<0.05$)

2.4.6 Bacteria Growth Media and Agar Plate Preparation

Growth media was prepared by dissolving Lennox pellets of Lysogeny broth (LB, EMD Chemicals, Darmsadt, Germany) in 150 mL of distilled deionized water. The solution was set to mix prior to being autoclaved at 121 ºC for 45 minutes. The solution was set aside until it was cool enough to the touch. Antibiotic Kanamycin was added at a concentration of 100 µM. 50 mL aliquots of the LB solution were stored at 4 ºC. For agar plate preparation, the prior steps were followed. However, prior to the autoclave step, 2.25 g of agar (Fisher Scientific, Fair Lawn, NJ) was added. When ready, agar containing LB was poured in petri dishes and sat until the solution solidified at 4 ºC.

2.4.7 Bactria Growth

A green fluorescent protein (GFP) - expressing *Escherichia coli* (E. coli) was thoughtfully gifted by Michigan State Professor Dr. Chris Waters. GFP expressing E. coli was grown in LB containing kanamycin for 4-6 hours shaking at 200 rpm. Then, bacteria were streaked out onto an agar plate, incubating overnight to allow the growth of single colonies. A single colony was transferred from the agar plate to an LB solution, for replication of that specific colony overnight. Since the E. coli were GFP expressing, cell density was determined using flow cytometry. Prior to opsonization and exposure to neutrophils.

2.4.8 Opsonization of GFP E. coli

In vivo opsonization or antibody/complement coating of a pathogen was previously described. A plastic Vacutainer blood tube (BD, Franklin Lakes, NJ) was used for the collection of whole blood. The blood tube contains clot activator but is absent of anticoagulants and preservatives making it practical for serum isolation. The whole blood sat at room temperature for 40 minutes, then centrifuged at 1000g for 10 minutes at 4 ºC. Serum was collected, and equal volume of Hanks balanced salt solution (HBSS) was added to make a 50% serum solution. 2 mL of the GFP E. coli solution was added and incubated with the serum at 37 ºC for 45 minutes.

2.4.9 Phagocytosis Experimental Setup

Neutrophils were isolated as described earlier. The neutrophils were resuspended in PBS and cell density was determined using a hemocytometer. The cell density of each sample was adjusted to ~ $5x10^5$ neutrophils per sample. A variation of the C-peptide/Zn^{2+}/albumin complex was added to directly to the neutrophils for an incubation period of 1 hour at 37 ºC. GFP E. coli was then added to the solution and incubation continued for 30 minutes in a CO_2 incubator at 37 ºC. Samples were then centrifuged at 250g for 10 minutes, separating free from ingested bacteria. The cell pellet was resuspended in 200 µL of HBSS and transferred to a black 96 well plate. Quantification of GFP in the cell pellet was determined measuring fluorescence at excitation 488 and emission 510. A simplified workflow of the assay is shown in figure

2.14. Unshown determination of the selected excitation and emission were made using flowcytometry. Quantification of phagocytosis is shown in figure 2.15. There was no significant difference observed between the control group and the experimental group at n=2. However, looking at percent increase (seen in figure 2.16), there is indication of the 20 nM C-peptide/Zn^{2+} sample being slightly proficient in increasing phagocytosis. With increasing the sample size, we conclude that there would be a statistical difference between the control group and the 20 nM C-peptide/Zn^{2+} sample.

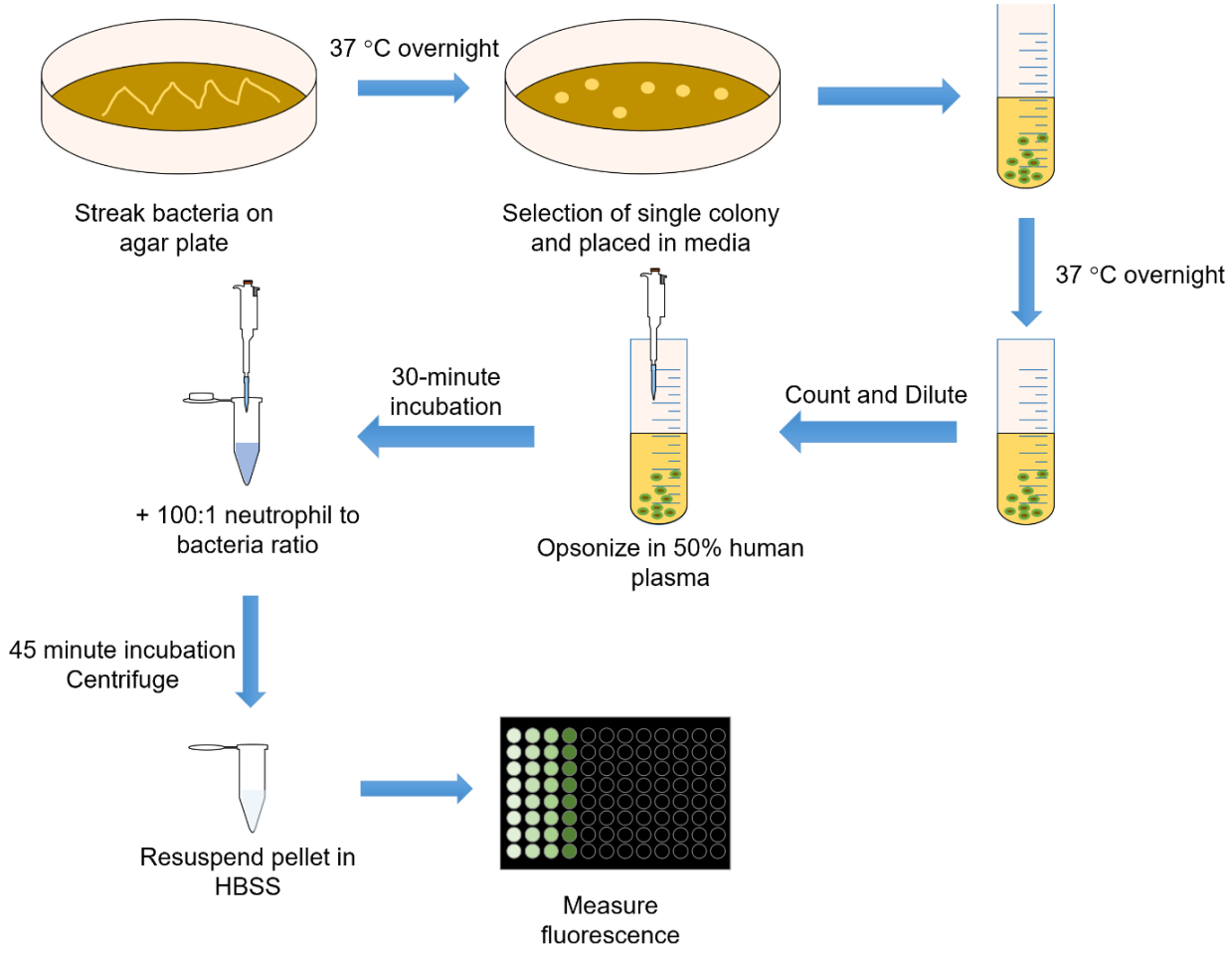

Figure 2.14: Procedure for phagocytosis assay. Bacteria from stock was scratched out on a fresh agar plate. A single colony of bacteria is transferred to the LB media where it will proliferate overnight. The cells were counted then optimized in 50% human serum. A concentrated solution of GFP E. coli was added to neutrophil samples previously stimulated with formulations of C-peptide, Zn^{2+}, and albumin at a 100:1 ratio. After incubation the samples were centrifuged, and the cell pellet was resuspended. Fluorescence was used to quantify the ingulfed bacteria using excitation 488 emission 510.

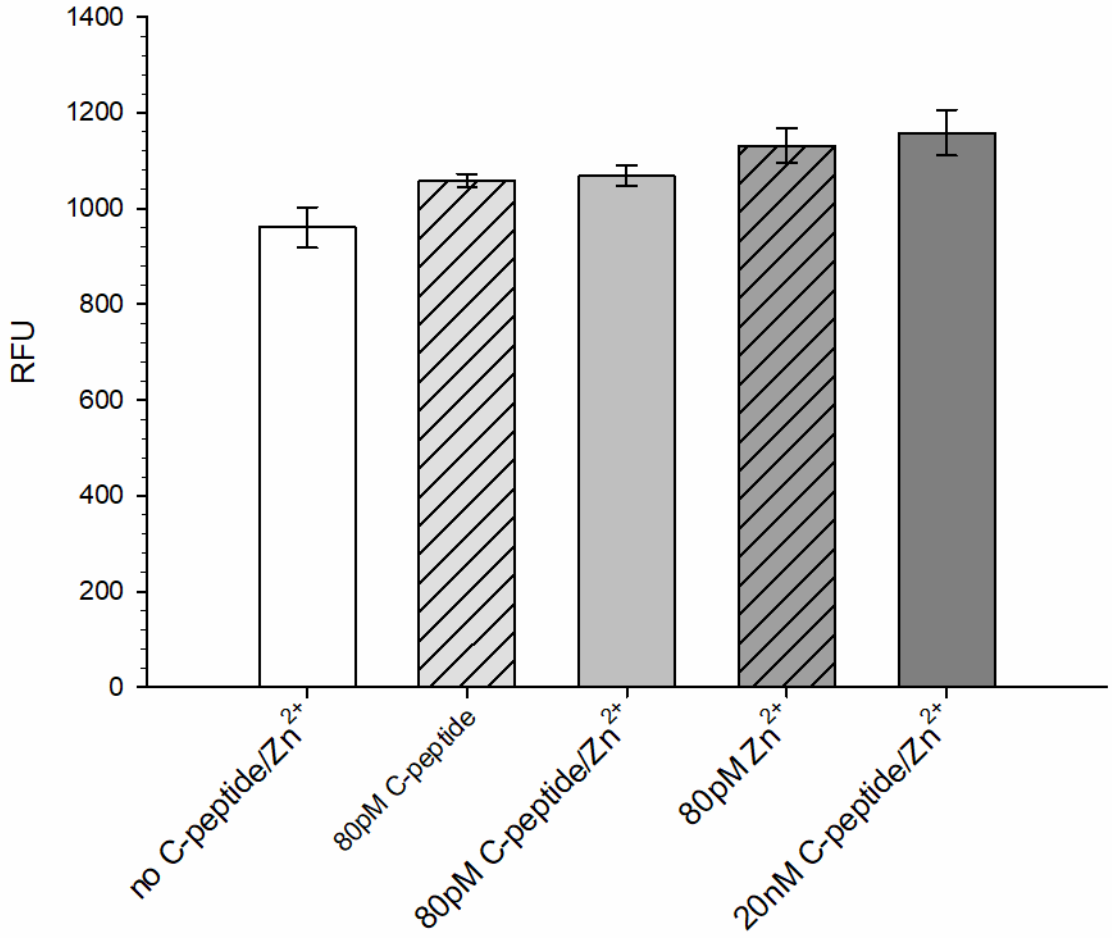

Figure 2.15: Quantification of phagocytosis. Following the workflow in figure 2.14, in each sample there was ~ 50,000 neutrophils to 5,000 GFP E. coli. Using fluorescence detection, no observed statistical difference was identified through the experimental groups to the control. (n=2) (error bars=SEM)

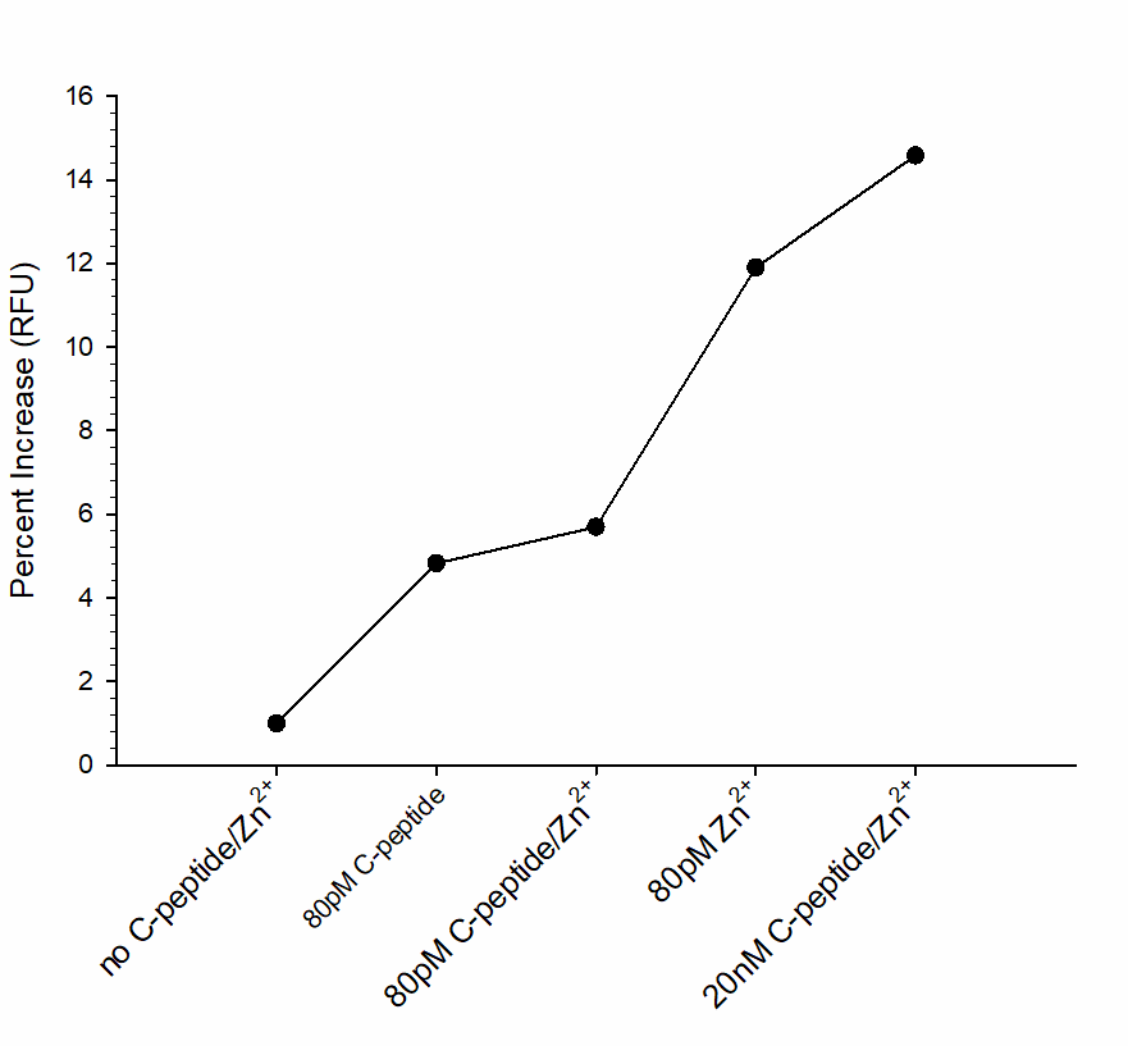

Figure 2.16: Percent increase of phagocytosis. Percent change compared to the control shows an approximate 14% increase in phagocytosis as measured by fluorescence. The percent change is indicative of a positive trend in the rate of phagocytosis of E. coli when variations of C-peptide and Zn^{2+} are added.

2.5 Discussion

Data presented shows evidence of a binding association of C-peptide to immune cells. While the value of molecules per cell reported is slightly higher than what was observed to human RBCs, specific binding of C-peptide to human neutrophils is at a

similar binding constant when you take in account differences in surface area.(*105, 106*) Data presented indicates albumin is necessary for C-peptide uptake in neutrophils, similar to what was observed in RBCs. In the case of Zn^{2+} binding, neutrophils bind more Zn^{2+} in the presence of C-peptide. T-cells show distinctive characteristics of C-peptide binding than neutrophils. C-peptide binding occurred at a much higher molecules per cell. Additionally, C-peptide binding was observed in the absence of albumin. It can be hypothesized that the heterogeneous surface receptors may non-specifically bind to the peptide. Since the C-peptide receptor has not been identified it is inconclusive how receptor variation among cell types changes binding quantities.

There is no difference seen in Zn^{2+} binding to T-cells when C-peptide is present or absent. Zn^{2+} is a known chemoattractant for immune cells, so it follows that Zn^{2+} would bind to the T-cells in the absence of C-peptide. Zn^{2+} homeostasis plays a pivotal role in immune cell function. A Zn^{2+} flux occurs seconds to minutes following immune cell activation by toll like receptors. The flux of Zn^{2+} acts as a secondary messenger in immune cell activation by initiating several signaling cascades similarly to a Ca^{2+} flux.(*57, 107*)

In a recent systematic review, it was reported that patients suffering from autoimmune diseases, including T1D, had less serum and plasma concentrations of Zn^{2+}.(*108*) Potentially, a decrease in Zn^{2+} concentration, coupled with dysregulation in Zn^{2+} binding due to a lack of C-peptide, could ultimately lead to irregular immune functions in individuals with T1D. Here we further show C-peptide with albumin, exhibits the ability to efficiently transport Zn^{2+} to a GLUT1 containing cell, as previously reported.(*95*)

C-peptide's anti-oxidant, anti-inflammatory, and anti-apoptotic effects have been described: the reduction of reactive oxygen species (ROS) through inhibition of nicotinamide adenine dinucleotide phosphate (NADPH) oxidase, inhibition of caspase-3, and slowing of apoptosis,(*109-111*) downregulation of nuclear factor nuclear factor κB (NF-κB) activity, decreased secretion of pro-inflammatory cytokines and chemokines,(*112*) and reduction of cellular adhesion molecules such as vascular endothelial growth factor (VEGF),(*113*) transforming growth factor β (TGF-β)(*114, 115*) and plasminogen activator inhibitor 1 (PAI-1).(*116*) However, these studies had a knowledge gap that the Spence group has solved, the need of Zn^{2+} and albumin in the experimental design. This is the first evidence that C-peptide directly interacts and binds to immune cells, and further confirms that albumin and Zn^{2+} are necessary for C-peptide to have a physiological effect. Increases in key early factors of immunity have been observed, contrary to the small sample sizes of similar C-peptide research. These increases in ROS activity, as well as phagocytosis by C-peptide and Zn^{2+} provide distinct evidence that this peptide has potential to provide insulin-like action in the bloodstream.

Overall, these *in vitro* results indicate that C-peptide may act as an immune system mediator, acting to increase the action of neutrophils and T-cells. Further research is necessary to further describe what C-peptide is doing bioenergetically and functionally to these immune cells. These findings further describe the potential role of C-peptide, as a biologically relevant molecule and a potential therapeutic. Acting on neutrophils, the first cell mediated line of defense in infections, and T-cells a powerhouse for the immune system, C-peptide administration may be key in ameliorating immunodeficiencies related to T1D complications.

REFERENCES

REFERENCES

1. Centers for Disease Control and Prevention. National Diabetes Statistics Report and its Burden in the United States. 2017.

2. Centers for Disease Control and Prevention, "National Diabetes Statistics Report," (U.S. Department of Health and Human Services, Atlanta, GA, 2020).

3. American Diabetes Association, Economic Costs of Diabetes in the U.S. in 2017. *Diabetes Care* **41**, 917-928 (2018).

4. M. Blair, Diabetes Mellitus Review. *Urol Nurs* **36**, 27-36 (2016).

5. L. Rosenfeld, Insulin: discovery and controversy. *Clin Chem* **48**, 2270-2288 (2002).

6. H. A. Keenan *et al.*, Residual insulin production and pancreatic ß-cell turnover after 50 years of diabetes: Joslin Medalist Study. *Diabetes* **59**, 2846-2853 (2010).

7. P. D. Brewer, E. N. Habtemichael, I. Romenskaia, C. C. Mastick, A. C. Coster, Insulin-regulated Glut4 translocation: membrane protein trafficking with six distinctive steps. *J Biol Chem* **289**, 17280-17298 (2014).

8. E. Karnieli *et al.*, Insulin-stimulated translocation of glucose transport systems in the isolated rat adipose cell. Time course, reversal, insulin concentration dependency, and relationship to glucose transport activity. *J Biol Chem* **256**, 4772-4777 (1981).

9. T. Kono, K. Suzuki, L. E. Dansey, F. W. Robinson, T. L. Blevins, Energy-dependent and protein synthesis-independent recycling of the insulin-sensitive glucose transport mechanism in fat cells. *J Biol Chem* **256**, 6400-6407 (1981).

10. American Diabetes Association, Abridged for Primary Care Providers. *Clin Diabetes* **39**, 14-43 (2021).

11. F. Ferri, *Diabetes mellitus. In: Ferri's Clinical Advisor*. (Elsevier, Philadelphia, PA, 2018).

12. Diabetes. Mayo Clinic. https://www.mayoclinic.org/diseasesconditions/diabetes/diagnosis-treatment/drc-20371451

13. A1C Test. Mayo Clinic. https://www.mayoclinic.org/tests-procedures/a1c-test/about/pac-20384643

14. L. Poretsky, *Principles of Diabetes Mellitus*. (Springer, New York, NY, ed. 2nd, 2010).

15. M. G. White, J. A. Shaw, R. Taylor, Type 2 Diabetes: The Pathologic Basis of Reversible β-Cell Dysfunction. *Diabetes Care* **39**, 2080-2088 (2016).

16. D. J. Mahoney, G. Parise, M. A. Tarnopolsky, Nutritional and exercise-based therapies in the treatment of mitochondrial disease. *Curr Opin Clin Nutr Metab Care* **5**, 619-629 (2002).

17. L. B. Rojas, M. B. Gomes, Metformin: an old but still the best treatment for type 2 diabetes. *Diabetol Metab Syndr* **5**, 6 (2013).

18. F. Porcellati *et al.*, Comparison of pharmacokinetics and dynamics of the long-acting insulin analogs glargine and detemir at steady state in type 1 diabetes: a double-blind, randomized, crossover study. *Diabetes Care* **30**, 2447-2452 (2007).

19. F. O. Magalhães *et al.*, Metformin increases blood flow and forearm glucose uptake in a group of non-obese type 2 diabetes patients. *Horm Metab Res* **38**, 513-517 (2006).

20. P. J. Grant, Beneficial effects of metformin on haemostasis and vascular function in man. *Diabetes Metab* **29**, 6S44-52 (2003).

21. A. Katsarou *et al.*, Type 1 diabetes mellitus. *Nat Rev Dis Primers* **3**, 17016 (2017).

22. P. Luppi, P. Drain, C-peptide antioxidant adaptive pathways in β cells and diabetes. *J Intern Med*, (2016).

23. M. A. Atkinson, G. S. Eisenbarth, A. W. Michels, Type 1 diabetes. *Lancet* **383**, 69-82 (2014).

24. M. B. Davidson, Insulin Therapy: A Personal Approach. *Clin Diabetes* **33**, 123-135 (2015).

25. P. Gkogkolou, M. Böhm, Advanced glycation end products: Key players in skin aging? *Dermatoendocrinol* **4**, 259-270 (2012).

26. Obstetrics, ACOG Practice Bulletin No. 201: Pregestational Diabetes Mellitus. *Obstet Gynecol* **132**, e228-e248 (2018).

27. J. M. Forbes, M. E. Cooper, Mechanisms of diabetic complications. *Physiol Rev* **93**, 137-188 (2013).

28. E. J. Barrett *et al.*, Diabetic Microvascular Disease: An Endocrine Society Scientific Statement. *J Clin Endocrinol Metab* **102**, 4343-4410 (2017).

29. D. M. Nathan, Long-term complications of diabetes mellitus. *N Engl J Med* **328**, 1676-1685 (1993).

30. Y. Zheng, M. He, N. Congdon, The worldwide epidemic of diabetic retinopathy. *Indian J Ophthalmol* **60**, 428-431 (2012).

31. R. N. Frank, Diabetic retinopathy. *N Engl J Med* **350**, 48-58 (2004).

32. F. Cunningham *et al.*, *Diabetes Miletus*. Williams Obstetrics (McGraw Hill, 2018).

33. "Chronic Kidney Disease in the United States," (US Department of Health and Human Services, Centers for Disease and Control and Prevention, Atlanta, GA, 2021).

34. M. Afkarian *et al.*, Clinical Manifestations of Kidney Disease Among US Adults With Diabetes, 1988-2014. *JAMA* **316**, 602-610 (2016).

35. K. Matoba *et al.*, Unraveling the Role of Inflammation in the Pathogenesis of Diabetic Kidney Disease. *Int J Mol Sci* **20**, (2019).

36. A. K. Maiti, Development of Biomarkers and Molecular Therapy Based on Inflammatory Genes in Diabetic Nephropathy. *Int J Mol Sci* **22**, (2021).

37. R. Pop-Busui *et al.*, Diabetic Neuropathy: A Position Statement by the American Diabetes Association. *Diabetes Care* **40**, 136-154 (2017).

38. P. Shillo *et al.*, Painful and Painless Diabetic Neuropathies: What Is the Difference? *Curr Diab Rep* **19**, 32 (2019).

39. S. E. Geerlings, A. I. Hoepelman, Immune dysfunction in patients with diabetes mellitus (DM). *FEMS Immunol Med Microbiol* **26**, 259-265 (1999).

40. A. Y. Peleg, T. Weerarathna, J. S. McCarthy, T. M. Davis, Common infections in diabetes: pathogenesis, management and relationship to glycaemic control. *Diabetes Metab Res Rev* **23**, 3-13 (2007).

41. T. C. Alba-Loureiro, S. M. Hirabara, J. R. Mendonça, R. Curi, T. C. Pithon-Curi, Diabetes causes marked changes in function and metabolism of rat neutrophils. *J Endocrinol* **188**, 295-303 (2006).

42. T. C. Alba-Loureiro *et al.*, Neutrophil function and metabolism in individuals with diabetes mellitus. *Braz J Med Biol Res* **40**, 1037-1044 (2007).

43. J. Casqueiro, C. Alves, Infections in patients with diabetes mellitus: A review of pathogenesis. *Indian J Endocrinol Metab* **16 Suppl 1**, S27-36 (2012).

44. J. I. Casey, B. J. Heeter, K. A. Klyshevich, Impaired response of lymphocytes of diabetic subjects to antigen of Staphylococcus aureus. *J Infect Dis* **136**, 495-501 (1977).

45. N. Joshi, G. M. Caputo, M. R. Weitekamp, A. W. Karchmer, Infections in patients with diabetes mellitus. *N Engl J Med* **341**, 1906-1912 (1999).

46. T. Mahlangu *et al.*, A systematic review on the functional role of Th1/Th2 cytokines in type 2 diabetes and related metabolic complications. *Cytokine* **126**, 154892 (2020).

47. M. Han *et al.*, Immunological Characteristics in Type 2 Diabetes Mellitus Among COVID-19 Patients. *Front Endocrinol (Lausanne)* **12**, 596518 (2021).

48. E. L. Pearce, E. J. Pearce, Metabolic pathways in immune cell activation and quiescence. *Immunity* **38**, 633-643 (2013).

49. N. J. Maciver *et al.*, Glucose metabolism in lymphocytes is a regulated process with significant effects on immune cell function and survival. *J Leukoc Biol* **84**, 949-957 (2008).

50. R. M. Loftus, D. K. Finlay, Immunometabolism: Cellular Metabolism Turns Immune Regulator. *J Biol Chem* **291**, 1-10 (2016).

51. R. P. Donnelly, D. K. Finlay, Glucose, glycolysis and lymphocyte responses. *Mol Immunol* **68**, 513-519 (2015).

52. C. B. Thompson, Rethinking the regulation of cellular metabolism. *Cold Spring Harb Symp Quant Biol* **76**, 23-29 (2011).

53. J. Jung, H. Zeng, T. Horng, Metabolism as a guiding force for immunity. *Nat Cell Biol* **21**, 85-93 (2019).

54. S. M. Houten, R. J. Wanders, A general introduction to the biochemistry of mitochondrial fatty acid β-oxidation. *J Inherit Metab Dis* **33**, 469-477 (2010).

55. L. Yang, S. Venneti, D. Nagrath, Glutaminolysis: A Hallmark of Cancer Metabolism. *Annu Rev Biomed Eng* **19**, 163-194 (2017).

56. B. J. van Raam, A. J. Verhoeven, T. W. Kuijpers, Mitochondria in neutrophil apoptosis. *Int J Hematol* **84**, 199-204 (2006).

57. N. Borregaard, T. Herlin, Energy metabolism of human neutrophils during phagocytosis. *J Clin Invest* **70**, 550-557 (1982).

58. D. C. Dale, L. Boxer, W. C. Liles, The phagocytes: neutrophils and monocytes. *Blood* **112**, 935-945 (2008).

59. M. V. Liberti, J. W. Locasale, The Warburg Effect: How Does it Benefit Cancer Cells? *Trends Biochem Sci* **41**, 211-218 (2016).

60. P. Chen *et al.*, Mitochondrial Apoptotic Pathway Is Activated by H2O2-Mediated Oxidative Stress in BmN-SWU1 Cells from Bombyx mori Ovary. *PLoS One* **10**, e0134694 (2015).

61. T. Finkel, Signal transduction by reactive oxygen species. *J Cell Biol* **194**, 7-15 (2011).

62. G. Fossati *et al.*, The mitochondrial network of human neutrophils: role in chemotaxis, phagocytosis, respiratory burst activation, and commitment to apoptosis. *J Immunol* **170**, 1964-1972 (2003).

63. R. I. K. Geltink, R. L. Kyle, E. L. Pearce, Unraveling the Complex Interplay Between T Cell Metabolism and Function. *Annu Rev Immunol* **36**, 461-488 (2018).

64. C. J. Fox, P. S. Hammerman, C. B. Thompson, Fuel feeds function: energy metabolism and the T-cell response. *Nat Rev Immunol* **5**, 844-852 (2005).

65. P. J. Murray, J. Rathmell, E. Pearce, SnapShot: Immunometabolism. *Cell Metab* **22**, 190-190.e191 (2015).

66. P. A. Kramer, S. Ravi, B. Chacko, M. S. Johnson, V. M. Darley-Usmar, A review of the mitochondrial and glycolytic metabolism in human platelets and leukocytes: implications for their use as bioenergetic biomarkers. *Redox Biol* **2**, 206-210 (2014).

67. G. J. van der Windt *et al.*, Mitochondrial respiratory capacity is a critical regulator of CD8+ T cell memory development. *Immunity* **36**, 68-78 (2012).

68. E. L. Pearce *et al.*, Enhancing CD8 T-cell memory by modulating fatty acid metabolism. *Nature* **460**, 103-107 (2009).

69. H. W. Davidson, (Pro)Insulin processing: a historical perspective. *Cell Biochem Biophys* **40**, 143-158 (2004).

70. J. C. Hutton, Insulin secretory granule biogenesis and the proinsulin-processing endopeptidases. *Diabetologia* **37 Suppl 2**, S48-56 (1994).

71. P. E. MacDonald, M. B. Wheeler, Voltage-dependent K(+) channels in pancreatic beta cells: role, regulation and potential as therapeutic targets. *Diabetologia* **46**, 1046-1062 (2003).

72. G. M. Martin, P. C. Chen, P. Devaraneni, S. L. Shyng, Pharmacological rescue of trafficking-impaired ATP-sensitive potassium channels. *Front Physiol* **4**, 386 (2013).

73. G. Wilcox, Insulin and insulin resistance. *Clin Biochem Rev* **26**, 19-39 (2005).

74. C. C. Quianzon, I. Cheikh, History of insulin. *J Community Hosp Intern Med Perspect* **2**, (2012).

75. F. S. Thong, P. J. Bilan, A. Klip, The Rab GTPase-activating protein AS160 integrates Akt, protein kinase C, and AMP-activated protein kinase signals regulating GLUT4 traffic. *Diabetes* **56**, 414-423 (2007).

76. Y. C. Long, Z. Cheng, K. D. Copps, M. F. White, Insulin receptor substrates Irs1 and Irs2 coordinate skeletal muscle growth and metabolism via the Akt and AMPK pathways. *Mol Cell Biol* **31**, 430-441 (2011).

77. K. R. Feingold *et al.* The Insulin Receptor and Its Signal Transduction Network. *Endotext.* (2000).

78. P. R. Shepherd, D. J. Withers, K. Siddle, Phosphoinositide 3-kinase: the key switch mechanism in insulin signalling. *Biochem J* **333 (Pt 3)**, 471-490 (1998).

79. V. Aguirre *et al.*, Phosphorylation of Ser307 in insulin receptor substrate-1 blocks interactions with the insulin receptor and inhibits insulin action. *J Biol Chem* **277**, 1531-1537 (2002).

80. P. D. Venieratos, G. I. Drossopoulou, K. D. Kapodistria, E. C. Tsilibary, P. V. Kitsiou, High glucose induces suppression of insulin signalling and apoptosis via upregulation of endogenous IL-1beta and suppressor of cytokine signalling-1 in mouse pancreatic beta cells. *Cell Signal* **22**, 791-800 (2010).

81. S. Kang *et al.*, Insulin can block apoptosis by decreasing oxidative stress via phosphatidylinositol 3-kinase- and extracellular signal-regulated protein kinase-dependent signaling pathways in HepG2 cells. *Eur J Endocrinol* **148**, 147-155 (2003).

82. D. F. Steiner, D. Cunningham, L. Spigelman, B. Aten, Insulin biosynthesis: evidence for a precursor. *Science* **157**, 697-700 (1967).

83. D. Brandenburg, History and diagnostic significance of C-peptide. *Exp Diabetes Res* **2008**, 576862 (2008).

84. F. Melani, A. H. Rubenstein, P. E. Oyer, D. F. Steiner, Identification of proinsulin and C-peptide in human serum by a specific immunoassay. *Proc Natl Acad Sci U S A* **67**, 148-155 (1970).

85. S. Sjöberg *et al.*, Residual insulin production, glycaemic control and prevalence of microvascular lesions and polyneuropathy in long-term type 1 (insulin-dependent) diabetes mellitus. *Diabetologia* **30**, 208-213 (1987).

86. C. W. Pinger, K. E. Entwistle, T. M. Bell, Y. Liu, D. M. Spence, C-Peptide replacement therapy in type 1 diabetes: are we in the trough of disillusionment? *Mol Biosyst* **13**, 1432-1437 (2017).

87. B. L. Johansson, B. Linde, J. Wahren, Effects of C-peptide on blood flow, capillary diffusion capacity and glucose utilization in the exercising forearm of type 1 (insulin-dependent) diabetic patients. *Diabetologia* **35**, 1151-1158 (1992).

88. J. Wahren, H. Foyt, M. Daniels, J. C. Arezzo, Long-Acting C-Peptide and Neuropathy in Type 1 Diabetes: A 12-Month Clinical Trial. *Diabetes Care* **39**, 596-602 (2016).

89. J. Wahren *et al.*, Role of C-peptide in human physiology. *Am J Physiol Endocrinol Metab* **278**, E759-768 (2000).

90. T. Forst *et al.*, Biological activity of C-peptide on the skin microcirculation in patients with insulin-dependent diabetes mellitus. *J Clin Invest* **101**, 2036-2041 (1998).

91. T. Forst, T. Kunt, Effects of C-peptide on microvascular blood flow and blood hemorheology. *Exp Diabesity Res* **5**, 51-64 (2004).

92. T. Kunt *et al.*, The effect of human proinsulin C-peptide on erythrocyte deformability in patients with Type I diabetes mellitus. *Diabetologia* **42**, 465-471 (1999).

93. M. Henriksson *et al.*, Specific binding of proinsulin C-peptide to intact and to detergent-solubilized human skin fibroblasts. *Biochem Biophys Res Commun* **280**, 423-427 (2001).

94. R. Rigler *et al.*, Specific binding of proinsulin C-peptide to human cell membranes. *Proc Natl Acad Sci U S A* **96**, 13318-13323 (1999).

95. Y. Liu, C. Chen, S. Summers, W. Medawala, D. M. Spence, C-peptide and zinc delivery to erythrocytes requires the presence of albumin: implications in diabetes explored with a 3D-printed fluidic device. *Integr Biol (Camb)* **7**, 534-543 (2015).

96. J. Carroll *et al.*, An altered oxidant defense system in red blood cells affects their ability to release nitric oxide-stimulating ATP. *Mol Biosyst* **2**, 305-311 (2006).

97. R. A. Cohen, Role of nitric oxide in diabetic complications. *Am J Ther* **12**, 499-502 (2005).

98. M. L. Ellsworth *et al.*, Erythrocytes: oxygen sensors and modulators of vascular tone. *Physiology (Bethesda)* **24**, 107-116 (2009).

99. R. S. Sprague *et al.*, Extracellular ATP signaling in the rabbit lung: erythrocytes as determinants of vascular resistance. *Am J Physiol Heart Circ Physiol* **285**, H693-700 (2003).

100. J. González-Alonso, D. B. Olsen, B. Saltin, Erythrocyte and the regulation of human skeletal muscle blood flow and oxygen delivery: role of circulating ATP. *Circ Res* **91**, 1046-1055 (2002).

101. J. A. Meyer, J. M. Froelich, G. E. Reid, W. K. Karunarathne, D. M. Spence, Metal-activated C-peptide facilitates glucose clearance and the release of a nitric oxide stimulus via the GLUT1 transporter. *Diabetologia* **51**, 175-182 (2008).

102. Z. Keltner *et al.*, Mass spectrometric characterization and activity of zinc-activated proinsulin C-peptide and C-peptide mutants. *Analyst* **135**, 278-288 (2010).

103. K. M. Piafsky, Disease-induced changes in the plasma binding of basic drugs. *Clin Pharmacokinet* **5**, 246-262 (1980).

104. C. Lennicke, J. Rahn, R. Lichtenfels, L. A. Wessjohann, B. Seliger, Hydrogen peroxide - production, fate and role in redox signaling of tumor cells. *Cell Commun Signal* **13**, 39 (2015).

105. Y. Liu, C. Chen, S. Summers, W. Medawala, D. M. Spence, C-peptide and zinc delivery to erythrocytes requires the presence of albumin: implications in diabetes explored with a 3D-printed fluidic device. *Integrative Biology*, (2015).

106. R. E. Roberts, M. B. Hallett, Neutrophil Cell Shape Change: Mechanism and Signalling during Cell Spreading and Phagocytosis. *Int J Mol Sci* **20**, (2019).

107. P. W. Marks, F. R. Maxfield, Transient increases in cytosolic free calcium appear to be required for the migration of adherent human neutrophils. *J Cell Biol* **110**, 43-52 (1990).

108. A. Sanna, D. Firinu, P. Zavattari, P. Valera, Zinc Status and Autoimmunity: A Systematic Review and Meta-Analysis. *Nutrients* **10**, (2018).

109. M. P. Bhatt, Y.-C. Lim, Y.-M. Kim, K.-S. Ha, C-peptide activates AMPKα and prevents ROS-mediated mitochondrial fission and endothelial apoptosis in diabetes. *Diabetes* **62**, 3851-3862 (2013).

110. V. Cifarelli *et al.*, C-peptide reduces high glucose-induced apoptosis of endothelial cells and decreases NAD(P)H-oxidase reactive oxygen species generation. *Diabetologia* **54**, 2702-2712 (2011).

111. M. P. Bhatt *et al.*, C-peptide prevents hyperglycemia-induced endothelial apoptosis through inhibition of reactive oxygen species–mediated transglutaminase 2 activation. *Diabetes* **62**, 243-253 (2013).

112. P. Luppi, V. Cifarelli, H. Tse, J. Piganelli, M. Trucco, Human C-peptide antagonises high glucose-induced endothelial dysfunction through the nuclear factor-κB pathway. *Diabetologia* **51**, 1534-1543 (2008).

113. Y.-C. Lim *et al.*, Prevention of VEGF-mediated microvascular permeability by C-peptide in diabetic mice. *Cardiovascular Research*, cvt238 (2013).

114. C. E. Hills, G. B. Willars, N. J. Brunskill, Proinsulin C-peptide antagonizes the profibrotic effects of TGF-β1 via up-regulation of retinoic acid and HGF-related signaling pathways. *Molecular Endocrinology* **24**, 822-831 (2010).

115. Y. Maezawa *et al.*, Influence of C-peptide on early glomerular changes in diabetic mice. *Diabetes/metabolism research and reviews* **22**, 313-322 (2006).

116. N. Lindenblatt, B. Braun, M. Menger, E. Klar, B. Vollmar, C-peptide exerts antithrombotic effects that are repressed by insulin in normal and diabetic mice. *Diabetologia* **49**, 792-800 (2006).

Chapter 3 - Blood Circulating Components Contributing to the Exacerbation of NETosis

3.1 Introduction into NETosis

Neutrophils are an innate immune cell typically regarded as the first to respond to foreign antigens. A specific defense mechanism of neutrophils can cause damage to self-tissue when unregulated. Neutrophil extracellular traps (NETosis) is a form of programmed cell death that neutrophils undergo in response to a pathogen.(*1*) Extracellular traps (ETosis) was first discovered in the late 2000s. These early studies identified the role of ETosis in innate immunity. Along with neutrophils, Etosis has been described in macrophages, eosinophils, dendritic cells, basophils, and more recently lymphocytes.(*2*) Brinkmann et al. reported regulation of infectious agents by neutrophil de-condensation, or the loosing of chromatin texture, and release of DNA, which was coined NETs.(*3*) Further verification promoted the release of nuclear DNA from NETs to NETosis. NETosis was initially characterized as a form of programmed cell death that could not be described as necrosis or apoptosis, due to the lack of caspase activity and receptor interacting serine/threonine kinase (RIPK) signaling, respectfully.(*1, 4, 5*) In 2018, the Nomenclature Committee on Cell Death recommended the term NETosis to be replaced by NET formation. The recommendation was in discovering that NET formation can occur without cell death.(*6*)

NETosis functions to stop the spread of pathogens in the extracellular space, or pathogens that resist phagosome degradation.(*7*) Formation of NETosis is induced by several stimuli such as: Infectious microorganisms (bacteria, viruses, and fungi), cytokines, damage associated molecular patterns (DAMPs), microcrystals (cholesterol, calcium carbonate). In vitro studies found success in inducing NETosis through phorbol ester (PMA) and ionophores (Calcimycin) stimulation.(*8, 9*) NETosis, shown in figure 3.1, is a release of chromatin modified with bactericidal peptides.(*10*) This “net” traps bacteria and degrades them from outside in. NETs are a 3D structure containing DNA, granular proteins (elastase, myeloperoxidase (MPO), cathepsin G, proteinase 3, lysozyme C, and antimicrobial peptides).(*11*) Subcellular regulation of NETosis has been investigated, however exact mechanisms remain unclear. Cases have been made that the initial collapse of the nuclear envelope and subsequent chromatin decondensation is dependent on reactive oxygen species (ROS), histone citrullination, and autophagy.(*12*) The proceeding section aims to explain cellular mechanisms that regulate NET formation.

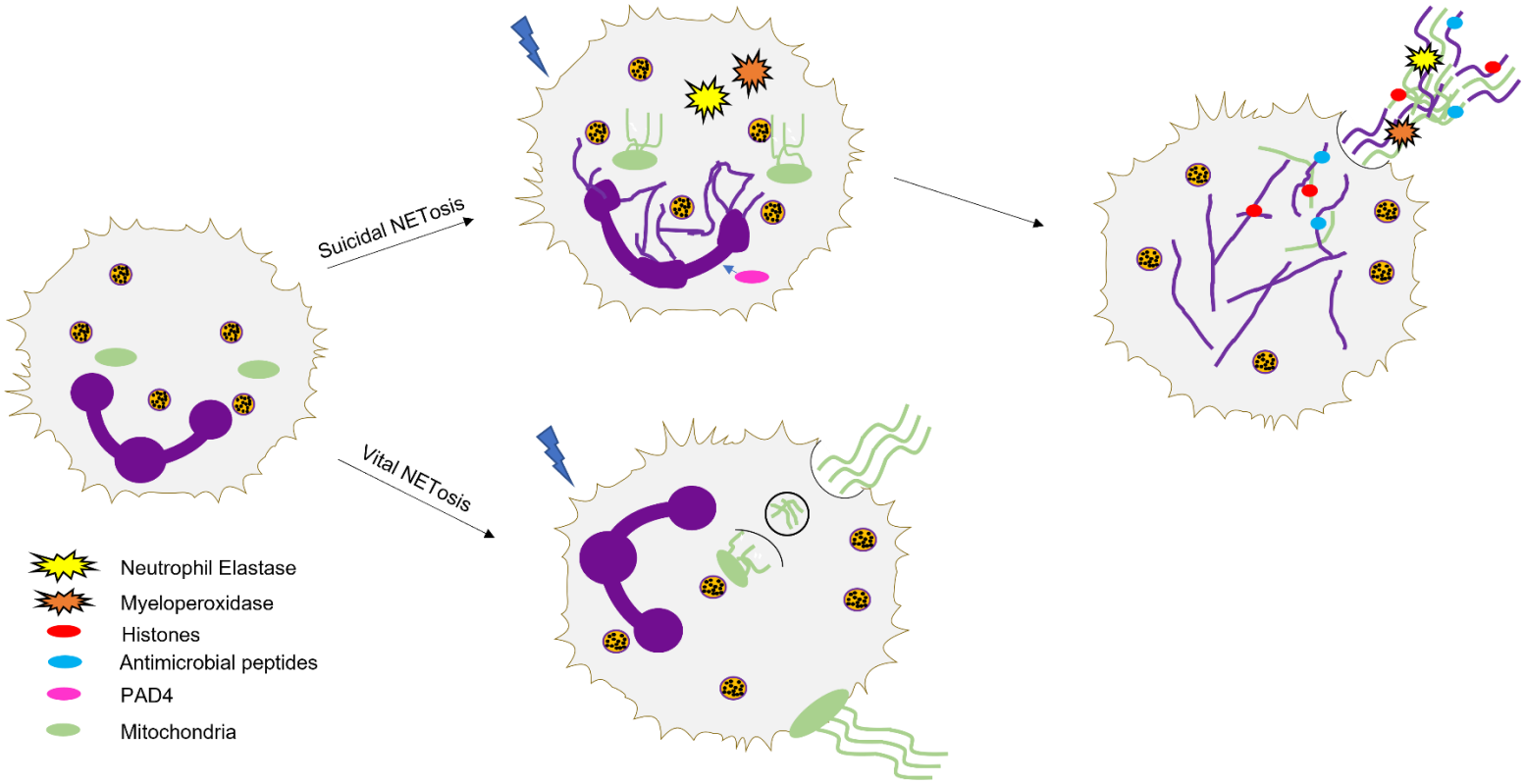

Figure 3.1: Graphical depiction of two forms of NETosis. Suicidal NETosis proceeds 3-8 hours post stimulation and leads to the cell death. Initial steps include chromosomal decondensation and the breakdown of the nuclear membrane, followed by DNA release from the mitochondria. Further, the cytoplasmic membrane disintegrates and the subsequent release of granular contents attatched to nuclear and mitochondrial DNA to the extracellular space. Vital NETosis occurs more rapidly, ~ 50-60 minutes post activation. Vital NETosis pathway allows neutrophils to maintain their viability, and antipathogenic functions such as phagocytosis. There have been two pathways of mitochondrial expulsion proposed. First, a release of mitochondrial DNA into the cytosol leading to translocation into vesicles. Second, fusion of the mitochondria to the plasma membrane, and the subsequent direct release of DNA into the extracellular space. In vivo stimuli inducing both pathways of NETosis include pathogens, cytokines, complement proteins, autoantibodies and activated platelets.

3.1.1 Regulation of NETosis

Autophagy is cellular function where cytosolic components are degraded and recycled through lysosomes as a way to maintain homeostasis.(*13, 14*) Broken down auto means “self” and phagy means “eat”. Vacuolization, or the process of forming vacuoles, is a process of autophagy that has been linked to NETosis.(*15*) Prior to intracellular chromatin decondensation and formation of “nets”, chronologically, vacuolization, and autophagy occurs.(*16*) Reportedly, PMA-induced Nicotinamide adenine dinucleotide phosphate (NADPH) oxidase is not affected by inhibition of autophagy, however, inhibition of autophagy prevents intracellular chromatin decondensation, which is essential for NETosis. The fate of neutrophils that have pharmacological inhibition of autophagy encompass cell death by classic apoptosis. In totality, apoptosis seems to run as a backup fate for neutrophils when NETosis is hindered by autophagy or NADPH oxidase malfunction.(*17*)

Dependency of ROS formation for NETosis execution has been investigated.(*17, 18*) However, a universal answer has yet to be concluded. Researchers have documented that inhibition of NADPH oxidase through redox metabolism indicated complete abolishment of “net” release. Additionally, neutrophils isolated from individuals with chronic granulomatous disease, who lack NADPH oxidase function, fail to release NETs when exposed to PMA. There have been reports of ROS activity playing a role in

the deactivation of caspase activity (evading apoptosis) through the production of NF-*κ*B, a regulator of antiapoptotic gene expression.(*19, 20*)

Citrullination is the process of converting positively charged arginine side chains into polar, neutrally charged citrulline side chains. One of the peptidylarginine deiminases (PAD) isomers has been shown to regulate the citrullination process. PAD4 is a known immune modulator that is heavily expressed in leukocytes, in particular neutrophils.(*21*) PAD4 leaves the cytoplasm and migrates to the nucleus where it will catalyze the citrullination process. Unique to the PAD4, compared to the isomers, is that PAD4 contains a nuclear localization signal. Inhibiting PAD4 activity with the use of Ca^{2+} ionophores ceased NET formation. Additionally, neutrophils obtained from PAD4 knockout mice were unable to produce NET formation.(*22*)

Recent reports have indicated that adenosine triphosphate (ATP) and pannexin1 (Panx1) contribute to NETosis.(*23*) This report identified the relevance of ATP in the formation of NETosis using several verification steps. Initially, the researchers investigated ATP alone and found no difference in SYTOX™ fluorescence. The addition of ionophore (calcimycin), a known stimulate of NETosis, along with ATP, resulted in no observed difference. However, when PMA and ATP were added, there was a significant increase in measured extracellular DNA. Utilizing neutrophils from Panx1 -/- mice, altered kinetics were observed. Sensitivity to calcimycin and PMA were both decreased, therefore resulting in decreased NETosis activity. The researchers observed when

exposed to A23187, the number of neutrophils undergoing DNA release was reduced. Secondly, in response to PMA, DNA release occurred with slower kinetics. In conjunction with observed decrease of ATP release in Panx1 -/- neutrophils, it was concluded that Panx1 accelerates the initial phases of NETosis leading to chromatin swelling through the release of ATP from intracellular to extracellular space.(*23*) Intracellular calcium (Ca^{2+}) levels as a result of purinergic stimulation have been identified as a regulator of NETosis as well. Purinergic signaling is involved in several intracellular signaling mechanisms, most of which involve Ca^{2+} translocation, which has been shown to have relevancy in NET formation.(*24, 25*) Both blocking the P2Y2 receptor or scavenging ATP decreased NETosis. Previous evidence showed the importance of P2Y2 signaling in NET formation in cattle neosporosis.(*26*) Further uridine diphosphate, a ligand of P2Y6 receptor, showed no response in “net” formation. Since the purinergic family has a diverse isomer pool, it is important that further investigation of purinergic receptors role in “net” formation is conducted.(*23, 27, 28*)

Mentioned earlier, neutrophil mitochondria do not function to produce ATP. Neutrophils utilize the Warburg effect, which interestingly, is a key component of NETosis. Neutrophil mitochondria maintain membrane potential through the glycerol-3-phosphate shuttle. This shuttle mechanism allows influx of electrons by the complex III of the electron transport chain via glycolysis.(*29*) Neutrophil mitochondria contribute to redox balance and the promotion of flux through the glycolytic pathway while avoiding apoptosis commitment.(*11*) The reliance on the Warburg effect may describe the ability of a neutrophil to remain viable through NETosis. Glycolysis may be a key factor in NETosis

since it has been described that NETosis is NADPH oxidase-dependent.(*30*) The proceeding sections will outline how disruption in NETosis have been linked to disease pathogeneses.

3.1.2 NETosis Dysfunction

At a brief glance this microbicidal function may seem highly regulated and beneficial, however, several studies have linked NETosis to several pathogenesis. Several infectious diseases and non-infectious diseases have had NETosis linked to pathogenesis.(*10*) Since the NETs contain DNA, it must be cleared immediately, in the case that DNA is not cleared, an immune response proceeds. The inflammatory response to extracellular DNA as well as other NET components have been linked to several autoimmune diseases, such as systemic lupus erythematosus and rheumatoid arthritis and various cardiovascular diseases.(*31-33*)

In the autoimmune disease lupus, components of released “nets” serve as specific autoantibodies. It was reported that individuals with lupus have impaired “net” clearance, allowing for cytotoxic and immune stimulation.(*34*) Specifically, in lupus nephritis (a kidney disorder), biopsies indicated autoantibodies specifically targeted NET components. The anti-“net” autoantibodies disallows DNase1, a DNA cleaving enzyme, to perform it’s degradative function.(*35*) Lack of “net” removal plays a potential role in the autoimmune cycle by the increased chance of “net” autoantigens being presented to

autoreactive B cells. Similar mechanisms have been identified in vasculitis. NETosis was shown to be dysregulated in vasculitis (blood vessel inflammation, and higher levels of circulating “net” components were observed in individuals in remission compared to healthy counterparts.(*36*)

In rheumatoid arthritis (RA), a method to diagnose is quantifying anti-citrullinated protein antibodies. Specifically, citrullinated fibrinogen is one of the commonly used markers.(*37*) Autoantibodies to citrullinated fibrinogen are specific to RA at 98%.(*38, 39*) Citrullination is the conversion of arginine to citrulline, which is not one of the 20 amino acids encoded by DNA.(*40*) Due to the foreign aspect of citrulline, autoantibodies to the citrullinated fibrinogen are produced leading to an autoimmune response.(*41, 42*) While the exact mechanism is not confirmed, PAD isomers have been identified as a potential player in this conversion.(*43*) Since hepatocytes, the producer of fibrinogen, do not contain PAD, a secondary source for citrullination was investigated. In the synovial fluid of individuals with RA, there is an increase of both free PAD4, a “net” component.(*42-44*)

Microbes have created defenses to elude NETs by stimulating neutrophil receptors which suppress neutrophil activation, allowing free bacterial replication and prolonged infection. Survival mechanisms used by microbes, viruses, and fungi include direct cell to cell interactions and enzymatic reaction. The surface capsule of streptococci, a common bacteria involved in sepsis, contains sialic acid which engage sialic acid binding immunoglobulin like receptors (Siglecs) on leukocytes.(*45*) The binding cascade leads to

a decrease in ROS formation and subsequent “net” formation.(*46*) In addition to cell mediated evasion, streptococci release β-protein that binds to Siglec-5.(*47*) Similarly, pneumonia causing bacteria P. aeruginosa, can encapsulate themselves with host sialyated glycoproteins, suppressing the efficacy of antimicrobial mediators associated with NETosis.(*48*) A secondary pathway of downregulating ROS production is through the litigation of signal inhibitory receptor on leukocytes 1 (SIRL1). This pathway is regularly used by the common bacteria S. aureus.(*49*) A common characteristic of bacteria is the formation of biofilms, the aggregation of one or more bacterium, forming a thick wall as a form of defense.(*50*) Bacterial biofilms are a target of NETosis activation.(*51*) While NETosis is successful in degradation of the film, reports show that fungal biofilms are elusive to NET degradation, through increased resistance and attenuation of NET formation.(*52*) Lastly, enzymatic reactions have been reported to slow or completely abolish NETosis efficiency. Examples include pathogen release of immunosuppressive cytokines and the release of DNase enzymes such as endonucleases and nucleosidases.(*45, 53*)

3.1.3 Dysregulated NETosis Treatment

Although NETosis is an important biological function, any dysregulation can be detrimental to the body as NETosis has been implicated in several pathologies.(*54*) This section will focus on potential therapeutics (anti-inflammatory, antithrombotic, NADPH/ROS inhibitors, nucleases) related to NETosis mitigation (see table 3.1). The

extracellular pH at the site of infection may play a role in “net” function.(*55*) As neutrophils leave circulation (pH ~7.4) to the site of tissue infection, neutrophils experience a change in extracellular pH. When NADPH oxidase is stimulated, there is a decrease in the intracellular pH due a large generation of H^+ ions.(*56, 57*) NETosis related enzymes such as elastase, proteinase, cathepsins, and MPO have both a basic (7.5-8.5) and an acidic (4.7-6.0) pH preference.(*58*) Decreasing the pH in vitro decreases “net” formation by disrupting MPO formation.(*59*) At higher pH “net” bound proteases were more effective in cleaving histones. Clinically, pH alterations through substances like sodium bicarbonate and TRIS base may play an important role in regulating pH.(*55*)

Table 3.1: Potential ant- NETosis therapeutics and mode of action.

ANTI-NET THERAPEUTICS	PHARMACOLOGICAL COMPOUNDS	TARGET	MODE OF ACTION
ANTI-INFLAMMATORY	Aspirin	Cyclooxygenase enzyme (COX),	Inhibits thromboxane A2 inhibiting platelets
ANTI-THROMBOSIS	Thrombomodulin	Protein C	Anticoagulant, decrease NETosis
ROS/NADPH INHIBITORS	Metformin	mTORC1, AMPK	Inhibits ROS production, inactivates PKC NADPH pathway
ANTI-THROMBOSIS	Recombinant DNase	DNA matrixes	Anticoagulant, inhibit NETosis
COMPOUNDS	Probiotics	PKC pathway	Decrease ROS production

Acetylsalicylic acid (aspirin) is a non-steroidal drug which manages inflammation through antithrombotic and anti-inflammatory mechanisms. Aspirin prevents arterial thrombosis through the inhibition of thromboxane A2, which activates platelet formation, platelet aggregation and subsequent vasoconstriction. Platelets regulate homeostasis, more specifically, initiating an innate immune response by interacting with recognize pathogen-associated molecular patterns (PAMPS).(*60, 61*) NETosis has been shown to be directly activated by platelets. Examples of platelet mediated NETosis include activation of P selectin expression and glycoprotein 1bα.(*62-64*) With this background knowledge, research looked to identify the effectiveness to indirectly decrease NETosis through decreasing platelet activation. Aspirin supplementation as a antiplatelet therapy, was investigated in acute lung injury, and transplantation.(*65-67*) The individual studies found that aspirin, is a successful therapy in preventing “net” formation, and subsequently increased the survival rate in mouse models, respectively.

Efforts to mediate NETosis using antithrombosis properties have been observed. Thrombosis is a formation of a blood clot caused by inflammatory mediators during injury, or prescription drug use.(*68*) Thrombin-thrombomodulin complex induces protein C, which initiates anticoagulant pathway synthesis.(*68, 69*) To combat, protein cofactor thrombomodulin modifies the substrate thrombin on endothelial cell surface. Excessive amounts of circulating DNA, which NETosis secretes, can influence thrombus formation by creating a scaffold for blood components to bind.(*70, 71*) This immune-thrombosis induced coagulation seems to contribute to excess hypercoagulability in pathologies.(*72*) In vitro, one study looked at supplementing thrombomodulin on a neutrophil/platelet co-

culture.(*73*) After the addition of lipopolysaccharide (LPS) for platelet activation, a decrease in coagulation, and subsequent decrease in abnormal NET formation was observed.

Metformin is a commonly prescribed drug which aims to regulate high blood glucose levels, typically in type 2 diabetes.(*74*) Metformin acts through stimulating AMP-activated protein kinase (AMPK). AMPK inhibits rapamycin, which subsequently activate glucose and fatty acid uptake, increasing cell metabolism when cellular energy is low. Rapamycin regulates cell metabolism through inhibition of mitochondrial ROS production. (*75*) As stated previously, ROS production is necessary for the function of NETosis. Inhibition of ROS indicates metformin may be a potential drug in not only ameliorating autoimmune disease, but specifically regulating NETosis. In vitro, studies have shown that metformin is effective in negating NETosis.(*76*) Interestingly, the same group reported no difference in NETosis when inducing glucose control with insulin. In a secondary pathway, metformin also has been shown to inhibit protein kinase c (PKC) translocation and NADPH oxidase activation, both of which a necessary for NETosis formation.(*77*)

Lastly, therapeutics disrupting extracellular or already secreted “nets” have been investigated. Pulmozyme, a recombinant human DNase that selectively cleaves DNA, has been used to cleave DNA in the mucus of individuals with cystic fibrosis, leading to decreased viscosity in the lungs.(*78*) It has been reported that DNases are effective in

disrupting immune complexes and DNA bound nucleoprotein, alleviating the severity of symptoms seen in systemic lupus and lupus nephritis.(*79*) Recombinant DNase has been evaluated on “net” formations, resulting in the reduction of NETosis and also reduced neutrophil recruitment.(*80, 81*) Several types of studies investigating decreasing neutrophil function and NETosis have been investigated. However, many of these treatment options may have adverse effects since they are not specific to NETosis, many treatments have been previously cleared for treatment of other diseases and/or disorders.

3.2 Introduction to Multiple Sclerosis

Multiple sclerosis (MS) is a debilitating autoimmune disease that affects the central nervous system.(*82*) The National Multiple Sclerosis Society estimated more than 2 million individuals are diagnosed worldwide, and over 700,000 in the United States. The annual total cost of MS research and treatment is estimated to be $12 billion. MS is more prevalent in the northern hemisphere and increasingly affects the female gender.(*82-85*) This progressive disease is produced by the destruction of myelin sheath which covers axons. The function of myelin sheath is facilitating nerve signal propagation by directing electric current along the axon. The production of myelin sheath come from oligodendrocytes. Demyelination leads to irregular signaling between neurons rendering the body unable to perform vital bodily functions.(*86*) Loss of blood brain barrier (BBB) integrity have also been reported in individuals with MS, contributing to both physical and cognitive decline.(*87*) One of the known physiologic features of many MS patients is the

breakdown of the BBB.(*87*) The destruction of the myelin has been shown to be due to the infiltration of autoreactive T-cells through the leaky BBB seen in figure 3.2.

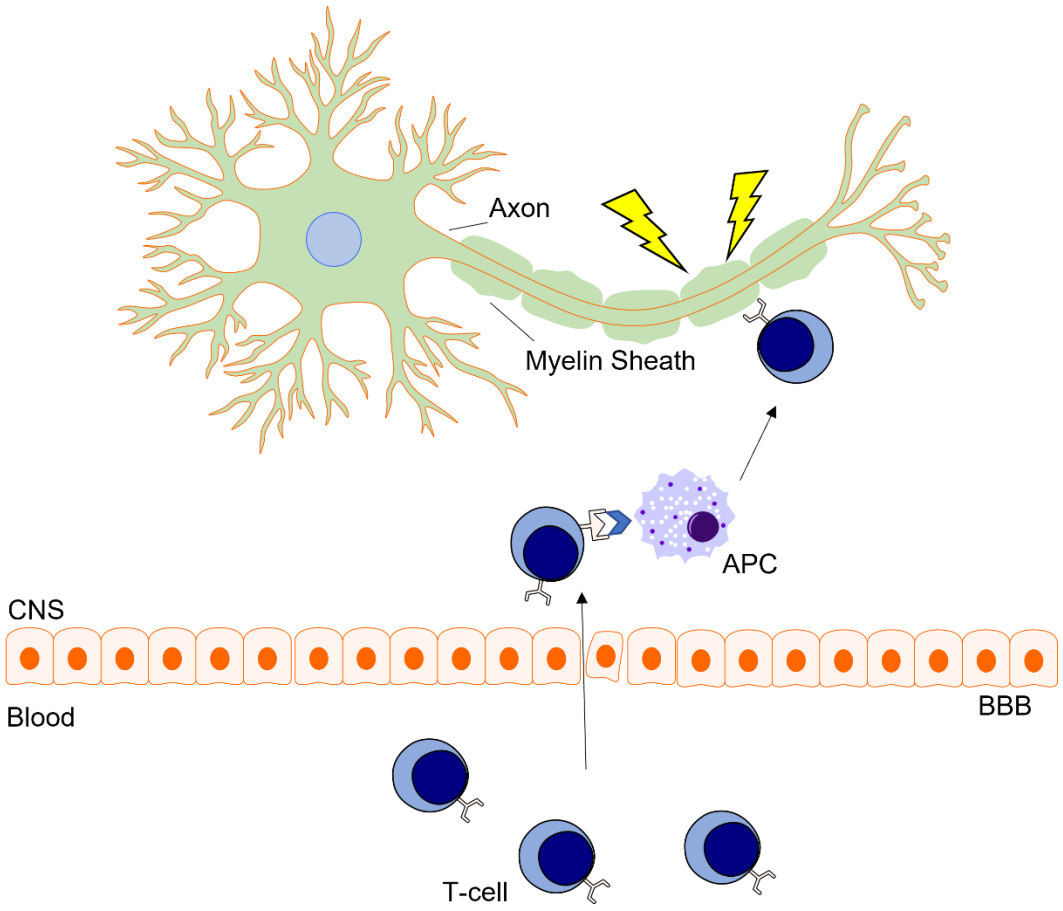

Figure 3.2: Cartoon depiction of MS pathology. Auto reactive T-cells migrate through a damaged blood brain barrier. The infultrated T-cells are then presented an autoantigen from an antigen presenting cell, activating the T-cell against self mylin. The autroreactive T-cell then migrates to the axon covered in mylin, selectively destroying mylin, leading to subsequent symptoms related to MS.

MS severity is often unpredictable, and intensity can vary. Common symptoms include numbness and fatigue, and in more severe cases, vision loss, paralysis and deficient brain function can occur due to demyelination. Symptoms of MS can also include

bladder, balance, sexual health, hearing, taste, and breathing dysfunctions.(*88*) Vision complications are the most common symptom of MS. Hyper inflammation in the optic nerve, brain stem, and cranial nerve are hypothesized to be precursors to three common vision complications of MS: Optic neuritis, nystagmus, diplopia. Individuals with MS often experience numbing, tingling, and burning in their extremities. Fatigue and muscular atrophy can be categorized as intermittent, reoccurring, and constant chronic. Chronic pain and muscle spasms symptoms are observed, possibly due to neuropathic pain, and include Lhermitte's sign, paroxysmal spasms, and trigeminal neuralgia. Lastly, cognitive dysfunctions for individuals with MS include memory loss, shortened attention span, and concentration issues.

3.2.1 Diagnosis of MS

The cause of MS has not been concluded. Evidence has been collected showing a combination of genetic and environmental factors contributing to the onset of MS. Evidence for environmental factors include Epstein-Barr virus (EBV), smoking, and vitamin D deficiency.(*89, 90*) Genetically, family recurrence has been shown to be as high as 15%, with twins showing a higher diagnosis rate.(*91, 92*) The X chromosome has been indicated in having a direct role in autoimmunity.(*93*) Using the mouse model for autoimmune encephalomyelitis (EAE), which has similar symptoms and characteristics to MS, two X chromosomes increase susceptibility to disease pathology.(*94*) Additionally, the X chromosome rendered inactive in women is much higher than men, potentially

contributing to the disproportional rate of MS in women compared to men.(*95*) The most convincing genetic factor related to the onset of MS is the human leukocyte allele (HLA) HLA-DRB1*1501.(*96*)

The first attack of MS is defined as clinically isolated syndrome (CIS). The common characteristics of CIS include detectable conditions such as optic neuritis, spinal cord involvement through cerebral spinal fluid (CSF), brainstem syndrome, and hemispheric involvement. Secondly, radiological isolated syndrome (RIS) involves inflammatory demyelination and lesions measured through magnetic resonance imaging (MRI), which suggests a patient has MS patients even if they never experienced symptoms. Diagnosis is directly related to the clinical subtypes of MS, defined in 1996.(*97*) Examples include relapse remitting, secondary progressive, primary progressive, and progressive relapsing shown in figure 3.3. Relapse remitting is the most common form of diagnosed MS utilizing the CIS criteria, representing 80-85% of total CIS diagnosis. Once MS is in a remitting state, new symptoms do not occur, making the progression of the disease difficult to track, and increases the chance of increased amplified when an individual leaves the remittent state.

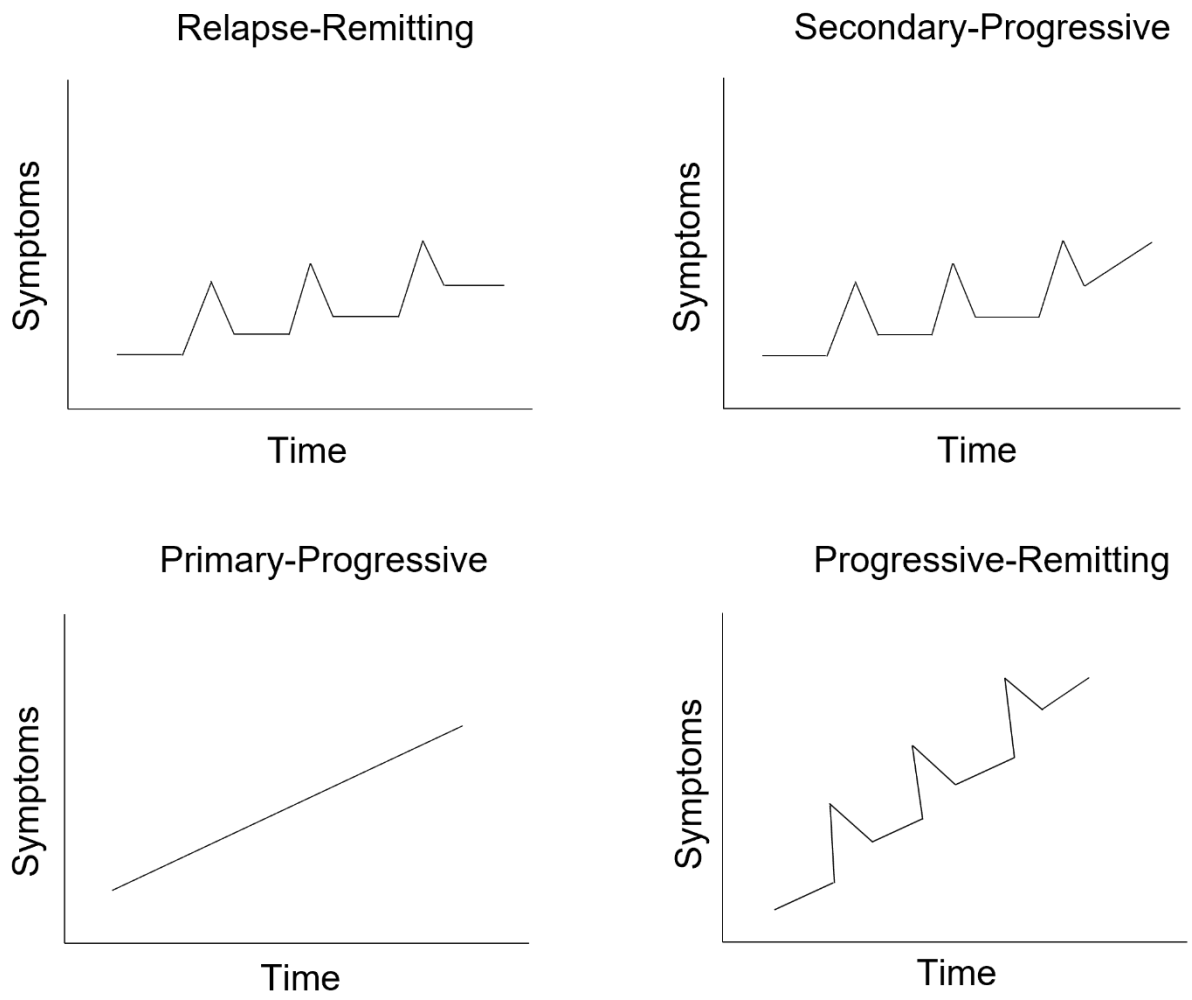

Figure 3.3: Illustration of the four types of MS progression. Relapsing-remitting MS consists of relapses followed by periods of symptomatic remission. Secondary-progressive MS presents as relapse-remitting, however, unexpected progression occurs. Primary-progressive MS consists of a steady increase in symptoms without remission, and progressive-remitting MS consists of a steady increase in MS symptoms with periodic relapses.

When left untreated, an individual moves to a secondary progressive state. Symptoms seen in the secondary progressive state include a drastic increase in neurological dysfunction and increased disability. Over time, the relapse and progression fluctuation are on a trend for increased disability, and individuals typically do not see

decreases in symptoms as compared to individuals in the relapse remitting state. Estimated 15% of MS diagnosis occurs in the primary progressive, where individuals do not experience any relapses or remissions. Lastly, progressive remission is a blend of relapse remission and primary progressive, effecting ~5% of MS patients.

Due to the lack of specific markers for MS, clinical diagnosis relies on family history and neurological examinations. However, reliance on these criteria has led to several cases of misdiagnosis.(*98*) Further, clinical symptoms of MS can be similar to several other infections and diseases, making misdiagnosis common.(*99*) Initial diagnosis using the McDonald criteria, a set of guidelines for diagnosis of MS, is often described as unreliable.(*100*) Sequentially, misdiagnosis coupled with a two year time frame for diagnosis, can be detrimental to the individuals health, as prolonged symptoms with no treatment can lead to irreversible disease progression.(*99*)

3.3 The Role of MS and ATP

The role of ATP in MS has been previously investigated. ATP works through purinergic receptor signaling, found on many cell types, including the myelin sheath producing oligodendrocytes and the immune cell responsible for autoreactivity to myelin sheath, T-cells. Further, ATP stimulation to purinergic receptor P2X, a Ca^{2+} permeable purinergic receptor, reversibly allows Ca^{2+} influx.(*101*) Prolonged stimulation of ATP can lead to irreversible opening of the Ca^{2+} channel, causing cytotoxic effects, which has been

described in oligodendrocytes.(*102, 103*) The irreversible cation channel and subsequent cytotoxic effects produce similar lesions described in MS. When stimulated by ATP, T-cells undergo several Ca^{2+} dependent cellular changes, ultimately activating them. Overactive T-cells are observed in MS, presenting autoimmune characteristics.(*104*) Matute et al. reported that in the MS mouse model EAE, treatment with P2X7 antagonist significantly reduced demyelination and decreased MS associated neurological symptoms.(*105*) In the same study, western blot analysis showed elevated levels of P2X7 protein levels in the axons of individuals with MS. Interestingly, when P2X7 -/- mice were treated to become EAE mice, symptoms of these mice were significantly decreased, even though activated T-cells were observed infiltrating through the BBB.(*101*)

Knowing the relationship between ATP and various cell types, it was logical to investigate the role of ATP in MS. The source of the extracellular ATP had been elusive until a discovery in the Spence lab. We investigated ATP release by both healthy control RBC and MS RBC as shown in figure 3.4.(*106*) It was found that RBCs obtained from individuals with MS secreted significantly more ATP when subjected to flow induced shear stress.(*106*) Due to the previous reports that NETosis plays a potential role in MS via dysregulated NET formation(*107*), and having previously described the association between ATP and NETosis, we aim to link a correlation between RBC-derived ATP and NETosis dysregulation in MS pathology.

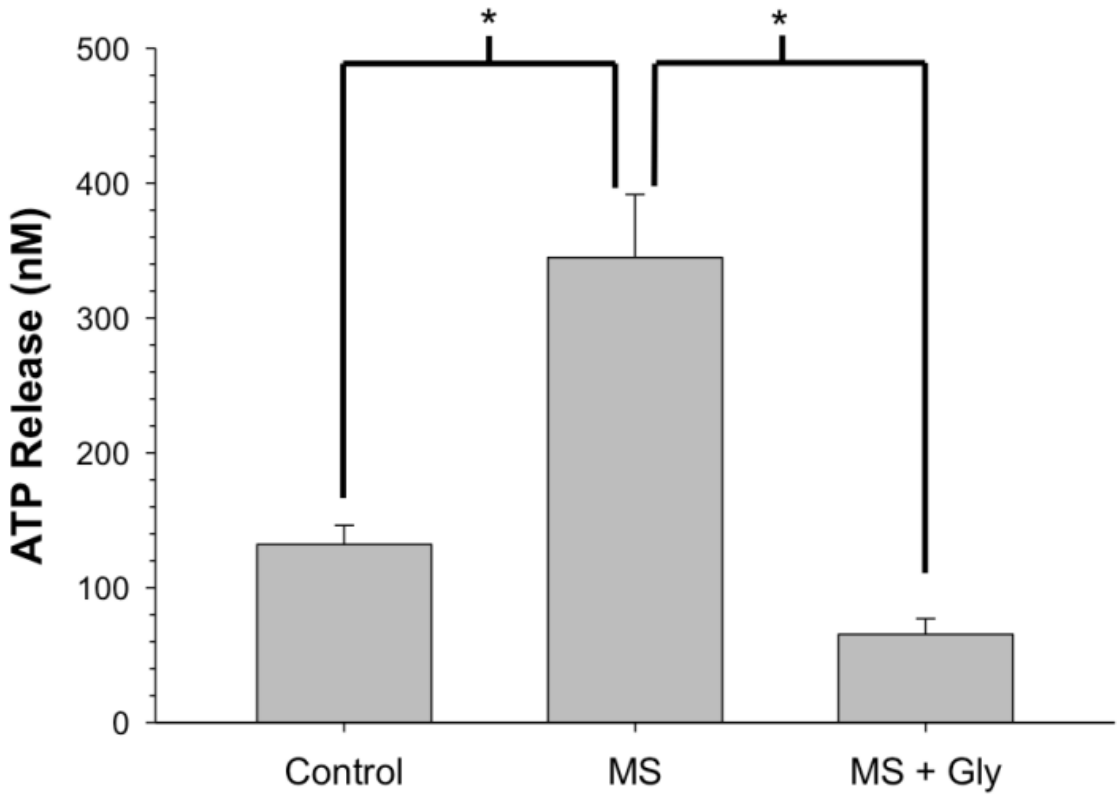

Figure 3.4: ATP release from RBCs of MS patients. The results of this study showed ATP release from the RBCs of MS patients was 345 ± 47 nM, where release from healthy controls was 132 ± 14 nM. When the RBCs of the MS patients were incubated with a Cystic fibrosis transmembrane conductance regulator (CFTR) inhibitor, glybenclamide, the ATP release is decreased to 65 ± 11 nM, below the amount of the healthy controls. Concluding that the increase in ATP release of the flowing RBCs of MS patients is not a result of RBC lysis. (error=SEM, for n = 19 MS patients, 10 healthy controls and 12 glybenclamide inhibitions. The asterisk represents $p < 0.001$)

3.4 Experimental

In the proceeding section, experiments are laid out to further investigate the role of extracellular molecules and proteins on the exacerbation of NETosis. Extracellular measurements of neutrophil elastase, a heavily concentrated enzyme in secreted NETs were used to determine rate of NETosis. Here, we investigated extracellular factors such

as ATP, albumin, Zn^{2+}, and C-peptide on NETosis. Further, we introduced pyridoxalphosphate-6-azophenyl-2',4'-disulfonic acid (PPAD) tetrasodium salt, a known purinergic receptor antagonist, and interferon β (IFN-β), a frequently used therapeutic for MS, to investigate NETosis mediation.

3.4.1 Isolation and Collection of Neutrophils

MS whole blood was collected into citrate tubes at Memorial Healthcare (Owosso, MI) and transported on ice. The whole blood was transferred to a 15 mL conical tube and a cell isolation kit was employed (EasySep Direct, STEMCELL Technologies, Vancouver, BC, Canada) to negatively separate the neutrophils from whole blood. Unwanted cells were bound by antibodies specific to their surface receptors, respectfully, a secondary antibody conjugated with a magnetic bead binds the initial antibody, and are magnetically separated from neutrophils. The neutrophils were resuspended in ~3 mL of PBS and used during experiments within 6 hours of isolation. Cell counts were determined using an automatic cell counter (Thermo Scientific, San Jose, CA, USA). The concentrated neutrophil suspension typically contained ~5 million cells/mL. In all cases, samples used during an analysis contained ~1 million neutrophils/mL.

3.4.2 C-peptide Binding to MS Neutrophils

MS whole blood samples were generously gifted from Memorial Healthcare's Institute for Neuroscience**.** Neutrophils were isolated by the neutrophil isolation methods described (section 3.4.1) and added to a known concentration of C-peptide in a buffered physiological salt solution (PSS; in mM: 4.7 KCl, 2.0 $CaCl_2$, 140.5 NaCl, 12 $MgSO_4$, 21.0 tris(hydroxymethyl) aminomethane (Invitrogen, Carlsbad, CA), 5.5 dextrose (Sigma Aldrich, St. Louis, MO), and 0.5% bovine serum albumin (Sigma Aldrich), final pH 7.40). C-peptide binding was investigated in the PSS buffer and a second version of PSS that was albumin-free. For studies involving C-peptide binding to immune cells in the presence of Zn^{2+}, the Zn^{2+} was mixed with C-peptide in a 1:1 molar ratio in 25 µL of distilled and deionized water (DDW, 18.0 MΩ). After 3 minutes, 375 mL of PSS or albumin-free PSS were added to the C-peptide/Zn^{2+} mixture, followed immediately by the addition of 100 µL of the concentrated/purified immune cells, and samples were incubated at 37 °C for 2 hours. Following incubation, samples were centrifuged and the amount of C-peptide remaining in the supernatant was determined using a commercially available C-peptide enzyme linked immunosorbent assay (ELISA) kit (Alpco, Salem, NH). Shown in figure 3.5, the absolute amount of C-peptide bound to neutrophils was determined by subtracting the moles of C-peptide measured in the supernatant from the number of moles initially added to the cell sample.

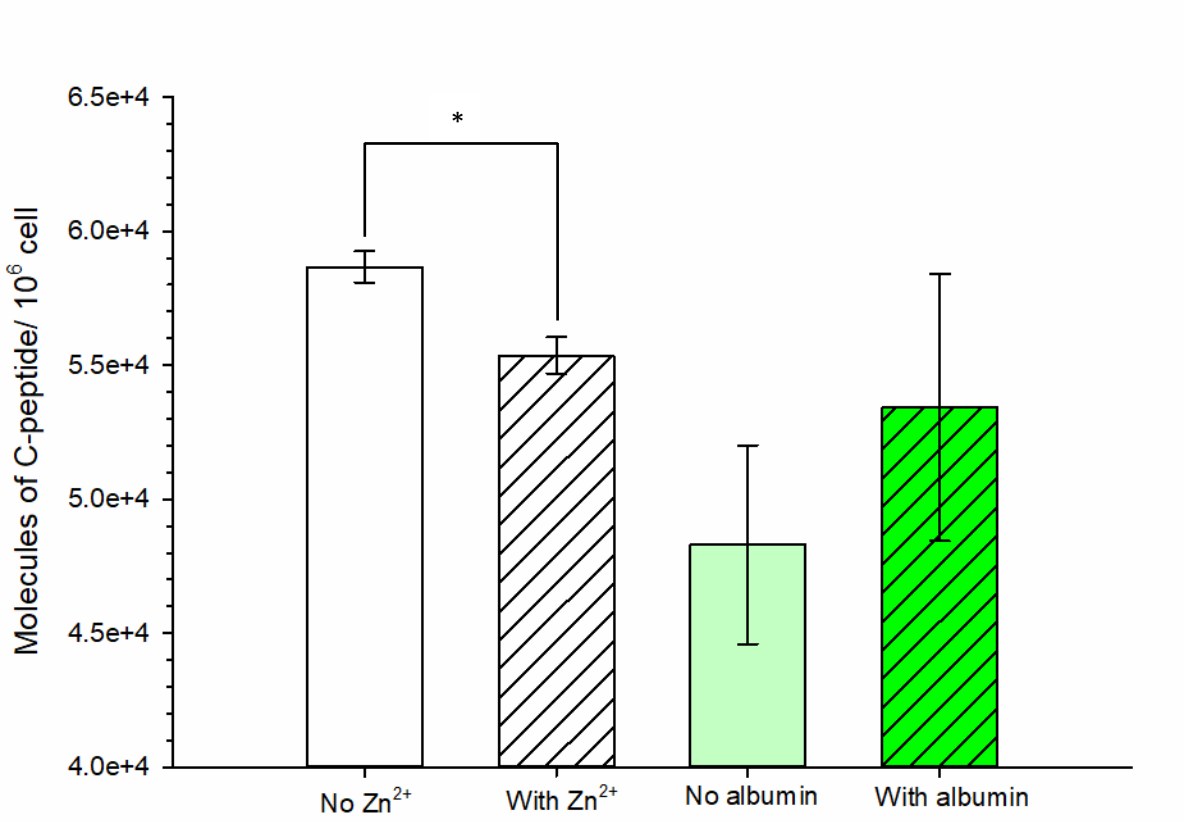

Figure 3.5: Determination of C-peptide binding to MS Neutrophils. Isolated MS neutrophils were exposed to different buffer formulations to determine changes in C-peptide binding. Stripped bars represent the removal of Zn^{2+} (white) and albumin (green) respectively. There was a statistical difference in the amount of C-peptide binding in the absence of Zn^{2+} when compared to the samples with Zn^{2+}. There was no statistical difference between the albumin groups. (error=SEM, n≥4 $p<0.05$)

The base PSS buffer for C-peptide binding studies contains albumin. Omitting albumin from the buffer results in a decrease in C-peptide binding to ~ $4.8x10^4$ molecules/10^6 cells, however, within error, there is no statistical difference when albumin is present (~ $5.4x10^4$ molecules/10^6 cells). When Zn^{2+} was removed from the solution, 5.9 $x10^4$ C-peptide molecules/10^6 cells was observed. Interestingly, when Zn2+ was present, we saw a significant decrease in the amount of C-peptide uptake to MS neutrophils (~ 5.5 $x10^4$ molecules/10^6 cells).

3.4.3 Radioisotopic Determination of Zn^{2+} Delivery to MS Neutrophils

MS neutrophils were isolated by negative separation as described above. Radioisotopic Zn^{2+}($^{65}Zn^{2+}$) was utilized to determine Zn^{2+} delivery to the neutrophils. A known concentration of $^{65}Zn^{2+}$ was added to a known cell density in PSS containing a concentration of C-peptide in a 1:1 ratio with $^{65}Zn^{2+}$. Samples were incubated at 37°C for 2 hours. After incubation, samples were centrifuged at 250 *g* for 10 minutes, and the amount of Zn^{2+} remaining in the supernatant was determined using gamma radiation emission counting (PerkinElmer Inc., Waltham, MA, USA). The centrifuged pellet was also analyzed to verify that $^{65}Zn^{2+}$ was not lost during the experiment. The moles of $^{65}Zn^{2+}$ bound to the immune cells were determined by subtracting the moles of $^{65}Zn^{2+}$ left in the supernatant from the $^{65}Zn^{2+}$ moles originally added to the sample (shown in figure 3.6).

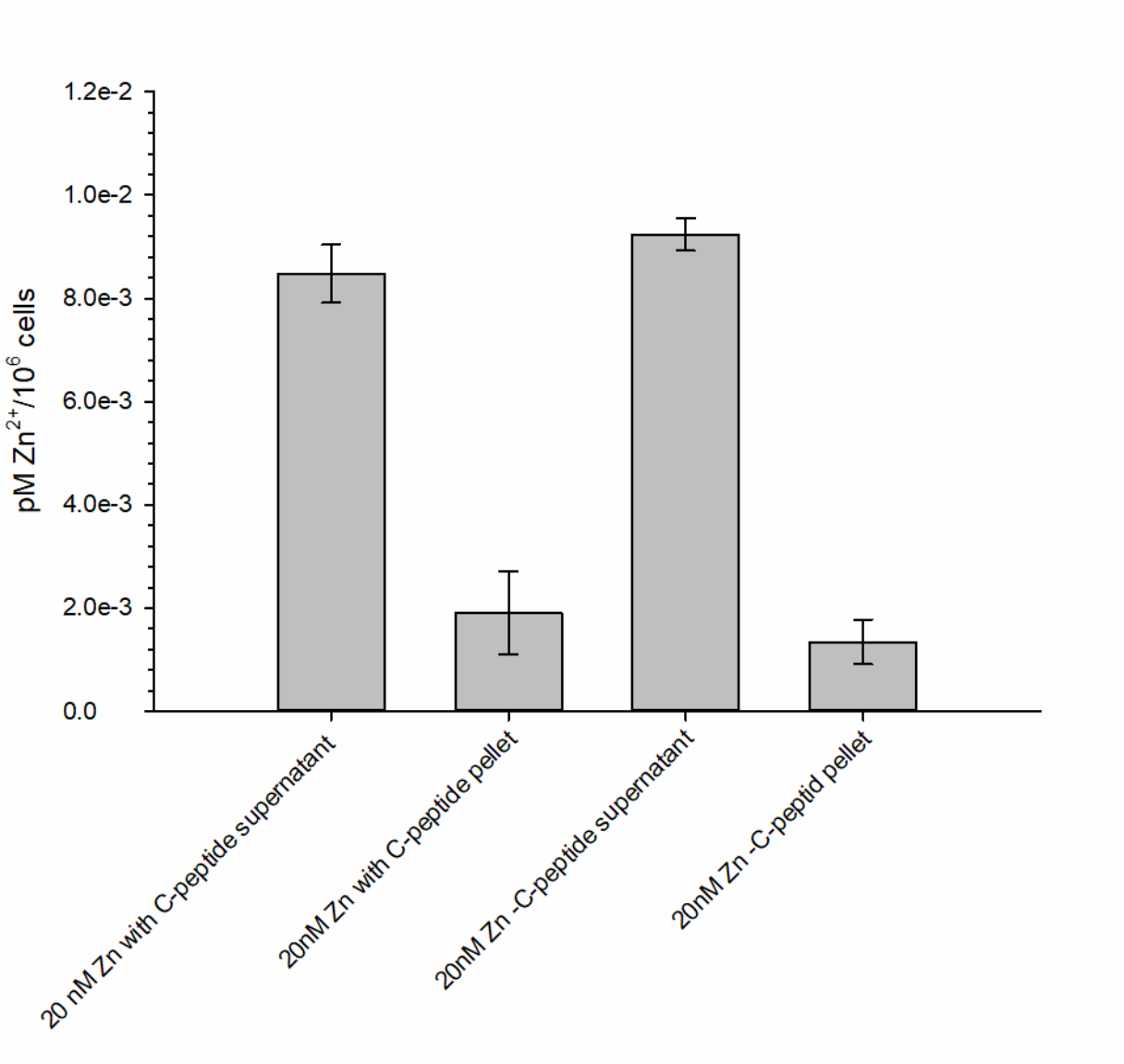

Figure 3.6: Zn^{2+} uptake by MS neutrophils. Zn^{2+} binding in the presence or absence of C-peptide. The presence or absence of C-peptide showed no statistically significant difference of Zn^{2+} uptake in MS neutrophils. (error=SEM, n=3)

Zn^{2+} binding to MS neutrophils was unaffected by the presence or absence of C-peptide. We observed uptake of ~ $2x10^3$ pM $Zn^{2+}/10^6$ cells in the presence of C-peptide. Further, when C-peptide was removed, ~ $1.7x10^3$ pM $Zn^{2+}/10^6$ cells was observed. Although not statistically significant, a decrease was observed, furthering the previously

reported statement that C-peptide binding may lead to downstream effects, increasing Zn^{2+} uptake. These early experiments aimed to investigate differences in C-peptide and Zn^{2+} binding from what was observed in control studies in chapter 2. The next section will investigate the experimental design and findings on blood circulating components effects on NETosis.

3.4.4 NETosis Measurement

Neutrophils were isolated as described in section 3.5.1. After isolating the neutrophils from whole blood, the cell pellet was resuspended in NETosis buffer (RPMI 1640, 1mM CaCl2, 5g BSA. Cayman Chemical, Ann Arbor, MI). 100 µL of phorbol 12-myristate 13-acetate (PMA) in NETosis buffer was added to 800 µL of neutrophils at a cell density of ~$8x10^5$ in a 24 well plate. 25 µL of 20nM Zn2+ was then added, followed by 75 µL of NETosis buffer, bringing the total volume to 1 mL. A NETosis assay kit (Cayman Chemical) was used to quantify DNA bound elastase in each sample, which is directly proportionate to NETosis activity, see figure 3.7.

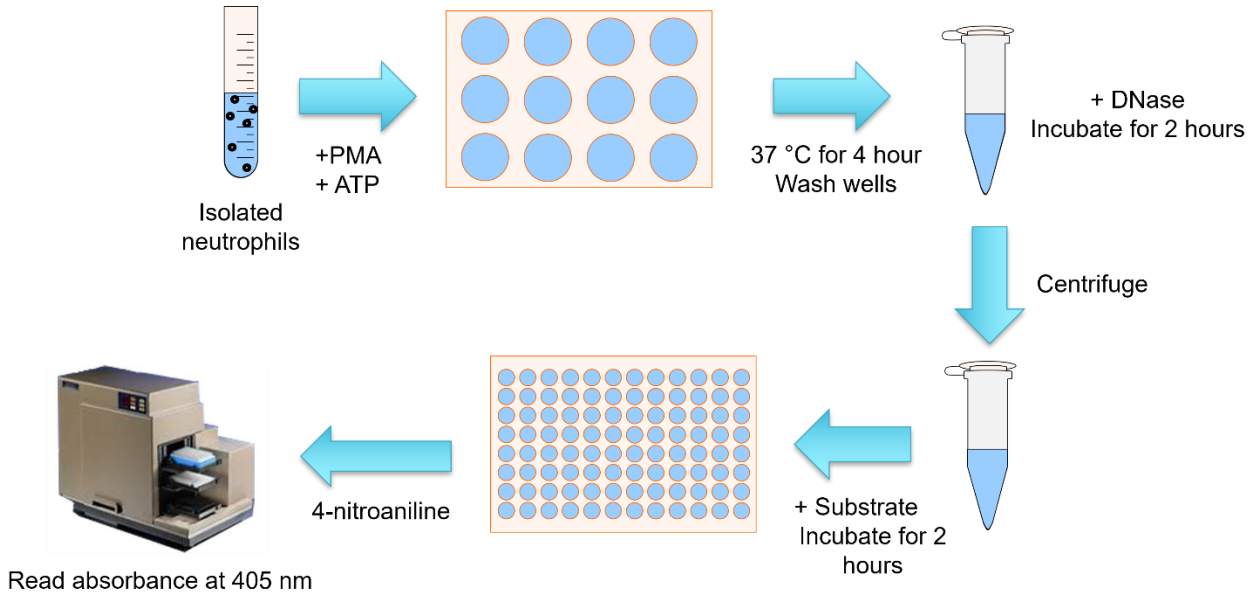

Figure 3.7: NETosis determination workflow. Quantification of NETosis is indirectly measured with elastase detection. Isolated neutrophils incubate in a 24 well plate, in media containing Ca^{2+} and albumin, along with the respected treatment formulation based on the experiment. After 4 hours, the wells are washed with media, removing substances unassociated with the NET, including non-bound elastase. A DNase is then added to digest NET DNA for 2 hours, freeing NETosis associated elastase. The samples are transferred to a centrifuge tube containing EDTA to stop any further reactions, then centrifuged. The supernatant is then transferred to a substrate containing 96 well plate, where the substrate is selectively cleaved by elastase to yield 4-nitroaniline that absorbs light at 405 nm.

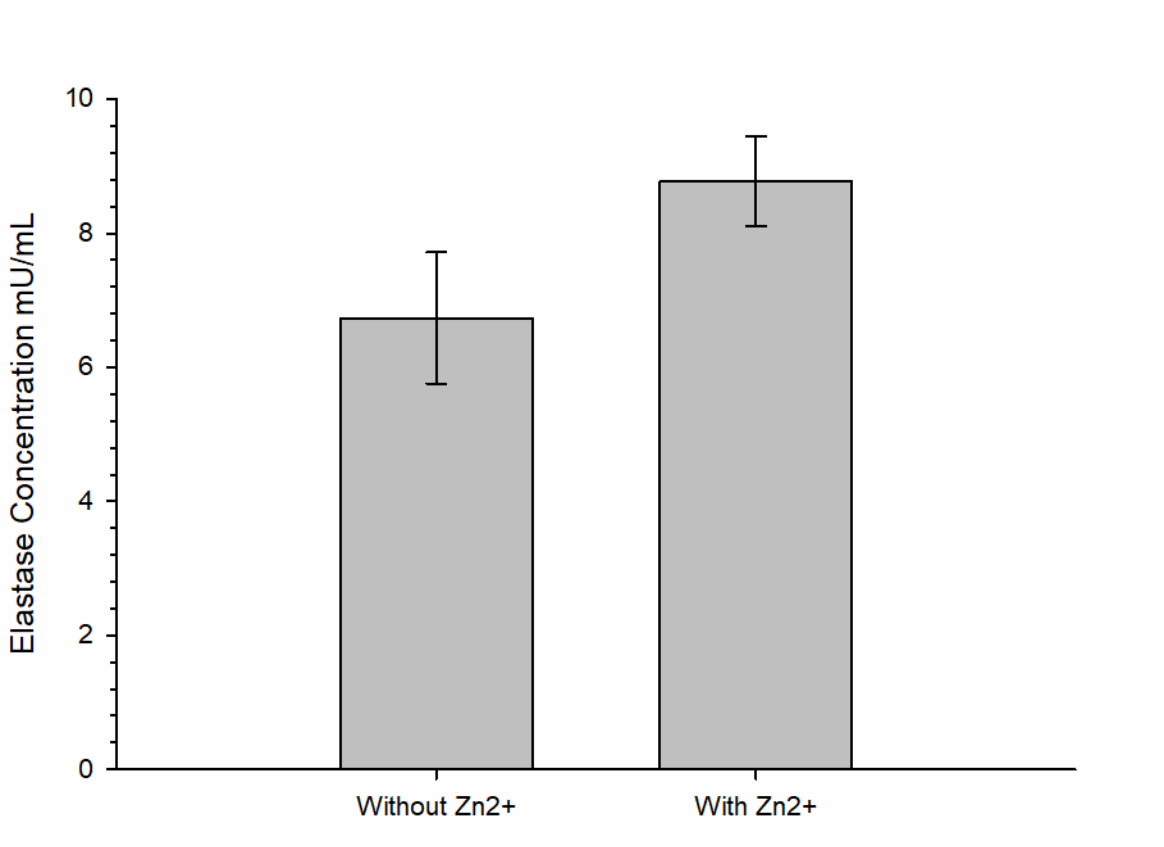

Figure 3.8: Determination of Zn^{2+} on NETosis. Following PMA stimulation, exogenous addition of 20nM Zn^{2+} we observe an increase in elastase release, however, not statistically significant. (error=SEM n=3)

For the first time, we reported the effects of Zn^{2+} on the rate of NETosis induction (see figure 3.8). In the presence of Zn^{2+}, measured elastase concentration is ~ 7 mU/mL, while the presence of Zn^{2+} increases elastase concentration by ~ 2 mU/mL at ~ 9 mU/mL. Although studies have indicated a relationship between ATP and NETosis, no research has looked at ATP released from RBCs on NETosis, a more biologically relevant model. The next section outlines the experimental set up to obtain ATP from RBCs.

3.4.5 Isolation and Collection of RBCs

Healthy control whole blood was collected into citrate tubes. MS whole blood was collected into citrate tubes from Memorial Healthcare (Owosso, MI) and transported on ice. These tubes were centrifuged at 500 g for 10 minutes and the plasma and buffy coat were removed. RBCs were washed 3 times with either PSS or albumin-free PSS, and the supernatant was aspirated off. The hematocrit was determined using a StatSpin® CritSpin™ microhematocrit centrifuge and hematocrit reader (Beckman Coulter, Brea, CA) and used in making 7% RBC samples.

3.4.6 ATP release from RBCs

A 7% RBC solution was incubated with 20 nM C-peptide and Zn^{2+}. These were incubated at 37 °C for 2 hours, inverting every 30 minutes. The samples were then centrifuged at 500 g for 5 minutes, and the supernatant was removed. Luciferin luciferase was prepared by diluting 5 mg of potassium luciferin (Gold Bio, St. Louis, MO) with 5 mL of 18 MΩ DDI H_2O. The 5 mL solution of potassium luciferin was then added to 100 mg of firefly lantern extract (Sigma Aldrich) and placed into a 15 mL tube. Standards were prepared by dissolving approximately 30 mg of ATP (Sigma Aldrich) into a 100 mL volumetric flask. 1 mL of this ATP solution was then added to another volumetric flask, and used to prepare all standards (160, 80, 40, 20, 10 nM). Using a FlexStation-3 spectrophotometer, ATP was quantified by adding 150 μL of each sample or standard to a 96-well black plate. At time zero, 15 μL of luciferin luciferase was added to the well and

mixed through pipetting. At 20 seconds, luminescence was measured. This was repeated 3 additional times per sample and averaged to determine the concentration ATP release. The ATP solution was added to the experimental design as shown in figure 3.7, we determined the impact of RBC derived ATP from both control RBCs and MS RBCs on NET formation (figure 3.9).

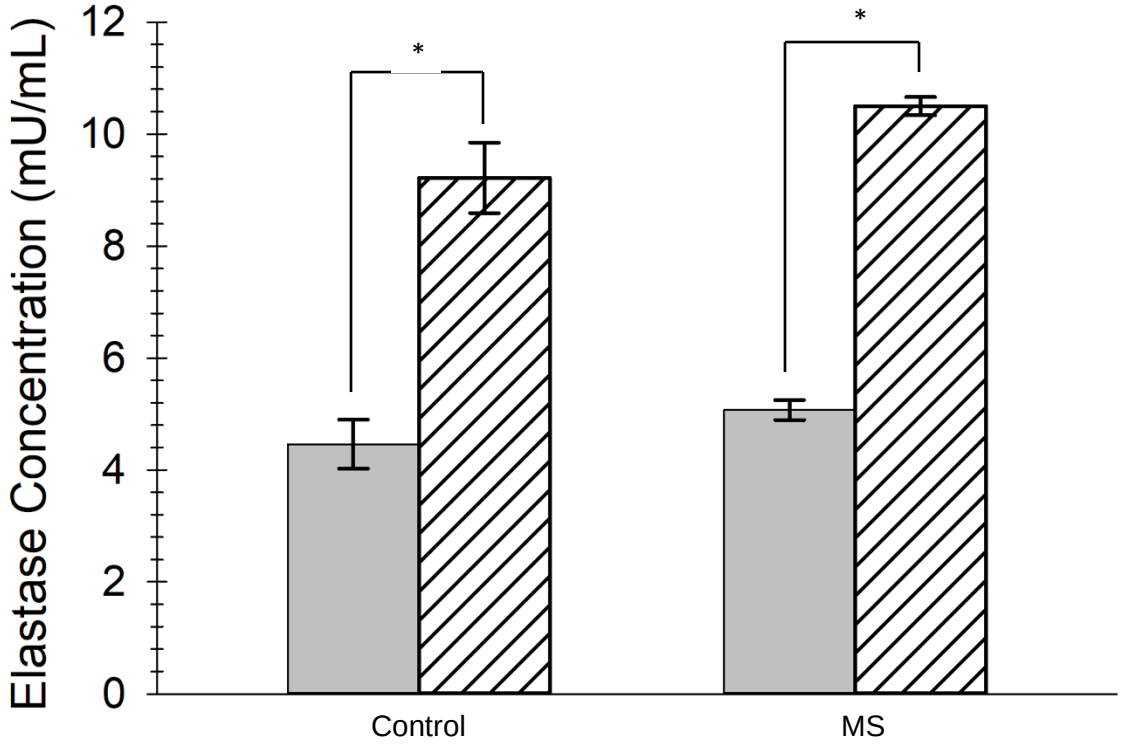

Figure 3.9: RBC derived ATP exacerbation of NETosis. Left cluster indicates a significant increase in NET formation when comparing no ATP (grey) and with ATP derived from control RBCs (striped). When observing ATP derived from MS RBCs in the right cluster (striped), we report a significant increase in NET formation when comparing no ATP (grey). Interestingly, we see a significant increase in NET formation when ATP is derived from RBCs from individuals with MS, indicating a potential source of NETosis dysregulation seen in MS. (error=SEM, n=3 (control) n=2 (MS) $p<0.05$)

We can conclude that ATP derived from RBCs has an exacerbator effect on NETosis. Investigating no addition of RBC ATP, 4.46 +/- .44 elastase concentration was measured compared to 9.22 +/- .63 when ATP from RBCs was added. However, we measured 10.5 +/- .16 elastase secretion when ATP from MS RBCs was added to control neutrophils, showing first time evidence of RBCs as a source for the high circulatory levels of ATP seen in MS, and subsequent downstream over stimulation of neutrophils, causing dysregulated NETosis.

To conclude our efforts on ATP inducing NETosis, we chemically blocked the ATP purinergic receptor with pyridoxal phosphate-6-azo (benzene-2,4-disulfonic acid) tetrasodium salt (PPAD) (see figure 3.10). PPAD is a non-selective purinergic receptor 2 antagonist.(*108*) It was observed that there was no statistical difference in elastase concentration when PPADs were present or absent, however, using the concentration of 10 µM may not have been sufficient enough as we do see a slight decrease in elastase. Lastly, we investigated INF-β, a highly prescribed therapeutic to determine effect on NETosis from neutrophils isolated from individuals with MS, seen in figure 3.11. Similar to the PPAD study, we see a non-significant decrease in elastase concentration when 2 and 4 µm IFN- β are added to the NETosis buffer. It can be concluded that, there may be a dose dependent response however, a significant treatment dose was not identified.

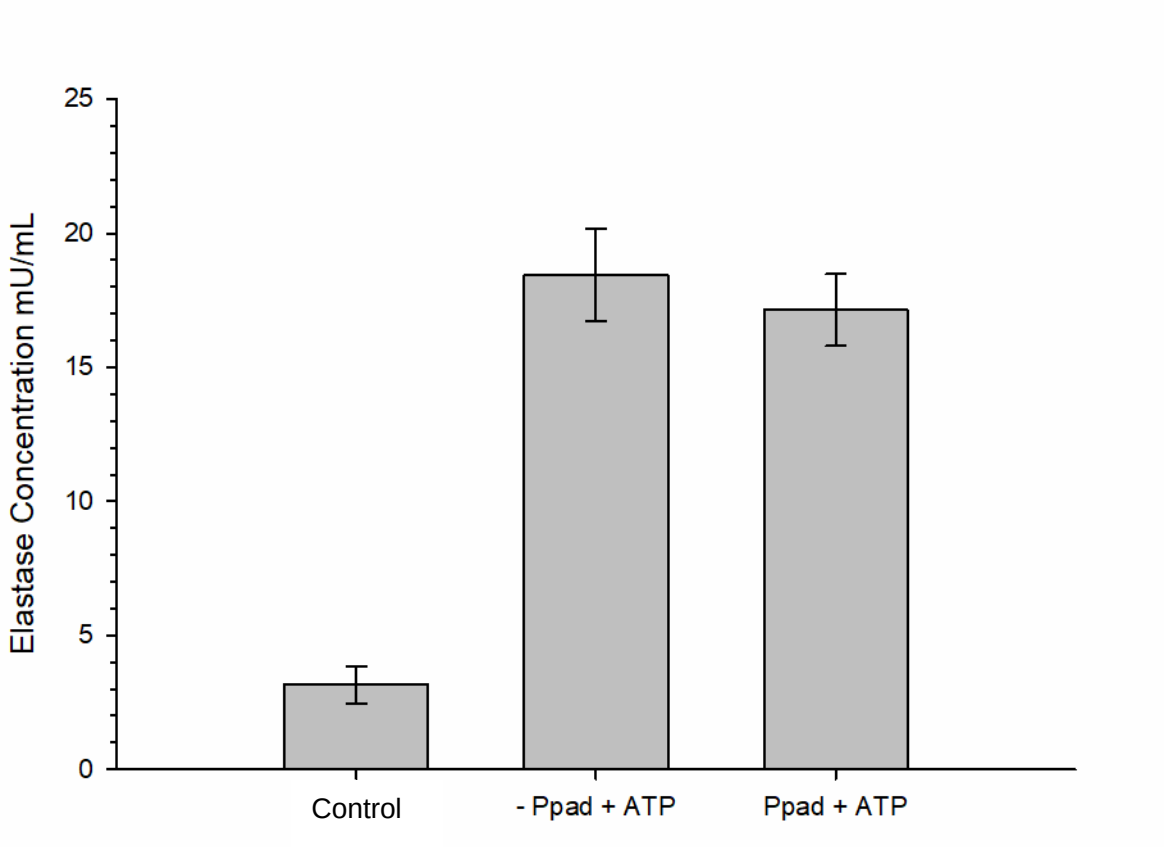

Figure 3.10: Purinergic receptor blocking and NETosis. In the presence or absence of the purinergic receptor blocking compound, there was no statistically different elastase concentration. The control sample does not contain ATP. (error=SEM, n=4)

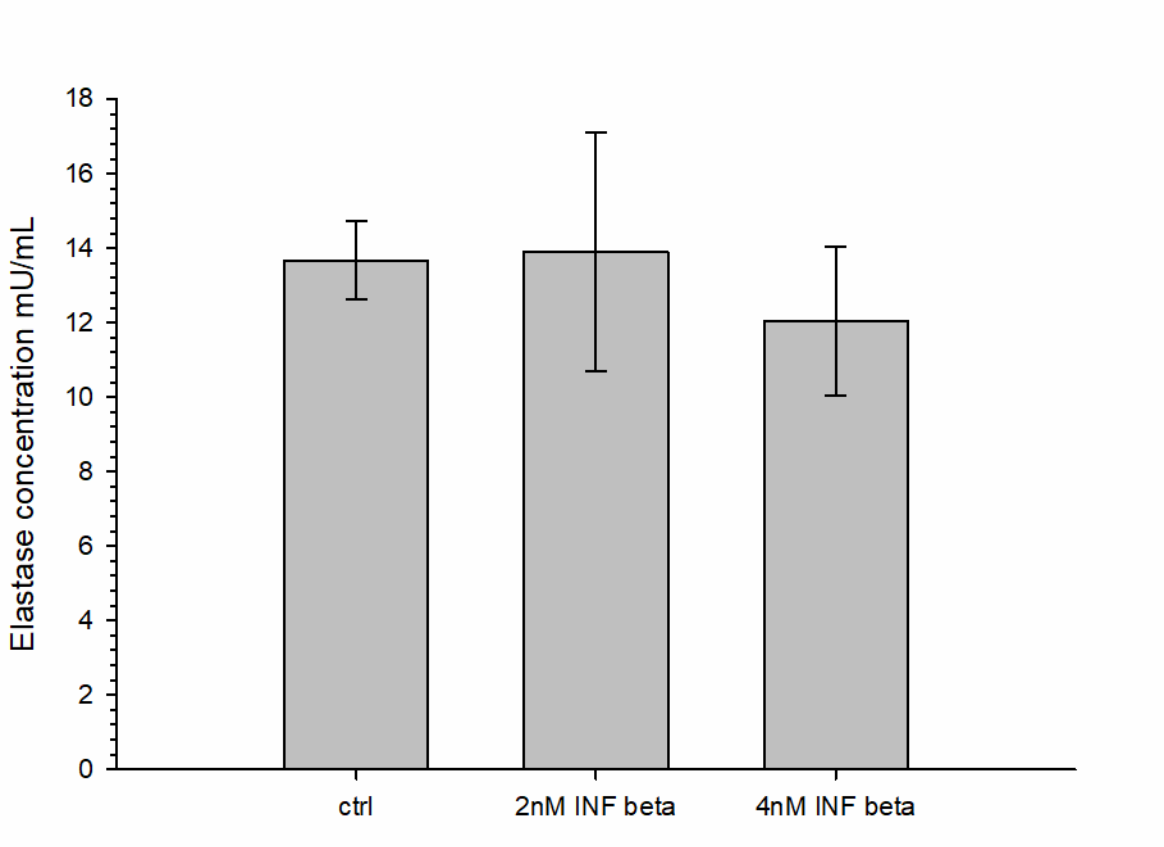

Figure 3.11: Determination of IFN- β on NETosis from MS neutrophils. Introducing the universally used therapeutic for MS, IFN- β, showed no statistical difference at 2 and 4 µM. The control sample was stimulated with PMA but had no IFN-β. A potential conclusion can be deduced for the effectiveness of INF-β on NETosis reduction, a higher concentration should be investigated. (error=SEM, n=3)

3.5 Discussion

This research is the first of its kind investigating C-peptide and Zn^{2+} binding to MS neutrophils. It was found that C-peptide binds to MS neutrophils in the absence of both albumin and Zn^{2+}, which is interesting when compared to C-peptide binding to RBCs requires albumin. It was previously reported that there was significantly more C-peptide binding to MS RBC when compared to control RBCs, at an alarming magnitude.(*106*) Our

findings further conclude that MS circulating cells tend to have a higher binding rate of C-peptide than their control counterparts. Mechanistically, it will be important to determine functional changes in MS neutrophils binding to C-peptide. Previous studies have shown C-peptide to have anti-inflammatory effects, therefore its role in MS should be identified.(*109, 110*)

In MS, Zn^{2+} has been discovered at higher concentrations in the blood stream compared to control patients. Zn^{2+} is a known chemoattractant for neutrophils, making it clear that Zn^{2+} binds to neutrophils in both the presence and absence of C-peptide.(*111*) Zn^{2+} homeostasis in immune cells is controlled by two families of Zn^{2+} transporters Zip1-14 and Zn1-10. These transporters are dispersed throughout the plasma membrane and intracellular organelle. It is known that Zn^{2+} plays a critical role in immunity via cellular function and signal transduction. Zn^{2+} deficiency is associated with several pathologies, however upregulation of Zn^{2+} concentration is lesser understood. Zn^{2+} has been identified as a potential mediator of MS pathology due to its high concentration in the CNS, however the mechanisms have not been identified. It will be important to further investigate the role of immune cell Zn^{2+} homeostasis in MS.(*111, 112*)

The major finding of this research is furthering evidence of ATP's role in NETosis. It was proven that ATP has an effect on NETosis, and we were able to prove that ATP secreted from RBC increases NETosis, proving a more biologically relevant measurement. This work can be directly correlated to the findings that individuals with

MS show an increased blood concentration of ATP. Additionally, previous work conducted in the Spence lab identified RBCs a potential source for the elevated levels. We have shown stimulating ATP release from MS RBC via flow induced shear stress, significantly increases the rate of NETosis. Blocking purinergic receptors and the addition of IFN-β decreased the amount of observed NETosis, however, repeating studies led to high error and lack of statistical significance. It will be important for us to continue to investigate higher concentrations to form a better conclusion on the impact of purinergic receptor blocking and INF-β supplementation, as a potential therapeutic to regulate NETosis in control patients and individuals with MS. In a preliminary study we removed albumin out of the buffer, and we observed a decrease in NETosis seen in figure 3.12. Albumin is a known carrier molecule that is able to carry ions, molecules, and peptides. In MS, albumin represents a large percentage of the proteins that become extravasated during BBB breakdown, it will be important to investigate what albumin is carrying to the BBB, as Zn^{2+} binding to albumin has been reported, and here we report Zn^{2+} increases NET formation.(*113*)

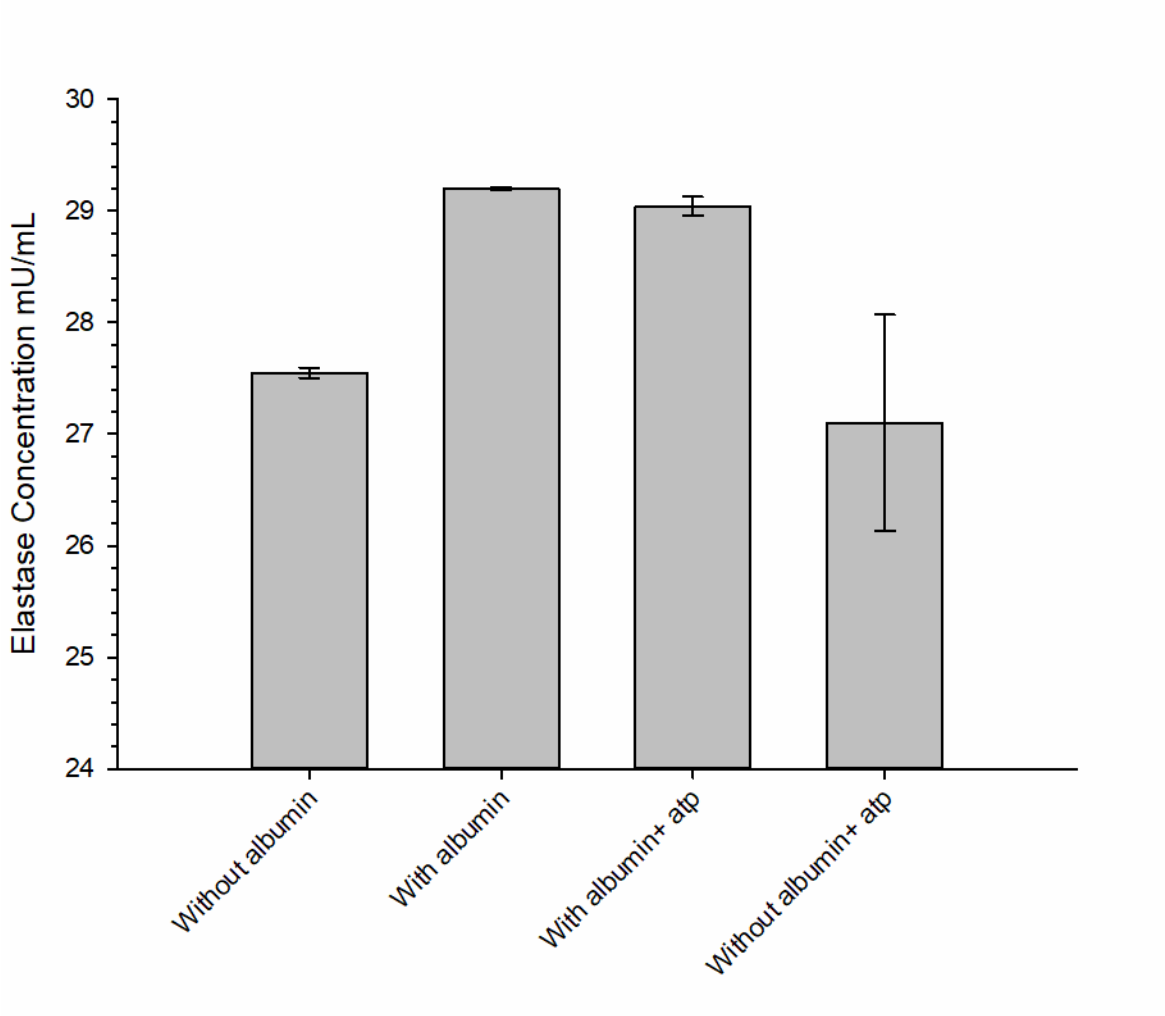

Figure 3.12: Preliminary evidence of albumin on NETosis. Without the presence of albumin, a decrease in elastase concentration was observed. (error= Standard deviation n=1)

It is hypothesized that ATP acts as a signaling molecule to increase circulating neutrophils to the BBB and CSF. Subsequently, the prolonged exposure to high ATP concentrations could cause neutrophils to undergo unregulated NETosis, ultimately causing damage to the BBB layer. It is key to note, in the event of cell death of any magnitude, there is an influx of several other immune cells due to the extracellular presence of damage associated proteins (DAMPS), DNA, and cytokines. T-cells could be

one of the recruited immune cells, giving the cell an opportunity to migrate through the damaged BBB and become autoreactive.

REFERENCES

REFERENCES

1. V. Brinkmann *et al.*, Neutrophil extracellular traps kill bacteria. *Science* **303**, 1532-1535 (2004).

2. Y. C. Rocha Arrieta, M. Rojas, G. Vasquez, J. Lopez, The Lymphocytes Stimulation Induced DNA Release, a Phenomenon Similar to NETosis. *Scand J Immunol* **86**, 229-238 (2017).

3. W. Antonin, H. Neumann, Chromosome condensation and decondensation during mitosis. *Curr Opin Cell Biol* **40**, 15-22 (2016).

4. H. Takei, A. Araki, H. Watanabe, A. Ichinose, F. Sendo, Rapid killing of human neutrophils by the potent activator phorbol 12-myristate 13-acetate (PMA) accompanied by changes different from typical apoptosis or necrosis. *J Leukoc Biol* **59**, 229-240 (1996).

5. B. L. Heckmann, B. Tummers, D. R. Green, Crashing the computer: apoptosis vs. necroptosis in neuroinflammation. *Cell Death Differ* **26**, 41-52 (2019).

6. L. Galluzzi *et al.*, Molecular mechanisms of cell death: recommendations of the Nomenclature Committee on Cell Death 2018. *Cell Death Differ* **25**, 486-541 (2018).

7. N. Branzk, V. Papayannopoulos, Molecular mechanisms regulating NETosis in infection and disease. *Semin Immunopathol* **35**, 513-530 (2013).

8. A. Hakkim *et al.*, Activation of the Raf-MEK-ERK pathway is required for neutrophil extracellular trap formation. *Nat Chem Biol* **7**, 75-77 (2011).

9. E. F. Kenny *et al.*, Diverse stimuli engage different neutrophil extracellular trap pathways. *Elife* **6**, (2017).

10. F. Conceição-Silva *et al.*, The Immune System Throws Its Traps: Cells and Their Extracellular Traps in Disease and Protection. *Cells* **10**, (2021).

11. Q. Remijsen *et al.*, Dying for a cause: NETosis, mechanisms behind an antimicrobial cell death modality. *Cell Death Differ* **18**, 581-588 (2011).

12. N. V. Vorobjeva, B. V. Chernyak, NETosis: Molecular Mechanisms, Role in Physiology and Pathology. *Biochemistry (Mosc)* **85**, 1178-1190 (2020).

13. M. Alirezaei *et al.*, Short-term fasting induces profound neuronal autophagy. *Autophagy* **6**, 702-710 (2010).

14. N. Kourtis, N. Tavernarakis, Autophagy and cell death in model organisms. *Cell Death Differ* **16**, 21-30 (2009).

15. I. Mitroulis *et al.*, Neutrophil extracellular trap formation is associated with IL-1β and autophagy-related signaling in gout. *PLoS One* **6**, e29318 (2011).

16. V. Brinkmann, A. Zychlinsky, Beneficial suicide: why neutrophils die to make NETs. *Nat Rev Microbiol* **5**, 577-582 (2007).

17. Q. Remijsen *et al.*, Neutrophil extracellular trap cell death requires both autophagy and superoxide generation. *Cell Res* **21**, 290-304 (2011).

18. T. A. Fuchs *et al.*, Novel cell death program leads to neutrophil extracellular traps. *J Cell Biol* **176**, 231-241 (2007).

19. M. A. Arruda, A. G. Rossi, M. S. de Freitas, C. Barja-Fidalgo, A. V. Graça-Souza, Heme inhibits human neutrophil apoptosis: involvement of phosphoinositide 3-kinase, MAPK, and NF-kappaB. *J Immunol* **173**, 2023-2030 (2004).

20. B. C. Albensi, What Is Nuclear Factor Kappa B (NF-κB) Doing in and to the Mitochondrion? *Front Cell Dev Biol* **7**, 154 (2019).

21. C. Anzilotti, F. Pratesi, C. Tommasi, P. Migliorini, Peptidylarginine deiminase 4 and citrullination in health and disease. *Autoimmun Rev* **9**, 158-160 (2010).

22. P. Li *et al.*, PAD4 is essential for antibacterial innate immunity mediated by neutrophil extracellular traps. *J Exp Med* **207**, 1853-1862 (2010).

23. A. Sofoluwe, M. Bacchetta, M. Badaoui, B. R. Kwak, M. Chanson, ATP amplifies NADPH-dependent and -independent neutrophil extracellular trap formation. *Sci Rep* **9**, 16556 (2019).

24. A. Schultze-Mosgau *et al.*, Characterization of calcium-mobilizing, purinergic P2Y(2) receptors in human ovarian cancer cells. *Mol Hum Reprod* **6**, 435-442 (2000).

25. A. K. Gupta, S. Giaglis, P. Hasler, S. Hahn, Efficient neutrophil extracellular trap induction requires mobilization of both intracellular and extracellular calcium pools and is modulated by cyclosporine A. *PLoS One* **9**, e97088 (2014).

26. R. Villagra-Blanco *et al.*, Bovine Polymorphonuclear Neutrophils Cast Neutrophil Extracellular Traps against the Abortive Parasite. *Front Immunol* **8**, 606 (2017).

27. G. Burnstock, Purinergic Signalling: Therapeutic Developments. *Front Pharmacol* **8**, 661 (2017).

28. S. W. Kim *et al.*, Adenosine Triphosphate Accumulated Following Cerebral Ischemia Induces Neutrophil Extracellular Trap Formation. *Int J Mol Sci* **21**, (2020).

29. B. J. van Raam *et al.*, Mitochondrial membrane potential in human neutrophils is maintained by complex III activity in the absence of supercomplex organisation. *PLoS One* **3**, e2013 (2008).

30. T. Kirchner *et al.*, The impact of various reactive oxygen species on the formation of neutrophil extracellular traps. *Mediators Inflamm* **2012**, 849136 (2012).

31. C. M. de Bont *et al.*, Autoantibodies to neutrophil extracellular traps represent a potential serological biomarker in rheumatoid arthritis. *J Autoimmun* **113**, 102484 (2020).

32. T. M. Hofbauer *et al.*, Neutrophil Extracellular Traps Induce MCP-1 at the Culprit Site in ST-Segment Elevation Myocardial Infarction. *Front Cell Dev Biol* **8**, 564169 (2020).

33. L. Yang *et al.*, DNA of neutrophil extracellular traps promotes cancer metastasis via CCDC25. *Nature* **583**, 133-138 (2020).

34. A. Bonanni *et al.*, Multi-antibody composition in lupus nephritis: isotype and antigen specificity make the difference. *Autoimmun Rev* **14**, 692-702 (2015).

35. A. Hakkim *et al.*, Impairment of neutrophil extracellular trap degradation is associated with lupus nephritis. *Proc Natl Acad Sci U S A* **107**, 9813-9818 (2010).

36. D. Söderberg *et al.*, Increased levels of neutrophil extracellular trap remnants in the circulation of patients with small vessel vasculitis, but an inverse correlation to anti-neutrophil cytoplasmic antibodies during remission. *Rheumatology (Oxford)* **54**, 2085-2094 (2015).

37. Y. Takizawa *et al.*, Citrullinated fibrinogen detected as a soluble citrullinated autoantigen in rheumatoid arthritis synovial fluids. *Ann Rheum Dis* **65**, 1013-1020 (2006).

38. B. Vander Cruyssen *et al.*, Diagnostic value of anti-human citrullinated fibrinogen ELISA and comparison with four other anti-citrullinated protein assays. *Arthritis Res Ther* **8**, R122 (2006).

39. D. Coenen, P. Verschueren, R. Westhovens, X. Bossuyt, Technical and diagnostic performance of 6 assays for the measurement of citrullinated protein/peptide antibodies in the diagnosis of rheumatoid arthritis. *Clin Chem* **53**, 498-504 (2007).

40. E. Girbal-Neuhauser *et al.*, The epitopes targeted by the rheumatoid arthritis-associated antifilaggrin autoantibodies are posttranslationally generated on various sites of (pro)filaggrin by deimination of arginine residues. *J Immunol* **162**, 585-594 (1999).

41. K. Shin *et al.*, Role of citrullinated fibrinogen peptides in the activation of CD4 T cells from patients with rheumatoid arthritis. *Immune Netw* **13**, 116-122 (2013).

42. E. Corsiero *et al.*, Single cell cloning and recombinant monoclonal antibodies generation from RA synovial B cells reveal frequent targeting of citrullinated histones of NETs. *Ann Rheum Dis* **75**, 1866-1875 (2016).

43. N. E. Blachère, S. Parveen, J. Fak, M. O. Frank, D. E. Orange, Inflammatory but not apoptotic death of granulocytes citrullinates fibrinogen. *Arthritis Res Ther* **17**, 369 (2015).

44. C. Sur Chowdhury *et al.*, Enhanced neutrophil extracellular trap generation in rheumatoid arthritis: analysis of underlying signal transduction pathways and potential diagnostic utility. *Arthritis Res Ther* **16**, R122 (2014).

45. V. Papayannopoulos, Neutrophil extracellular traps in immunity and disease. *Nat Rev Immunol* **18**, 134-147 (2018).

46. Y. C. Chang *et al.*, Group B Streptococcus engages an inhibitory Siglec through sialic acid mimicry to blunt innate immune and inflammatory responses in vivo. *PLoS Pathog* **10**, e1003846 (2014).

47. S. R. Ali *et al.*, Siglec-5 and Siglec-14 are polymorphic paired receptors that modulate neutrophil and amnion signaling responses to group B Streptococcus. *J Exp Med* **211**, 1231-1242 (2014).

48. B. Khatua, K. Bhattacharya, C. Mandal, Sialoglycoproteins adsorbed by Pseudomonas aeruginosa facilitate their survival by impeding neutrophil extracellular trap through siglec-9. *J Leukoc Biol* **91**, 641-655 (2012).

49. K. Van Avondt, M. van der Linden, P. H. Naccache, D. A. Egan, L. Meyaard, Signal Inhibitory Receptor on Leukocytes-1 Limits the Formation of Neutrophil Extracellular Traps, but Preserves Intracellular Bacterial Killing. *J Immunol* **196**, 3686-3694 (2016).

50. L. Ma, S. Wang, D. Wang, M. R. Parsek, D. J. Wozniak, The roles of biofilm matrix polysaccharide Psl in mucoid Pseudomonas aeruginosa biofilms. *FEMS Immunol Med Microbiol* **65**, 377-380 (2012).

51. A. Thanabalasuriar *et al.*, Neutrophil Extracellular Traps Confine Pseudomonas aeruginosa Ocular Biofilms and Restrict Brain Invasion. *Cell Host Microbe* **25**, 526-536.e524 (2019).

52. S. Bates *et al.*, Role of the Candida albicans MNN1 gene family in cell wall structure and virulence. *BMC Res Notes* **6**, 294 (2013).

53. T. Saitoh *et al.*, Neutrophil extracellular traps mediate a host defense response to human immunodeficiency virus-1. *Cell Host Microbe* **12**, 109-116 (2012).

54. V. Mutua, L. J. Gershwin, A Review of Neutrophil Extracellular Traps (NETs) in Disease: Potential Anti-NETs Therapeutics. *Clin Rev Allergy Immunol* **61**, 194-211 (2021).

55. M. A. Khan *et al.*, Regulating NETosis: Increasing pH Promotes NADPH Oxidase-Dependent NETosis. *Front Med (Lausanne)* **5**, 19 (2018).

56. S. Grinstein, W. Furuya, P. E. Nasmith, O. D. Rotstein, Na+/H+ exchange and the regulation of intracellular pH in polymorphonuclear leukocytes. *Comp Biochem Physiol A Comp Physiol* **90**, 543-549 (1988).

57. L. Simchowitz, E. J. Cragoe, Intracellular acidification-induced alkali metal cation/H+ exchange in human neutrophils. *J Gen Physiol* **90**, 737-762 (1987).

58. B. Korkmaz, T. Moreau, F. Gauthier, Neutrophil elastase, proteinase 3 and cathepsin G: physicochemical properties, activity and physiopathological functions. *Biochimie* **90**, 227-242 (2008).

59. I. I. Vlasova, J. Arnhold, A. N. Osipov, O. M. Panasenko, pH-dependent regulation of myeloperoxidase activity. *Biochemistry (Mosc)* **71**, 667-677 (2006).

60. C. Leon, C. Ravanat, M. Freund, J. P. Cazenave, C. Gachet, Differential involvement of the P2Y1 and P2Y12 receptors in platelet procoagulant activity. *Arterioscler Thromb Vasc Biol* **23**, 1941-1947 (2003).

61. C. Weber, Platelets and chemokines in atherosclerosis: partners in crime. *Circ Res* **96**, 612-616 (2005).

62. A. Carestia, T. Kaufman, M. Schattner, Platelets: New Bricks in the Building of Neutrophil Extracellular Traps. *Front Immunol* **7**, 271 (2016).

63. M. Merza *et al.*, Human thrombin-derived host defense peptides inhibit neutrophil recruitment and tissue injury in severe acute pancreatitis. *Am J Physiol Gastrointest Liver Physiol* **307**, G914-921 (2014).

64. A. Caudrillier *et al.*, Platelets induce neutrophil extracellular traps in transfusion-related acute lung injury. *J Clin Invest* **122**, 2661-2671 (2012).

65. G. Ortiz-Muñoz *et al.*, Aspirin-triggered 15-epi-lipoxin A4 regulates neutrophil-platelet aggregation and attenuates acute lung injury in mice. *Blood* **124**, 2625-2634 (2014).

66. J. Tilgner *et al.*, Aspirin, but Not Tirofiban Displays Protective Effects in Endotoxin Induced Lung Injury. *PLoS One* **11**, e0161218 (2016).

67. D. M. Sayah *et al.*, Neutrophil extracellular traps are pathogenic in primary graft dysfunction after lung transplantation. *Am J Respir Crit Care Med* **191**, 455-463 (2015).

68. H. Weiler, B. H. Isermann, Thrombomodulin. *J Thromb Haemost* **1**, 1515-1524 (2003).

69. P. Fuentes-Prior *et al.*, Structural basis for the anticoagulant activity of the thrombin-thrombomodulin complex. *Nature* **404**, 518-525 (2000).

70. D. M. Arnold *et al.*, A systematic evaluation of laboratory testing for drug-induced immune thrombocytopenia. *J Thromb Haemost* **11**, 169-176 (2013).

71. C. M. de Bont, W. C. Boelens, G. J. M. Pruijn, NETosis, complement, and coagulation: a triangular relationship. *Cell Mol Immunol* **16**, 19-27 (2019).

72. S. Gando, Microvascular thrombosis and multiple organ dysfunction syndrome. *Crit Care Med* **38**, S35-42 (2010).

73. J. Helms *et al.*, Thrombomodulin favors leukocyte microvesicle fibrinolytic activity, reduces NETosis and prevents septic shock-induced coagulopathy in rats. *Ann Intensive Care* **7**, 118 (2017).

74. L. B. Rojas, M. B. Gomes, Metformin: an old but still the best treatment for type 2 diabetes. *Diabetol Metab Syndr* **5**, 6 (2013).

75. G. Rena, D. G. Hardie, E. R. Pearson, The mechanisms of action of metformin. *Diabetologia* **60**, 1577-1585 (2017).

76. L. Menegazzo *et al.*, The antidiabetic drug metformin blunts NETosis in vitro and reduces circulating NETosis biomarkers in vivo. *Acta Diabetol* **55**, 593-601 (2018).

77. A. Gallo *et al.*, Metformin prevents glucose-induced protein kinase C-beta2 activation in human umbilical vein endothelial cells through an antioxidant mechanism. *Diabetes* **54**, 1123-1131 (2005).

78. S. Shak, D. J. Capon, R. Hellmiss, S. A. Marsters, C. L. Baker, Recombinant human DNase I reduces the viscosity of cystic fibrosis sputum. *Proc Natl Acad Sci U S A* **87**, 9188-9192 (1990).

79. M. Macanovic *et al.*, The treatment of systemic lupus erythematosus (SLE) in NZB/W F1 hybrid mice; studies with recombinant murine DNase and with dexamethasone. *Clin Exp Immunol* **106**, 243-252 (1996).

80. R. D. Gray, B. N. McCullagh, P. B. McCray, NETs and CF Lung Disease: Current Status and Future Prospects. *Antibiotics (Basel)* **4**, 62-75 (2015).

81. T. Mohanty *et al.*, Neutrophil extracellular traps in the central nervous system hinder bacterial clearance during pneumococcal meningitis. *Nat Commun* **10**, 1667 (2019).

82. H. F. Harbo, R. Gold, M. Tintoré, Sex and gender issues in multiple sclerosis. *Ther Adv Neurol Disord* **6**, 237-248 (2013).

83. S. Simpson, L. Blizzard, P. Otahal, I. Van der Mei, B. Taylor, Latitude is significantly associated with the prevalence of multiple sclerosis: a meta-analysis. *J Neurol Neurosurg Psychiatry* **82**, 1132-1141 (2011).

84. C. Ahlgren, A. Odén, J. Lycke, High nationwide incidence of multiple sclerosis in Sweden. *PLoS One* **9**, e108599 (2014).

85. J. F. Kurtzke, Epidemiology in multiple sclerosis: a pilgrim's progress. *Brain* **136**, 2904-2917 (2013).

86. National Multiple Sclerosis Society. Understanding MS. https://www.nationalmssociety.org/What-is-MS/MS-FAQ-s

87. K. M. Boje, S. S. Lakhman, Nitric oxide redox species exert differential permeability effects on the blood-brain barrier. *J Pharmacol Exp Ther* **293**, 545-550 (2000).

88. N. Ghasemi, S. Razavi, E. Nikzad, Multiple Sclerosis: Pathogenesis, Symptoms, Diagnoses and Cell-Based Therapy. *Cell J* **19**, 1-10 (2017).

89. A. Ascherio, K. L. Munger, Epstein-barr virus infection and multiple sclerosis: a review. *J Neuroimmune Pharmacol* **5**, 271-277 (2010).

90. A. Tselis, Evidence for viral etiology of multiple sclerosis. *Semin Neurol* **31**, 307-316 (2011).

91. A. Compston, A. Coles, Multiple sclerosis. *Lancet* **359**, 1221-1231 (2002).

92. N. M. Nielsen *et al.*, Familial risk of multiple sclerosis: a nationwide cohort study. *Am J Epidemiol* **162**, 774-778 (2005).

93. C. Selmi, The X in sex: how autoimmune diseases revolve around sex chromosomes. *Best Pract Res Clin Rheumatol* **22**, 913-922 (2008).

94. D. L. Smith-Bouvier *et al.*, A role for sex chromosome complement in the female bias in autoimmune disease. *J Exp Med* **205**, 1099-1108 (2008).

95. G. P. Knudsen *et al.*, X chromosome inactivation in females with multiple sclerosis. *Eur J Neurol* **14**, 1392-1396 (2007).

96. S. Sawcer *et al.*, Genetic risk and a primary role for cell-mediated immune mechanisms in multiple sclerosis. *Nature* **476**, 214-219 (2011).

97. F. D. Lublin *et al.*, Defining the clinical course of multiple sclerosis: the 2013 revisions. *Neurology* **83**, 278-286 (2014).

98. A. J. Solomon, E. P. Klein, D. Bourdette, "Undiagnosing" multiple sclerosis: the challenge of misdiagnosis in MS. *Neurology* **78**, 1986-1991 (2012).

99. A. J. Thompson *et al.*, Diagnosis of multiple sclerosis: 2017 revisions of the McDonald criteria. *Lancet Neurol* **17**, 162-173 (2018).

100. S. Ömerhoca, S. Y. Akkaş, N. K. İçen, Multiple Sclerosis: Diagnosis and Differential Diagnosis. *Noro Psikiyatr Ars* **55**, S1-S9 (2018).

101. A. J. Sharp *et al.*, P2x7 deficiency suppresses development of experimental autoimmune encephalomyelitis. *J Neuroinflammation* **5**, 33 (2008).

102. M. Bradl, H. Lassmann, Oligodendrocytes: biology and pathology. *Acta Neuropathol* **119**, 37-53 (2010).

103. C. Stadelmann, S. Timmler, A. Barrantes-Freer, M. Simons, Myelin in the Central Nervous System: Structure, Function, and Pathology. *Physiol Rev* **99**, 1381-1431 (2019).

104. C. Cekic, J. Linden, Purinergic regulation of the immune system. *Nat Rev Immunol* **16**, 177-192 (2016).

105. C. Matute *et al.*, P2X(7) receptor blockade prevents ATP excitotoxicity in oligodendrocytes and ameliorates experimental autoimmune encephalomyelitis. *J Neurosci* **27**, 9525-9533 (2007).

106. S. Letourneau, L. Hernandez, A. N. Faris, D. M. Spence, Evaluating the effects of estradiol on endothelial nitric oxide stimulated by erythrocyte-derived ATP using a microfluidic approach. *Anal Bioanal Chem* **397**, 3369-3375 (2010).

107. T. Woodberry, S. E. Bouffler, A. S. Wilson, R. L. Buckland, A. Brüstle, The Emerging Role of Neutrophil Granulocytes in Multiple Sclerosis. *J Clin Med* **7**, (2018).

108. G. Lambrecht *et al.*, PPADS, a novel functionally selective antagonist of P2 purinoceptor-mediated responses. *Eur J Pharmacol* **217**, 217-219 (1992).

109. C. E. Hills, N. J. Brunskill, C-Peptide and its intracellular signaling. *Rev Diabet Stud* **6**, 138-147 (2009).

110. P. Luppi, P. Drain, C-peptide antioxidant adaptive pathways in β cells and diabetes. *J Intern Med*, (2016).

111. M. Maywald, I. Wessels, L. Rink, Zinc Signals and Immunity. *Int J Mol Sci* **18**, (2017).

112. B. Y. Choi, J. W. Jung, S. W. Suh, The Emerging Role of Zinc in the Pathogenesis of Multiple Sclerosis. *Int J Mol Sci* **18**, (2017).

113. S. M. LeVine, Albumin and multiple sclerosis. *BMC Neurol* **16**, 47 (2016).

Chapter 4 - 3D Printing Applications for in Vitro Studies

4.1 History of 3D Printing

In recent years device design and fabrication has emerged throughout science as a useful tool for the advancement of research. Use of fabrication comes in many forms, ranging from analytical tools and lab equipment to medical implantation.(*1*) Early fabricated equipment was constructed by hand using glass blowing or heavy machinery. Although useful for its time, these methods were time consuming and often out of reach for interested individuals. In addition to accessibility and time efficiency, early fabrication techniques led to disparities in end products from lab to lab. Any tool or measurement method, heavily relies on reproducibility.(*2*) Therefore, the advancement of fabricated devices needed to be revamped before the technology's relevancy ended.

Within the last 15 years, 3D printing has reemerged as a prominent technology in the research setting. The numerous forms of 3D printing will be described in detail in the proceeding sections, however, all forms share the same umbrella, namely, an additive manufacturing technique building models one layer at a time.(*3*) The first rendition of a 3D printer was developed by Charles Hull in the early 1980s.(*4*) Hull introduced the technology as a stereolithography apparatus (SLA), a light curable liquid resin to build layers producing a solid end product. Since the invention of the SLA printing technique, several advancements in the field of 3D printing have surfaced, improving the technology. Examples include inkjet printing, extrusion machines, lamination machines, and

bioprinting and more seen in table 4.1.(5) Advancements in the technologies have introduced numerous material properties as well that can produce metals, gradients of hard to rubber-like plastic, and biological components such as cells and extracellular matrices. The proceeding sections will describe each technology further, including the positive and negative aspects of the technologies.

Table 4.1: Different forms of 3D printing technologies and their respective properties.

3D printing Process	Technology	Material	Resolution	Common applications
Material extrusion	Fused deposition modeling (FDM)	Plastic filament (PLA, ABS, PET, Carbon fiber)	±0.5 mm	Electrical housings, form and fit testing
VAT polymerization	Stereolithography (SLA)	Photopolymer resin	±0.2 mm	Dental, injection mold, jewelry casting
Powder bed fusion	Selective laser sintering (SLS), Electron beam melting (EBM)	Thermoplastic powder, metal powder, ceramic	±0.3 mm	Functional parts, complex ducting
Ink jetting	Inkjet, polyjet	Photopolymer resin	±0.1 mm	Full color prototypes, medical models
Sheet lamination	Laminated object manufacturing (LOM), Ultrasonic consolidation (UC)	Paper, metal sheets, polymer	±0.1 mm	Prototyping, mold casting
Binder jetting	Binder jetting	Sand or metal powder, ceramic composites	±0.2 mm	Functional metal parts

4.2 Types of 3D Printing Technology

4.2.1 Stereolithography Apparatus

Now in its fourth decade of development, stereolithography apparatus (SLA) printing utilizes photopolymerization, a process in which a photocurable resin solidifies when exposed to a light source.(*6*) The initial design of SLA (figure 4.1) utilized a vat or pool of photocurable resin, with a computer guided laser as the light source. As the laser cured the top layer as designed, the print stage would drop, bringing a fresh uncured layer of resin to the top. This process would repeat until the design was complete. Other additives such as dyes, and UV absorbers were used to create full color products and softened plastic products.(*6, 7*)

Although effective, there are a few drawbacks to SLA technology. The use of a fine point laser resulted in prolonged and tedious print times, resulting in a lack of time efficiency. Optimization of the print parameters such as light exposure duration, wavelength selection, and laser power determination contribute to lengthy parameter selection. Further, the vat size is a limiting factor due to its predetermined dimensions, limiting the size of the part that can be produced. Further advancements in SLA technology led to the production of digital light process (DLP) printing. Functionally, DLP is similar in methodology to SLA, however, the key difference is DLP uses an arc lamp (rather than a laser), applying a single sheet of light to the top vat layer of photopolymer, curing one slice at a time.(*8*) Total print time is shorter compared to SLA, however, there is a loss in resolution due to the non-selective method of sheet curing. (*1*)

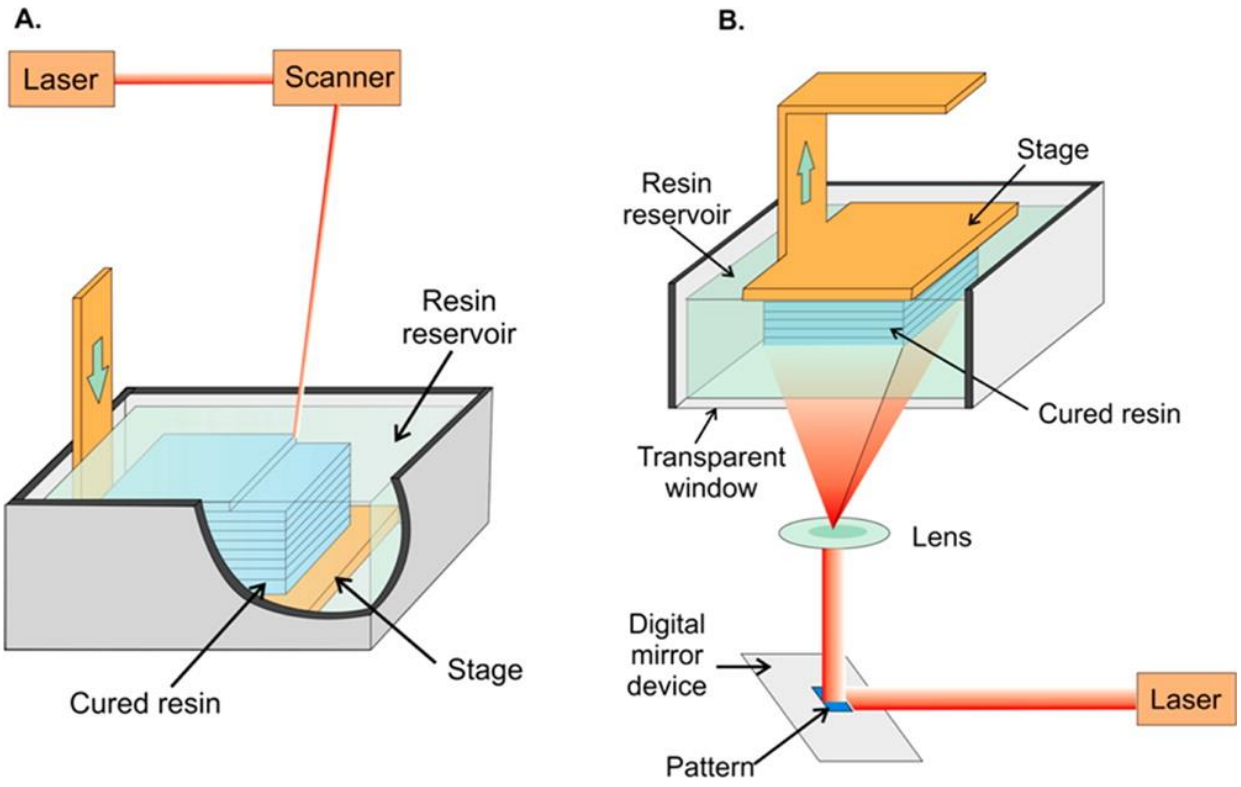

Figure 4.1: Schematic SLA printer configuration. with a direct write curing process. (A) Print stage is submerged in a vat of liquid resin. A pinpoint laser travels along the surface of the resin curing by row until the desired layer is fully cured. The stage drops lower into the vat, emerging a new layer of liquid resin covers the surface, the curing process then repeats. (B) Schematic of a layer configuration (DLP) SLA printer variant. In the DLP version of an SLA printer, similarly, the stage is submerged into a photopolymer reservoir. A laser is guided to the bottom of the stage to cure the material in the reservoir between the laser and the stage. DLP allows for simultaneously full layer curing, speeding up the overall print time. Once one layer is cured the stage raises by a defined distance allowing for the following layer to be cured.

4.2.2 Material Extrusion

Material extrusion is a process of material, typically plastic, extruded out of a heated nozzle onto a print stage. Material extrusion is typically used to print full color plastic with the possibility of multi-material applications.(*5*) This widely used form of 3D printing is commonly used in fused deposition modelling (FDM).(*9*) The high use of this technology stems from the low cost of machinery and plastic. FDM was developed by

Scott Crump of the company Stratasys to create a manufacturing technology for rapid prototyping.(*1*) Shown in figure 4.2, FDM fabricates parts through layer-by-layer addition of a semi molten thermoplastic filament.

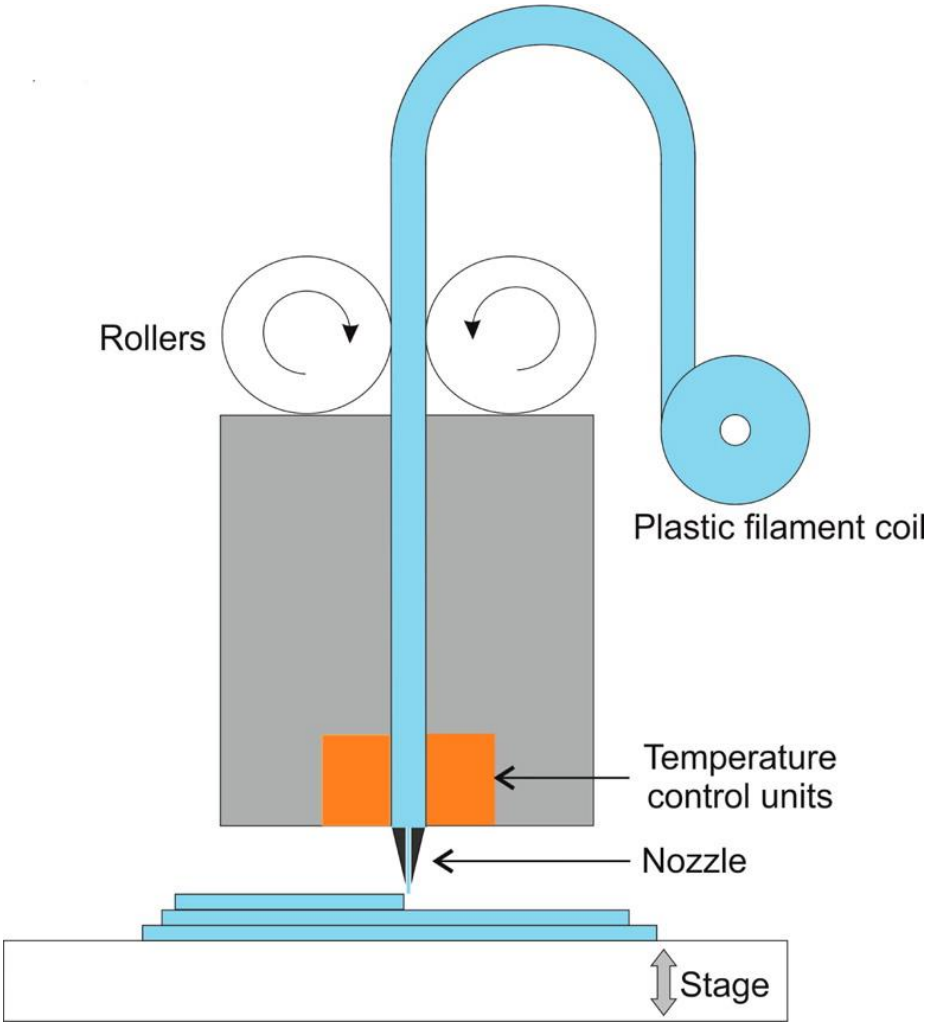

Figure 4.2: Mechanism of FDM technology. A coil of thermoplastic is fed through a set of rollers and through a print head. The temperature-controlled region of the print head will heat to the appropriate temperature, causing the thermoplastic to reach a semi molten state. The semi molten plastic is specifically extruded out of a nozzle, as the plastic cools on the print stage, it returns to its solid state in the shape of the desired design. The print head will then move up the Z-axis in single layer increments as the process is repeated until the part is complete.

The resolution of FDM printers are low at 200 um, making this technology more suitable for prototyping.(*10*) A highlight of FDM printing technology is the availability of printable materials. In addition to generic plastics such as polycarbonate, FDM printers can print polystyrene, acrylonitrile butadiene styrene (ABS), glass polymers, biocompatible materials, and metal.(*1, 11-13*)

4.2.3 Powder Bed Fusion

Powder bed fusion is a less commonly used 3D printing process in which an energy source induces fusion between powder particles inside a build tray.(*14*) Typical powders used in this technology include but are not limited to plastic, ceramic, and metal. The addition of applying additional powder while simultaneously smoothing, encases the final product in unused powder as support.(*15, 16*) Selective lasering sintering (SLS) is a low-cost method of 3D printing that utilizes powder bed fusion (figure 4.3). In SLS, a tray of polymer powder is heated to an optimum temperature just below the melting point of the polymer. A blade wipes across, forming a thin layer of powdered polymer, followed by a laser (fiber or CO_2), which scans across the surface sintering the powder forming a solidified cross-section. The platform is lowered one layer in height allowing the blade to redeposit a fresh layer of powder, repeating the previous steps until the design is complete. Although SLS is able to print a wide selection of material, with a resolution of 500 um, fine detailed prints are unachievable using this technique.(*1*)

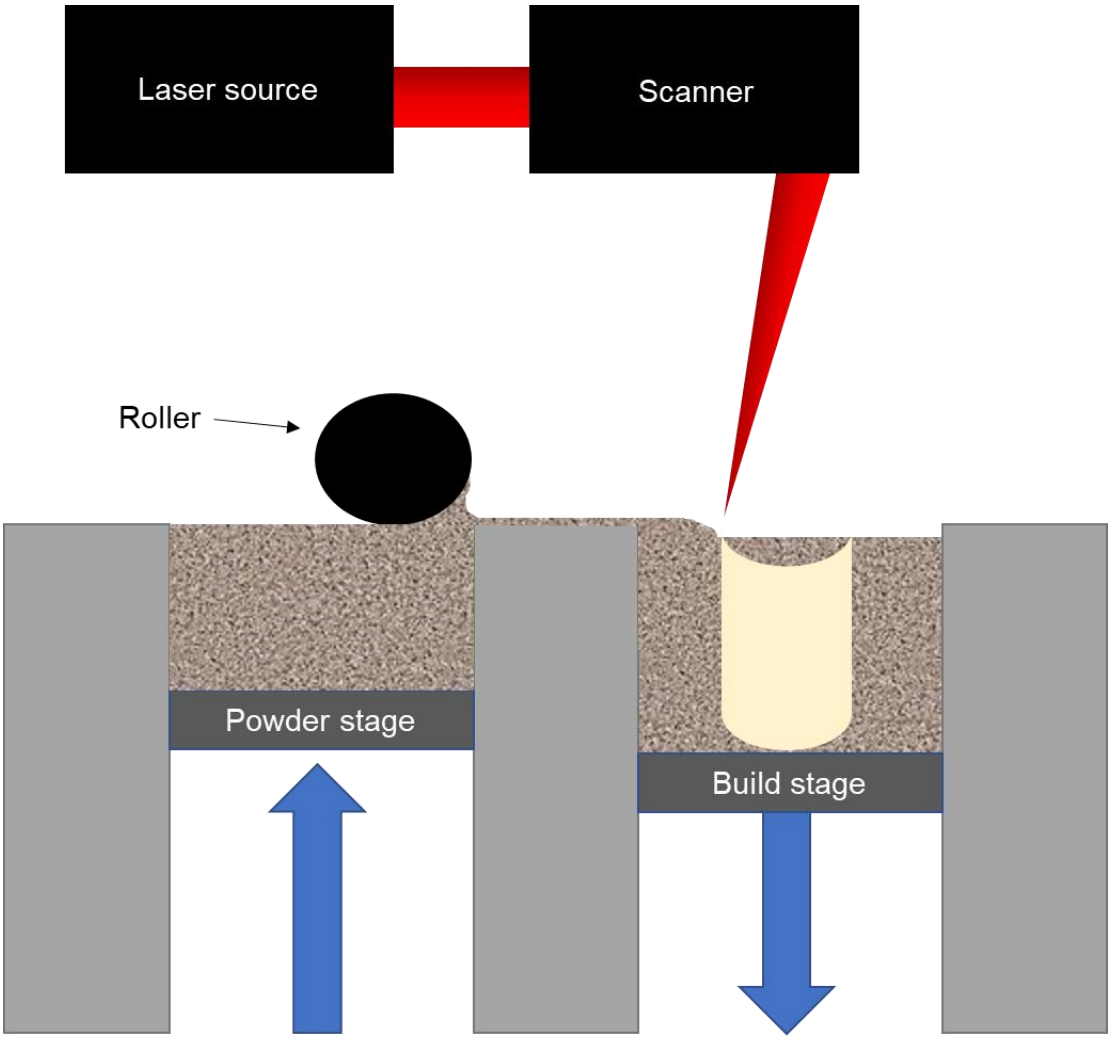

Figure 4.3: Schematic of SLS printing technology. Powdered material, typically metal, is sintered by a selective laser. Once the defined layer is sintered, the build stage drops as the powder stage raises, exposing a fresh layer of powder. The powder is transferred to the top layer in the build reservoir mechanically by a roller. The fresh layer undergoes the same sinter process, repeating until the solid product is complete.

4.2.4 Inkjet Printing

Inkjet printing is similar to a standard inkjet printer used for printing on paper, however, instead of printing a single layer of ink, inkjet 3D printing layers inks on top of each other forming a solid part.(*17*) Further, droplets of photopolymers are sprayed on a

print stage while simultaneously photocured, typically by ultraviolet light. Following a completion of a photocured layer, the print stage is dropped in layered increments allowing a new layer to be formed directly on top, repeating to build a 3D object.(*18*) A key feature of inkjet printing is the ability to print different materials in the same design. Additionally, having a large stage, and high Z axis resolution allows for large parts to be formed, and multiple designs can be printed in one print job. Overall, inkjet printers hold the highest resolution and print speed, however, inkjet printers require extensive maintenance and are the most expensive in regard to machinery and material cost.

Polyjet printing is one of the more recent installations to inkjet printing technology, with capabilities of multi-resin use through multiple print heads seen in figure 4.4. Resins available in poly jet printing include the full color spectrum and include chemical compositions allowing for production of hard to soft plastic measured by shore values.(*19*) The printing technology has many advantages over the previously described 3D printing technologies. Specifically, with the addition of multiple print heads render polyjet printers capable of material mixing, making designs highly customizable in aspects such as color and shore values. An additional advantage is the resolution, ranging from 14 to 100 um.(*20*) One of the disadvantages of polyjet printing is the support material, which stabilizes the design when complex geometries are incorporated in the design. Means of support material removal include physical removal by hand, pressure washing, or agitation in a 2% sodium hydroxide solution. Support material has shown problematic for applications such as microfluidic device fabrication or other designs with micron-scale

open spaces. Removal of support material in closed systems devices such as microfluidic device channels of micron dimension are nearly impossible to achieve.

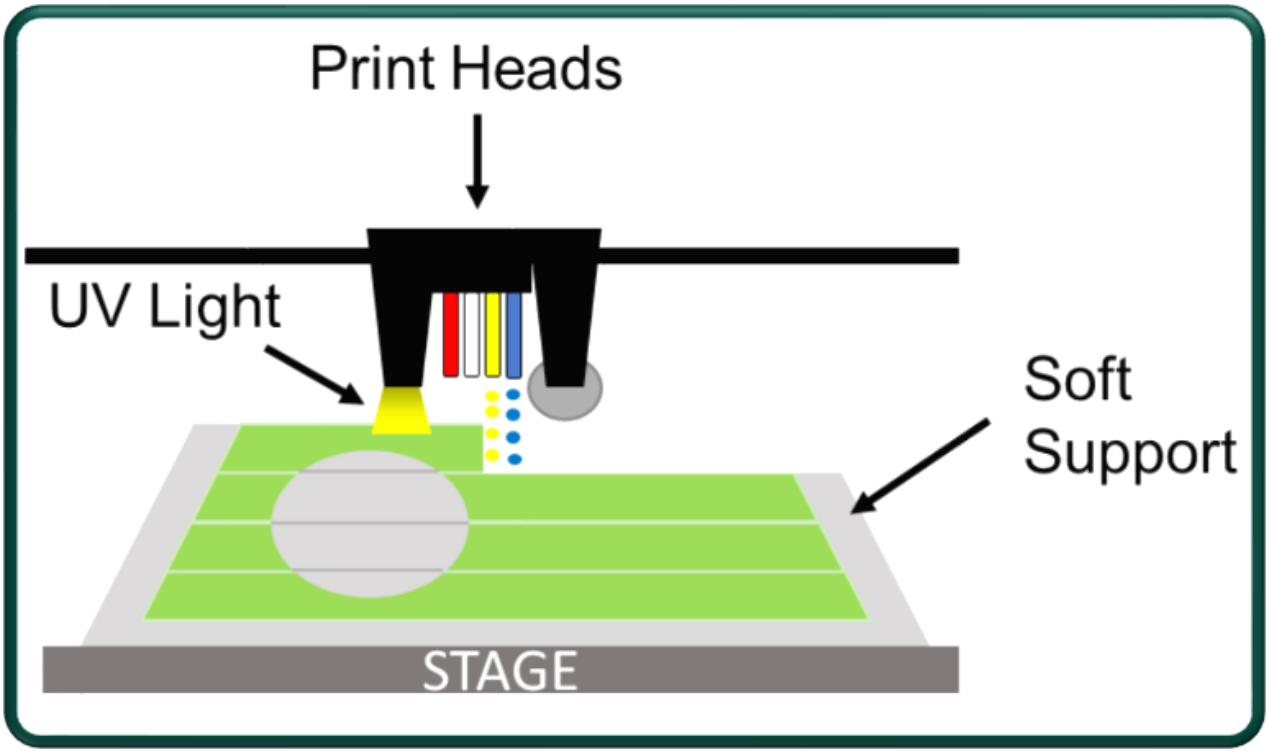

Figure 4.4: Schematic of polyjet printing technology. Polyjet printers contain multiple print heads, allowing for highly customizable prints. A variety of materials and colors can be created by blending resins from different print heads. As the print heads spray resin along the print stage, simultaneous polymerization of resin occurs through UV light exposure. A roller smooths the layer prior to the print stage dropping, creating a flat cured surface for a new layer to be added.

4.2.5 Bioprinting

3D printers have been used extensively for medical devices, laboratory tools, and analytical methods, however, recent efforts have pushed the technology to biological applications. A common problem of 3D printing is incompatibility with biological samples.(*21*) Complications with biocompatibility have been observed when biological

samples were introduced to 3D printed material. In recent years, there have been several technological advances, rendering 3D bioprinting possible. 3D bioprinters are capable of printing concentrated cell solutions, organoids, matrices, and various biologically relevant molecules into defined structures.(*22, 23*) Adapting from both FDM and inkjet technology, many 3D bioprinters utilize a blend of printing tactics for a desired biodesign.

Allevi is a recent company commercializing 3D bioprinters like the example shown in figure 4.5. The technology uses multiple commercially available that can be preloaded with solutions such as cells and/or gel matrices. The syringes are loaded into separate print heads capable of temperature control, ideal for homeostatic temperatures, and gel matrix consistency. Pressurized air is applied to the syringes extruding the contents of the syringes onto a desired well plate or dish that sits on a temperature-controlled stage. For certain 3D matrices requiring crosslinking, the instruments feature controllable UV curing. 3D printing does not begin with the machines themselves. Rather, users must create 3D sketches in computer software and export the sketches to a readable file for the 3D printers. The next few sections are dedicated to 3D printing design platforms and file types.

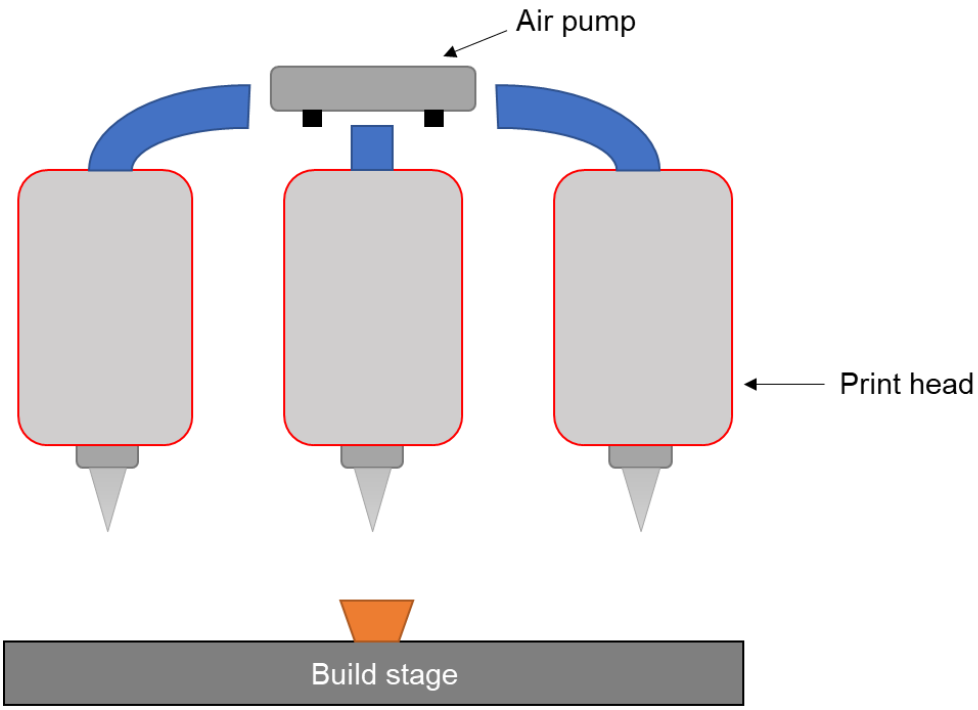

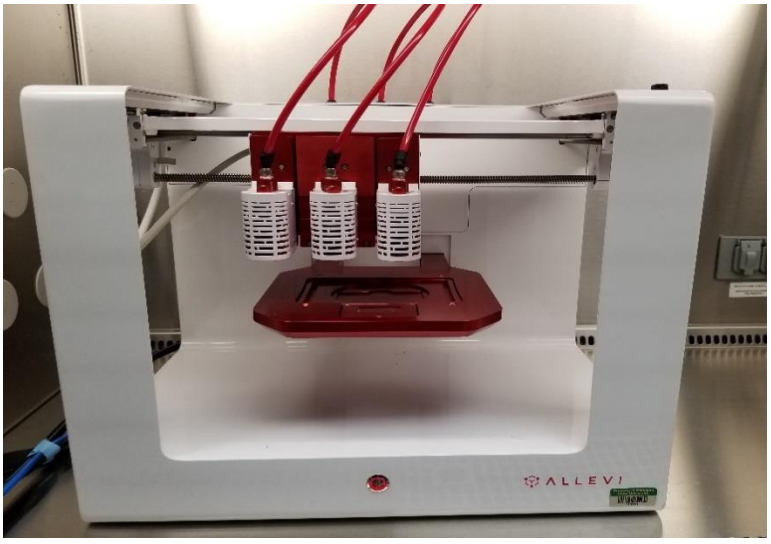

Figure 4.5: Example of bioprinting mechanism and machine. (Top) Several bioprinters have similar modes of action. Temperature controlled print heads extrude biological material out of a pre-loaded syringe, using pressurized air compressors. Typically, there is no photocuring, as UV light is damaging to cells, crosslinking agents are used instead to solidify the structure. Parameters such as extruding speed, print head and print stage temperature, and nozzle gauge size play an intricate part in creating a stable bioproduct. (Bottom) Allevi 3 bioprinter in the IQ 3D printing core.

4.3 Creating Printable Designs

Printable designs must be created on computer 3D printing software or downloaded from online websites. With the emerging popularity of 3D printing websites such as grabcad.com, thingiverse.com, and NIH 3D printing exchange, outlets for readily available files free to download already exist. Research publications that include novel 3D printed devices often include the files in supplementary materials section. However, if a novel device needs to be constructed, there is available computer modeling software online. Common software for designing 3D printed devices include Autodesk and SolidWorks. The premise of the software is to provide users freedom to design three dimensional structures and have integrated features enabling the conversion of the structures into readable print files. The following section will describe the common types of 3D printer file types listed in table 4.2.

Table 4.2: Most common 3D printing formats.

			SUPPORTED FEATURES		
EXTENSION	**Name**	**Description**	**Geometry**	**Colors**	**Texture**
.STL	Stereolithography	A mesh of surfaces as list of geometric features	x		
.OBJ	Wavefront OBJ	Text based format consisting of numbering of each line containing a key and values used for part rendering	x	x	x
.STP	Standard for the Exchange Product Data	Text format that describes objects instead of raw geometric data	x		
.AMF	Additive Manufacturing File	XML-based format allows computer design software to describe shape and composition	x	x	x
.U3D	Universal 3D	Compressed file format for 3D computer graphics software. Contains 3D model information such as triangle meshes, lighting, shading, motion data, lines and points with color and structure	x	x	x
.VRML	Virtual Reality Modeling Language	Intended for virtual reality. Text file format that specifies information such as vertices and edges of a 3D polygon.	x	x	x

4.3.1 Printable File Types

Once a 3D sketch is created in a 3D modeling software program, the object needs to be converted to a printable file recognizable by the printer. The 3D printed sketch is rendered into geometric slices or described in code through text file formats. Noteworthy in table 4.2, every 3D printing file is unique in how it renders 3D sketches, and the ability to support parameters such as texture and color. For example, stereolithography format

(.STL), the most popular 3D file format for 3D printing, however it only supports geometric features, lacking the ability to determine color and textures.(*24-26*)

Charles Hall, the inventor of SLA printer, is also responsible for the creation of the most common printing file type Standard Tessellation Language or stereolithography (.STL). The .STL file works by rendering information from each surface of the 3D sketch into triangulated sections, creating coordinates of the vertices in a text file.(*27*) Print resolution is directly correlated to the amount triangles that define a surface, henceforth, the more triangles (data) that exist, the better the resolution. Figure 4.6 visually depicts triangulation of defined surfaces in an .STL file.(*1*) The following sections will demonstrate 3D printing applications in various research demographics.

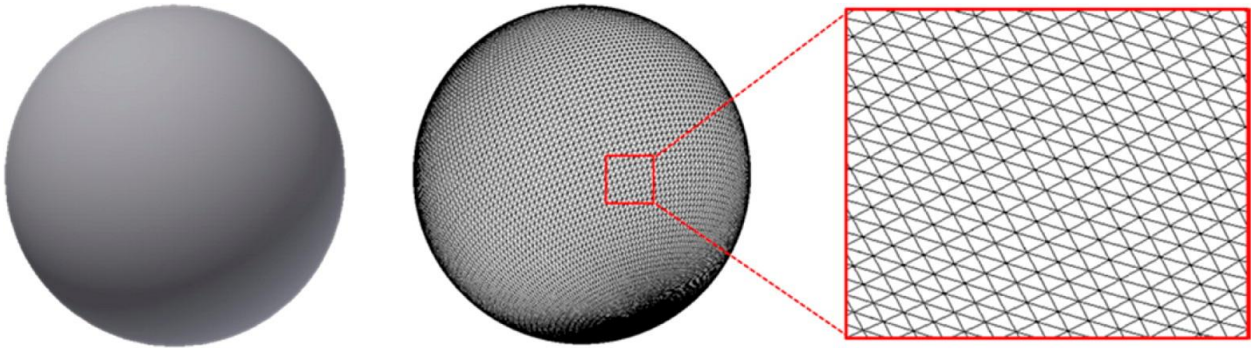

Figure 4.6: Depiction of information in an .STL file. The circle on the left, was created in Autodesk program and was subsequently saved as an .STL file. Comparing the same design, shown in the middle, is the triangulated surface of the object. The coordinates of the triangle vertices are stored in the .STL file and transmitted to the printer for fabrication.

4.4 3D Printing Applications

4.4.1 Microfluidics

3D printing has the potential to advance research in multiple fields. In the field of chemistry, 3D printed devices have extensively been used to create a variety of devices for analyte detection. For example, microfluidics, specifically, microfluidic devices produced by additive manufacturing, have been utilized for nearly a decade.(*18*) Microfluidics refers to the manipulation, control, and behavior of fluids in a small scale, often in geometrically unique channels.(*28*) To be considered truly “microfluidic” channels tend to be sub 100 µm in diameter. The first microfluidic device was constructed by gas chromatography by Terry et al.(*29*) In the 1990s, one of the first applications of microfluidics was electrophoresis based separations, on microfluidic chips constructed on silicon and glass, which was costly and time consuming.(*18*) A milestone in the field of microfluidics was the introduction of polydimethylsiloxane (PDMS) fabricated devices.(*30*) Since its discovery in device fabrication, PDMS molding has become one of the common methods to produce microfluidic devices for many reasons. Examples include ease of fabrication, cost, and properties of the material. PDMS surface is inert and does not react with many reagents, visually the material is transparent, non-cytotoxic, gas permeable, surface chemistry is modifiable, and curing occurs at lower temperatures.(*18, 31*)

However, PDMS fabrication has its disadvantages and limitations. PDMS fabrication tends to vary from lab to lab due to the tedious nature of methodologies required to generate the device. PDMS microfluidic devices have tendencies to be

rugged, enabling variations in applicable fluid levels and flow rates. However, the efficiency of soft lithography (molds) is low, resulting in labor intensive fabrication. Additionally, the properties for molds used for PDMS often have different properties, making the final PDMS product slightly different from lab to lab, and any variation in devices as small as microfluidics can cause irregularity in detection methods. 3D printing has been proposed to be the future of microfluidics as the process requires less human intervention and is highly time efficient compared to PDMS soft lithography. Recently, the Spence lab has reported novel techniques in 3D printing of truly microfluidic devices using polyjet 3D printing technologies.

Utilizing polyjet 3D printing, our group was able to create a protocol for manufacturing microfluidic devices. Importantly, there were multiple manipulations to our Stratasys J750 polyjet printer software to allow our success in printing a truly microfluidic closed system microfluidic device. For example, the 3D printer was programmed to print without the use of a carpet layer, or a bed of support material by accessing the Stratasys Parameters Manager application on the computer connected to the printer.(*32*) Within this application, the Carpet_height, Carpet_protectorZ, and ImproveSupport_ThickOfPedestal parameters were altered from their original values to zero millimeters. It should be noted that this is a nonstandard procedure and is not recommended by Stratasys. Then, the .STL file of the channel-containing device was loaded into GrabCAD Pro (Stratasys, Eden Prairie, MN).

The first device (Figure 4.7A) was printed in a rigid material (VeroClear or MED610) containing an open channel facing up. Then, without removing the device from the printer's build tray, the channel was overfilled with a solution of glycerol and isopropanol (IPA) (65:35) (Figure 4.7B). The excess solution was then removed (Figure 1C) with a 3D printed "squeegee" with a shore value of 50. The. STL of the second device was then loaded into GrabCAD in the exact position and orientation on the build-tray as the first device. By accessing the maintenance settings of the computer hosting the printer and selecting *Motor Control*, the build-tray was lowered by the exact height of the channel-containing device. The printer was instructed to print the second device directly on top of the first device, spraying the first layers of material directly onto the first device and the glycerol/IPA solution-filled channels (Figure 4.7D). The liquid photocurable resin was cured on top of the support solution sealing the two separate devices together as a single object. An exploded view (showing the order of assembly) of the entire device is shown in Figure 4.7E. For the three-component system (channels <200 μm), a base layer was printed, the build tray was lowered and then the channel layer printed. The build tray was lowered again, and the final cover layer printed.

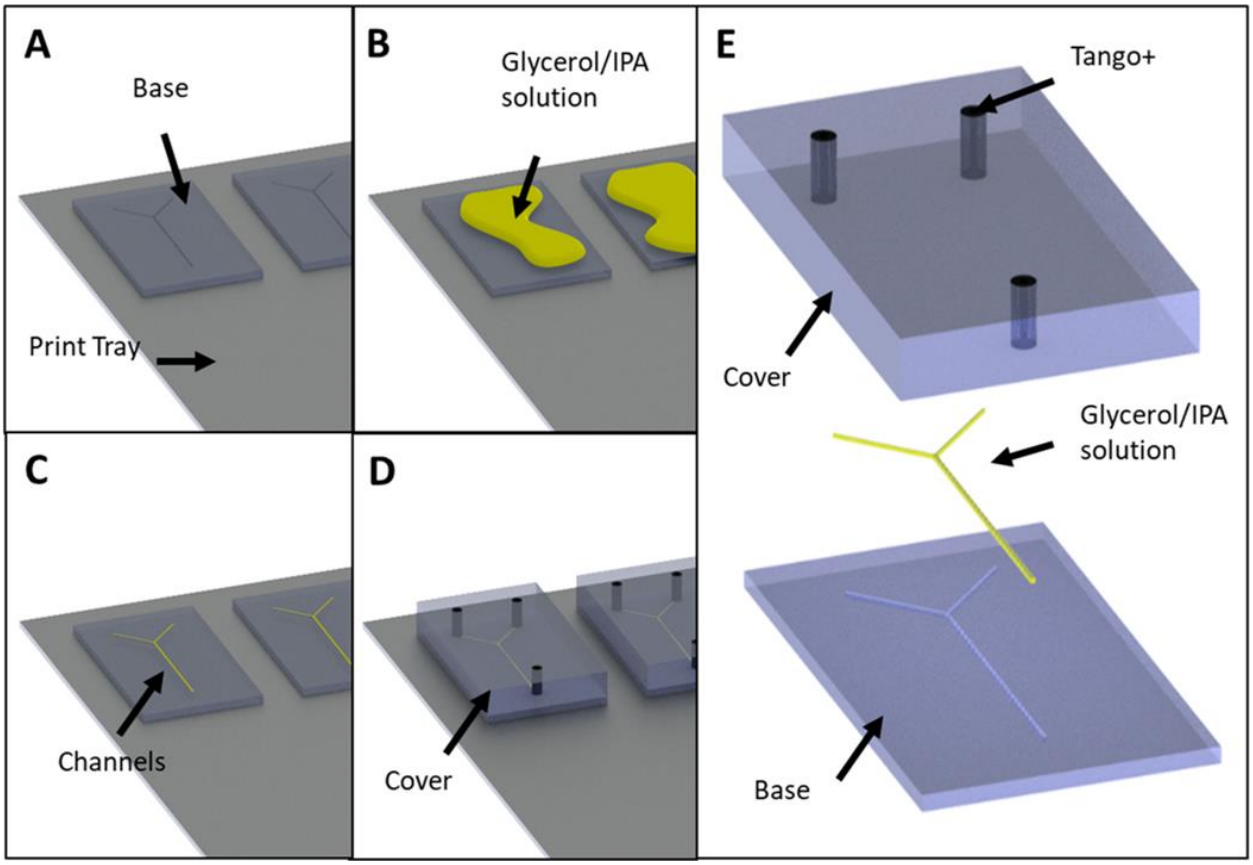

Figure 4.7: 3D sketch representation of the device fabrication process using glycerol/isopropanol support (A–E). (A) The initial base model is printed directly onto the printer stage with no support material. The surface of this base model contains an open channel. **(B)** A mixture of glycerol and isopropanol (65:35 v:v) is applied to the surface of the model, filling in the open channel. **(C)** The print stage is lowered by the height of the base model following removal of the excess glycerol mixture. **(D)** A new model is printed directly on top of the base model, thereby enclosing the channel. The ports shown in black are printed in Tango+, a rubber like material allowing for pressure-based connections to capillaries. **(E)** Exploded 3D sketch view of the final Y shaped mixing chip.

The multi material capability of the polyjet printer was utilized to make crucial connections to the device for flow-based determinations. Specifically, the rubber like resin Tango+ was incorporated into the access ports, enabling a pressure-based seal of either a steel pin or capillary. The steel pins were used when waste volume was less important,

such as the luciferin/luciferase outlet port (a continuous flow of reagent). A capillary (150 μm inner diameter, 365 μm outer diameter) was used to minimize waste volume of the injection port and could be connected directly to the device using commercially available capillary sleeves. This device has two inlets to allow RBCs to mix with the luciferin/luciferase solution and produce light in direct proportion to the concentration of ATP (figure 4.8A). A standard addition curve was generated for samples containing a 7% solution of RBCs (figure 4.8B). Data in figure 4.8C shows the statistical difference in the release of the ATP from RBCs (393 ± 137 nM) and RBCs stimulated with a prostacyclin analogue, treprostinil(*33, 34*) (1305 ± 436 nM). As stated previously, a closed system renders removal of polyjet support material difficult. We were able to manufacture a fully functional closed system without support material, to measure analyte concentrations in a biological stream of cells.

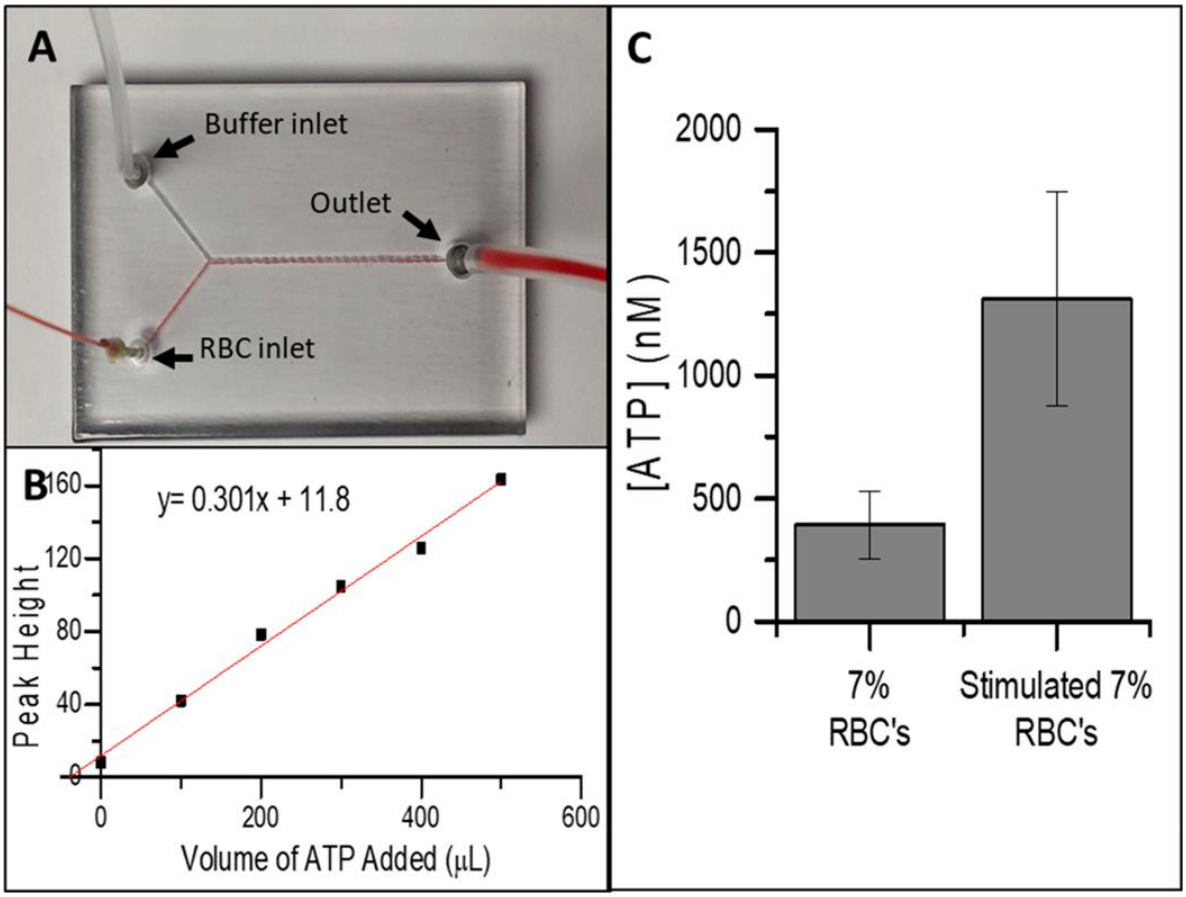

Figure 4.8: Analysis of ATP release from flowing RBCs. (A) 7% RBCs mixing with buffer. Connections made directly with capillary and compression sleeve for the RBC channel and with steel pins for the buffer and waste channels. **(B)** Standard curve for 7% RBCs. R^2 = 0.9917. **(C)** Comparison of the concentration of ATP in normal 7% RBCs and 7% RBCs stimulated with Treprostinil (n = 3).

4.4.2 Cellular Migration Devices

Cell migration is a fundamental cellular process conducted where cells migrate in response to chemical or mechanical stimuli. Commercial devices exist to measure migration, including the Boyden chamber, the micropipette-based assay, and the Dunn chamber, however, there are limitations to these devices.(*35-39*) Examples of limitations include but are not limited to, lack of real time quantification, cost, and lack of overall customization. For this reason, many researchers have resorted to fabrication of their own

migration device, typically, a microfluidic device. Here, we describe the use of polyjet printing technologies to fabricate cell migration devices.

As shown in figure 4.9, a microchannel with two reservoirs was printed directly on top of a glass slide. As described above, similar modifications to the printer software were essential in printing directly on a glass slide. The print stage was lowered to the same dimension as the thickness of a standard glass slide, while the glass slide was placed in top left corner of the print stage. An .STL file of the channel device was printed directly on top of the glass sliding. A transwell insert (Corning Inc., Corning, NY, USA) was placed in an extended slot, for the creation of a chemoattractant gradient along the channel. Fluorescein was used to characterize chemoattractant gradient, and seal (figure 4.10). This application allows for real time analysis of cell migration.

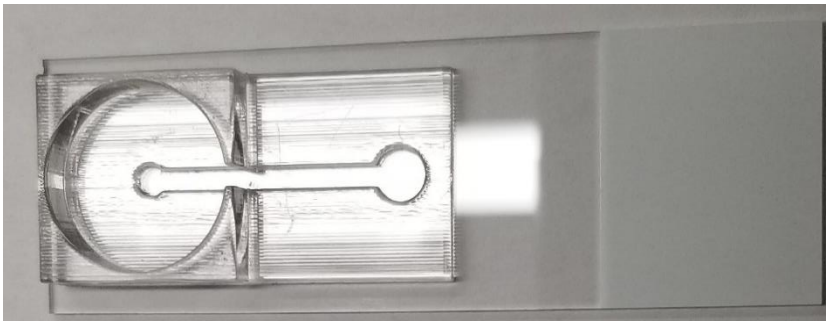

Figure 4.9: Microchannel migration device. Polyjet resin VeroClear, was sprayed directly on a glass slide forming a channel. The large opening was designed to integrate a transwell insert. The opposite well was designed with the same dimensions as the bottom of a 96 well plate to ensure proper cell densities can be calculated easily.

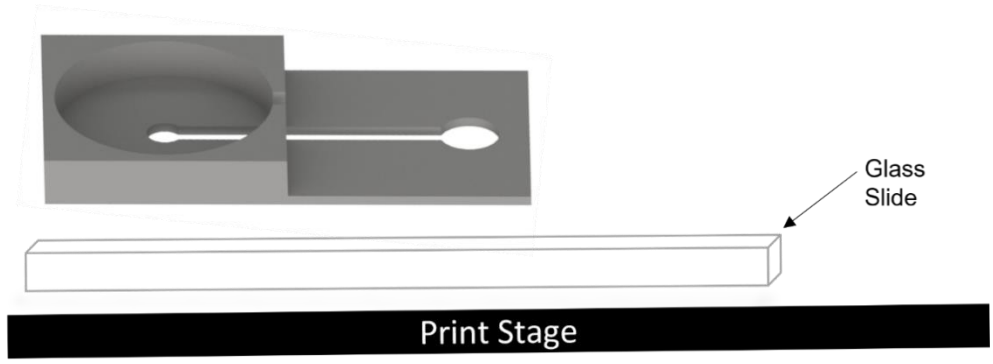

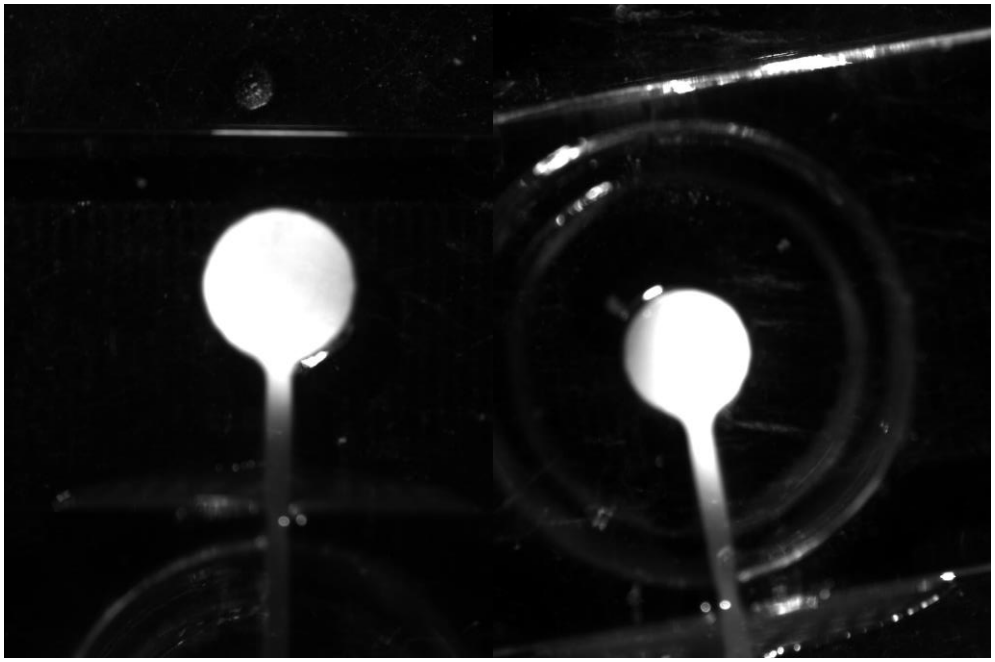

Figure 4.10: Device fabrication workflow and fluorescein detection. (Top) Stepwise, a glass slide was placed on the print stage, the stage was lowered by the same dimension as the thickness of the glass slide. The device was then printed directly on the slide and ready for use, no post print processing was necessary. (Bottom) Using fluorescein, diffusion through the transwell insert could be established in real time. The image on the left is 15 minutes after the addition of fluorescein, the image on the right is 30 minutes.

After successful fabrication of the microfluidic migration device, the next goal was to 3D print a Boyden chamber. Commercially available Boyden chambers are commonly used to determine cell migration and invasion through a polycarbonate membrane with

varying pore size. Cells are seeded in a cylinder-shaped insert on top of a membrane, the membrane separates the top and bottom well. A chemical gradient is manually created to initiate cell migration through the porous membrane. The migrant cells are quantified via staining and measurement of florescence emission in a plate reader. This system is widely accepted by researchers, however, it is known to have limitations. The lack of membrane customization has shown to be a common limitation of the product. Unless researchers purchase multiple iterations of the device, increasing cost, users are limited to few membrane types, protein matrix, pore size, and detection techniques. With polyjet printing technology, a cost effective, customizable extravasation device was created.

For the execution of this print, the printer software was modified to eliminate the printers use of support material. Additionally, there were several print-pause-print cycles used for the integration of the porous membrane (figure 4.11). Four separate .STL files were created representing the base, tango layer, and reservoir cover. After completion of the base, the staged was dropped to accommodate the height of the design, followed by printing of tango, a sticky rubber material, as an adhesive layer for the membrane. The stage was dropped to accommodate the height of the tango layer plus membrane, and immediately the reservoir cover was printed on top, sealing the device.

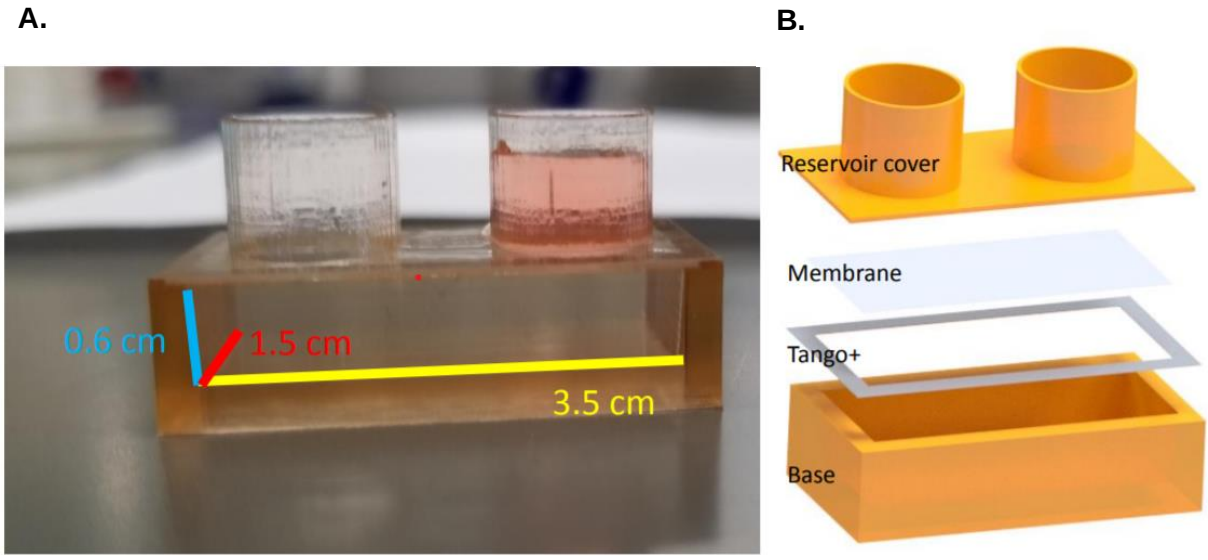

Figure 4.11: Cell migration device. (A) Cell migration device with an internal void of 0.6 cm x 1.5 cm x 3.5 cm. Reservoir for cell growth media is supported by a membrane and the membrane is intact after printing. **(B)** Exploded view of the cell migration device. In this case a tango+ layer was used to aid in adhesion of the membrane to the base layer.

While we have established 3D printing techniques for biological applications, such as the migration device capable of real time monitoring and a highly customizable cell invasion device. There are limitations to these approaches, mainly, cytotoxic effects. Early cell applications used on these devices varied daily, however, a few minor alterations to protocols were able to solve some of the cytotoxic effects. Initially, with the glass slide migration device, we observed T-cells dying shortly after their addition to the device. We found that there is residual uncured resin that leaks into the T-cell containing media. To counter act, the device was carefully wiped with 2% sodium hydroxide, then with deionized water. We observed more viable cells after this process, however, the percent viability was not sufficient. We then fully coated the device in 2.5 ug/mL fibronectin after the wiping step. The viability of the cells went up to 70%, but still needed improvement.

The next solution was coating the device in 4% polystyrene, prior to the addition of fibronectin. Through the combination of 2% sodium hydroxide cleaning, 4% polystyrene coating, and 2.5 ug/mL, we were able to obtain a satisfactory percent viability. In the cell invasion device, we were able to purchase a resin from Stratasys, MED610, a biocompatible resin, which has been graded for medical device and dental implantation. Switching to MED610 allowed us to successfully seed an endothelial monolayer on the integrated porous membrane. The next section will outline the 3D scaffolding efforts using FDM technology and fiber spinning technology.

4.4.3 3D Scaffolding and Tissue Engineering

Each year in the United States, there is an increase in individuals suffering from organ failure and dysfunction resulting from tissue damage or disease.(*40*) One way many researchers try to combat a lack of therapeutic actions using regenerative medicine, particularly, tissue engineering. The process of tissue engineering is discipline of biomedical engineering aimed to regenerate damaged tissue through cell manipulation, material science, and biochemical processes.(*41*) The first step in tissue engineering is the formation of scaffolds, a three dimensional base biochemically suitable for cells to adhere and proliferate.(*42*)

Historically, methods for creating scaffolds include solvent casting particulate leaching, fiber meshes, phase separation, and freeze drying.(*42*) Many limitations are associated with these methods, often resulting in poor distribution of cells from factors such as high mechanical strength and excess connectivity of scaffolds.(*42*) Adequate cell

distribution is necessary to promote an environment promoting proliferation and proper vessel formation.(*43*) For example, if endothelial cells placed on a scaffold are not aligned correctly, subsequent failure to form proper vessels follow.(*44*) Osteoblasts will form clusters if the environment of the scaffold are inadequate.(*45*) To overcome these obstacles, many tissue regenerative/scaffolding researchers have made a push to 3D printing to form scaffolds.

With a strong collaborative effort in the Spence lab with Cody Pinger PhD and Erin Bosman, we were able to modify an FDM printer to be equipped with a blow spinning apparatus for spinning fibers onto 3D printed devices and successfully attach endothelial cells in a 3D scaffold. Solution blow spinning is a process where a polymer solution is dissolved in a volatile solvent and pressurized air flows around the polymer solution to create and distribute fibers on a surface, seen in figure 4.12.(*46*) This method is capable of producing micro and nano scale fibers at a very high production rate. Figure 4.13 shows the holding apparatus and blow spinner attachment to the Prusa MKS3 FDM printer.

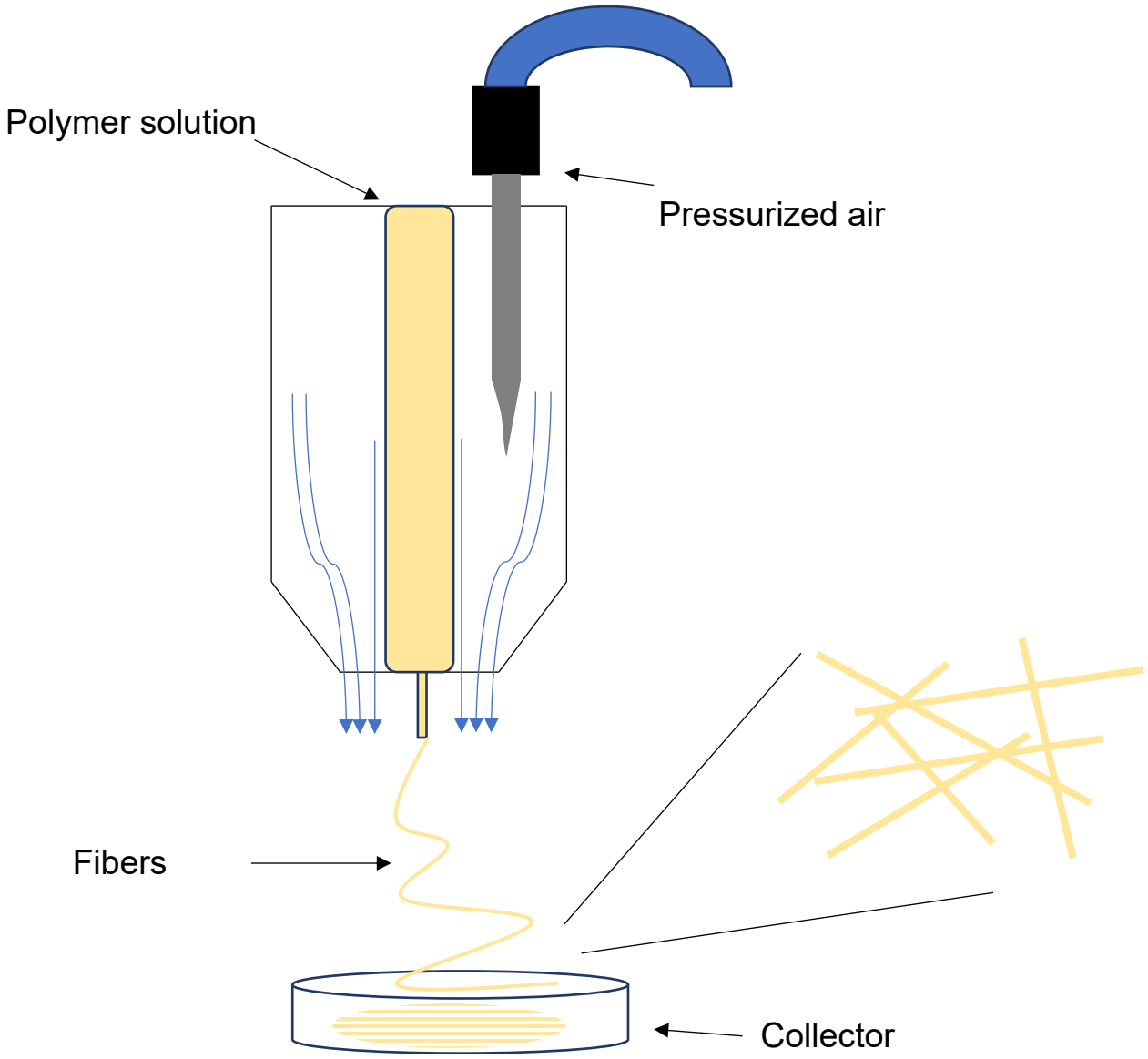

Figure 4.12: Schematic for a solution blow spinning device. A protein or polymer solution slowly flows through a tubing forming solution droplets. A stream of focused pressurized air acts on the solution, evaporating the solution, producing a web of fibers ejected towards a collector.

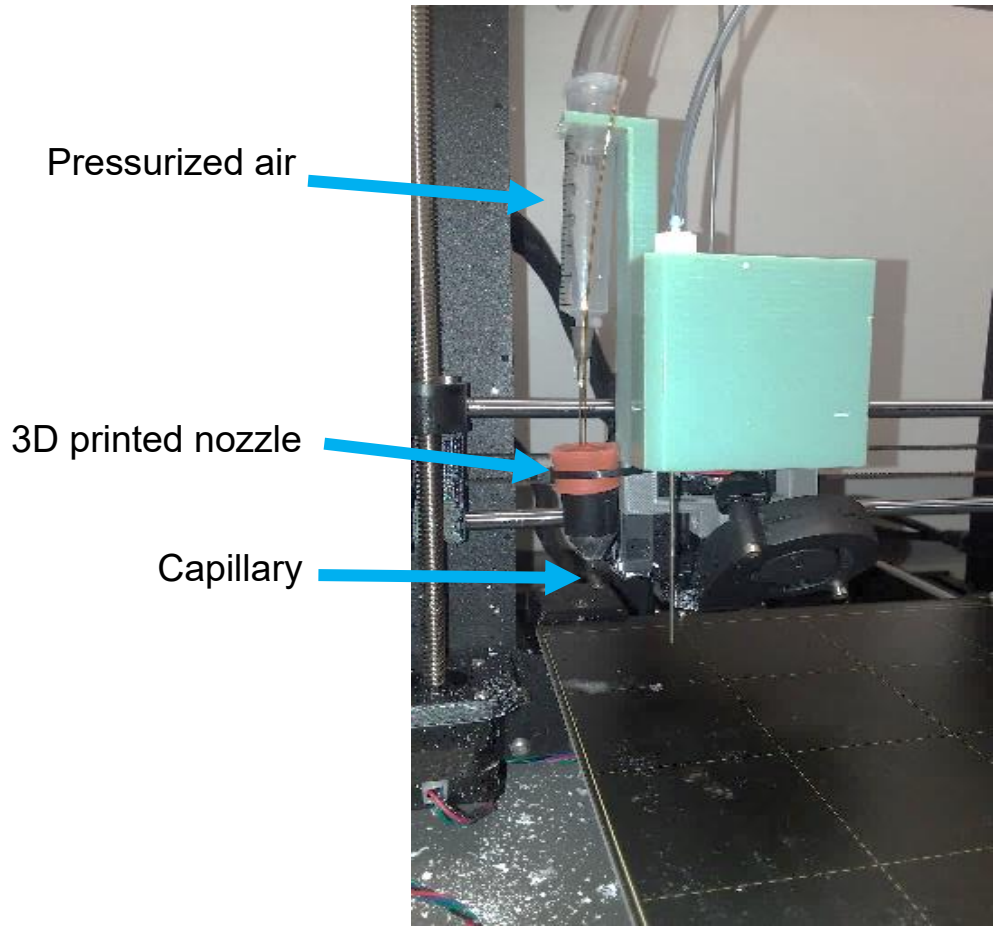

Figure 4.13: "Bioprinting" modification of a commercially available FDM printer. A holding apparatus was attached to the gantry of the FDM printer, containing an opening for a syringe which is the pressurized air source. The 3d-printed nozzle has a rubber septum on top, the compressed air comes through a syringe and through this septum. Additionally, the protein solution is flowed through a fused silica capillary (inner diameter 150 µm) runs through the nozzle and is exposed a centimeter out of the bottom of the nozzle. The design follows standard solution blow spinning protocol in which compressed air focuses around the end of the capillary which slowly extrudes protein solution, is immediately forced into a small stream of fibers.

With the success of modifying the FDM printer for solution blow spinning, the device was then characterized by blow spinning gelatin fibers. As listed in table 4.3, a series of parameters were optimized to produce sub 10 µm gelatin fibers directly integrated into a printed device. Capillary inner diameter, gelatin concentration, air pressure (PSI), and solution flow rate were optimized to produce an adequate 3D gelatin matrix seen in figure 4.14.

Table 4.3: Identified parameters for synthesis of gelatin fibers.

Gelatin solution	PSI	Capillary I.D.	Flow rate
40% (m/v) gelatin/acetic acid	55 psi air pressure	150 µm I.D.	200 µl/hr

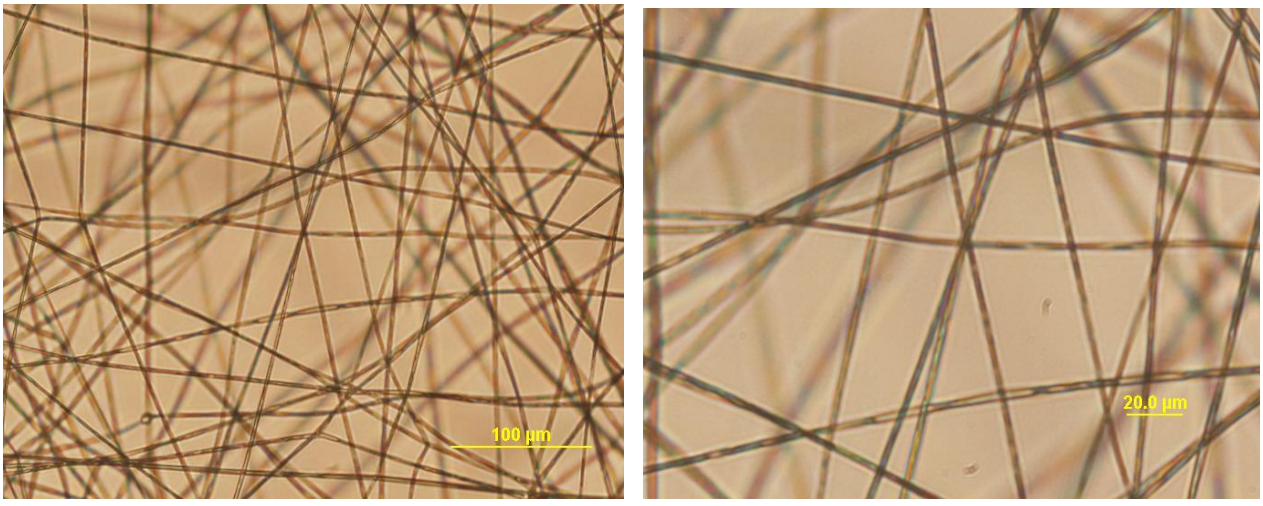

Figure 4.14: Microscopy analysis of blow spun gelatin fibers. Post optimization of parameters previously described, sub 10 µm gelatin fibers were produced in an overlapping orientation, similar to what is observed in in vivo matrices.

To test the effectiveness of our 3D matrix, bovine pulmonary arterial endothelial cells (BPAEC) were integrated into a three-channel 3D printed device. A 3D sketch of a channel device was created in Autodesk inventor, and converted to .gcode file, a computer language numerical control file, readable to the modified Prusa MKS3 FDM printer. Shown in figure 4.15, the printer began fabricating the channel device using polylactic acid (PLA) thermoplastic, prior to the layers containing the channels being laid, we paused the print. The gantry was raised, by manipulating the Z-axis, allowing proper distance to conduct gelatin blow spinning protocol. The gelatin fibers were produced directly on the part using the parameters described in table 4.3, until the device was fully covered in fibers. The printing was then resumed, fully integrating the fibers in the device. The gelatin fibers were then crosslinked using genipin, a chemical compound commonly used to crosslink gelatin and collogen.(*47*) RPMI media containing BPAEC's was added directly to the channels, adhering overnight in a CO2 incubator at 37 °C. Fluorescent microscopy of the cells was conducted using SYTOX^{TM} green staining (figure 4.16).

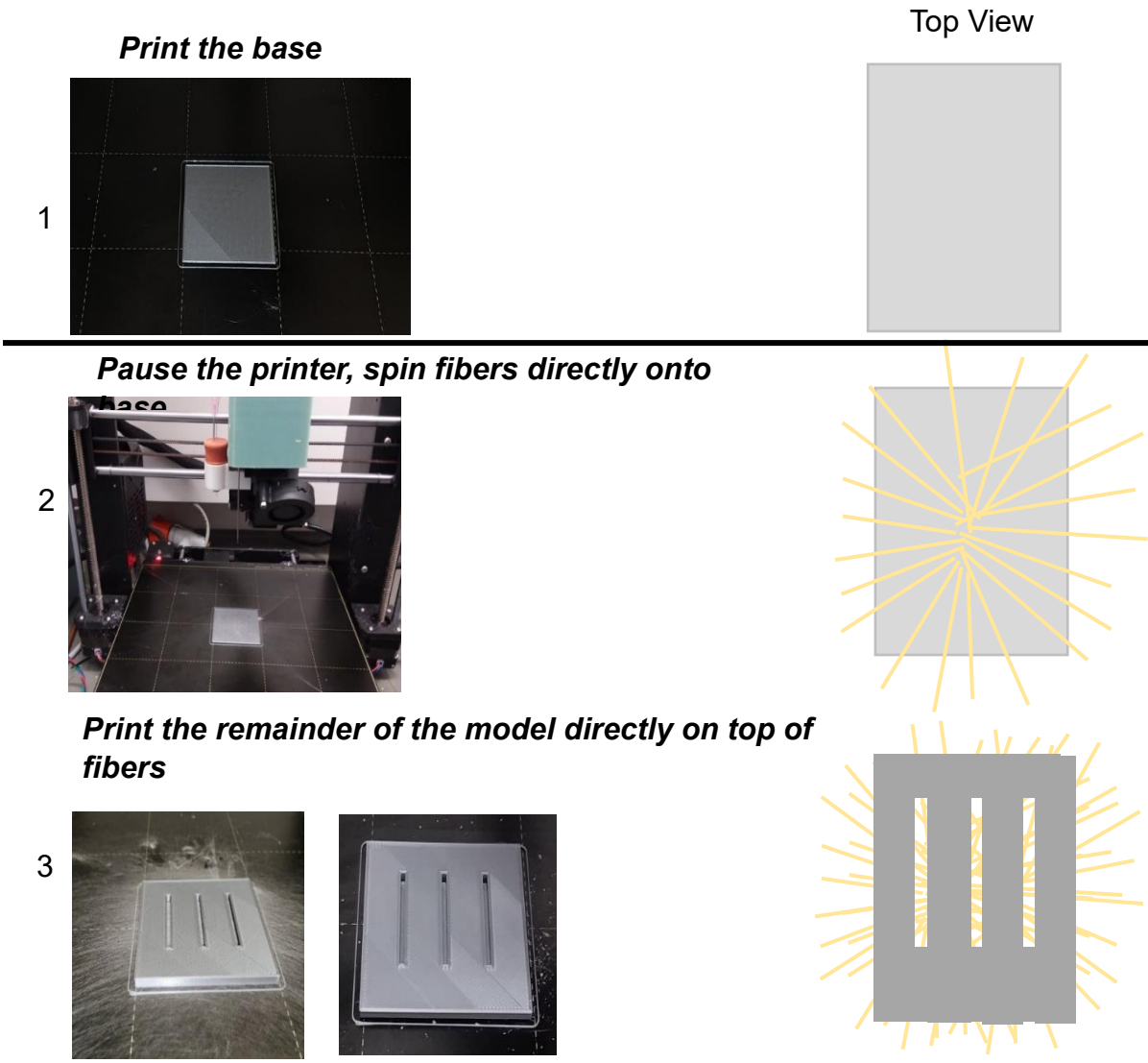

Figure 4.15: Integration of gelatin fibers in a 3D printed channel device. A PLA printed channel device was printed using FDM technology. The part was paused approximately halfway through the print process to blow spin gelatin fibers directly on the device. The orientation and stacking of the fibers are synonymous to in vitro orientation of extracellular matrices. Once covered in fibers, the print is resumed exposing fibers on the bottom of channels.

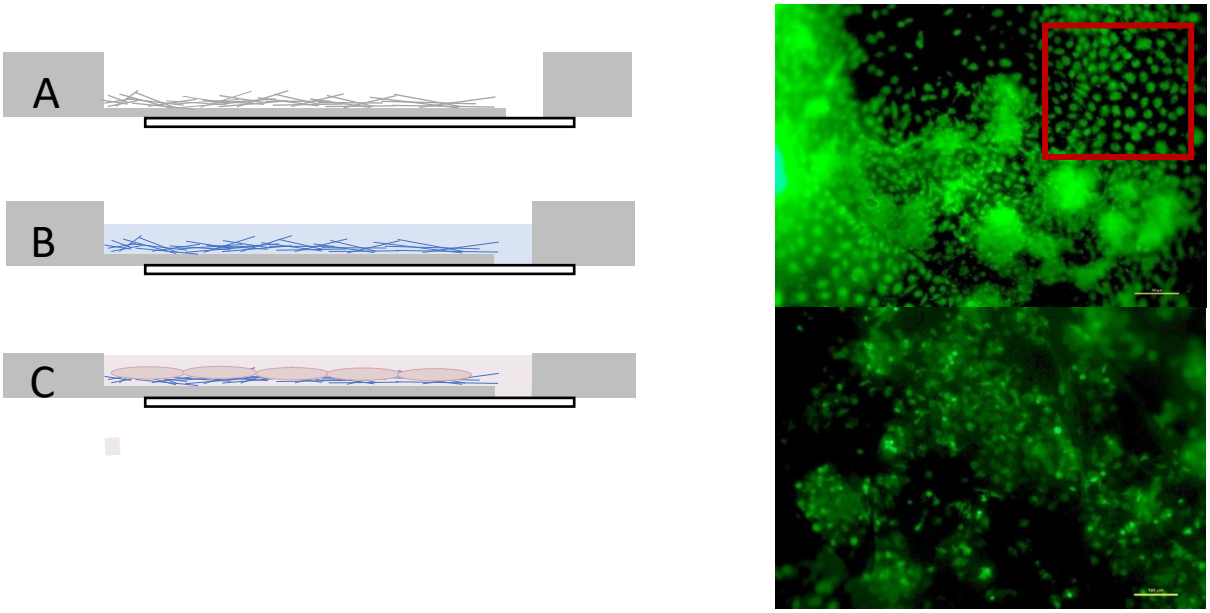

Figure 4.16: Integration of BPAECs. A. fabrication of gelatin fibers into channels. B. Cross linking step using a genipin solution. C. Seed BPAEC onto cross linked fibers overnight. Using SYTOX^{TM} green staining, visual representation of attachment and confirmation of morphological changes in endothelial cell elongation.

4.5 Discussion

Additive manufacturing has shown to be an effective tool for STEM research. Researchers can produce customized products specifically to their research needs. Here, we were able to utilize 3D printing technology to produce in vitro models, mimicking in vivo properties. A truly microfluidic device was fabricated that has potential applications in both analytical chemistry and biological disciplines. Further, we provided a technical method of modifying printer settings to rid the devices of problematic support material, while functionally proving successful analysis of analyte detection. Using our technique, µM levels of ATP release from RBC were quantified, showing reproducibility and detection limits of the microfluidic device. It is important to note that while we were able to

successfully produce support free microfluidic devices using poly jet technology, we did observe some cytotoxicity of the cells directly from the resin.

Along with the creation of microfluidic devices, we were able to fabricate two versions of cell migration devices rapidly, and at a fraction of the typical cost of these devices. To solve the lack of customization of commercially available migration devices, we established a rapid and effective method for the production for real time cell migration devices. Although the method posed limitations, we were able to troubleshoot using simple post processing modifications. Real time quantification of migration allows researchers to determine duration of assays, saving the research lab precious time and reagent resources. A novel method of printing on glass with a watertight seal, allows for fabrication of a microfluidic device that is not limited to only cell migration studies, but diffusion and pharmacokinetic measurements as well.

With the rise of regenerative medicine, we were able to establish a method for producing a fully functional gelatin 3D matrix using a modified FDM printer. Manipulation of specific parameters allowed for the production of sub 10 μm diameter gelatin fibers, directly integrated into a channel device. It was important to identify the elongation of endothelial cells, as that is a key indicator of proper attachment to the matrix.(*48*) Since the device was integrated into a channel device, there is potential to conduct flow based studies for the detection of several cellular functions, including immune cell attachment to the cultured monolayer, endothelial cell secretions, such as cytokines and nitric oxide, and organ on a chip applications. Figure 4.17 shows preliminary application of a flow-based system our lab synthesized.

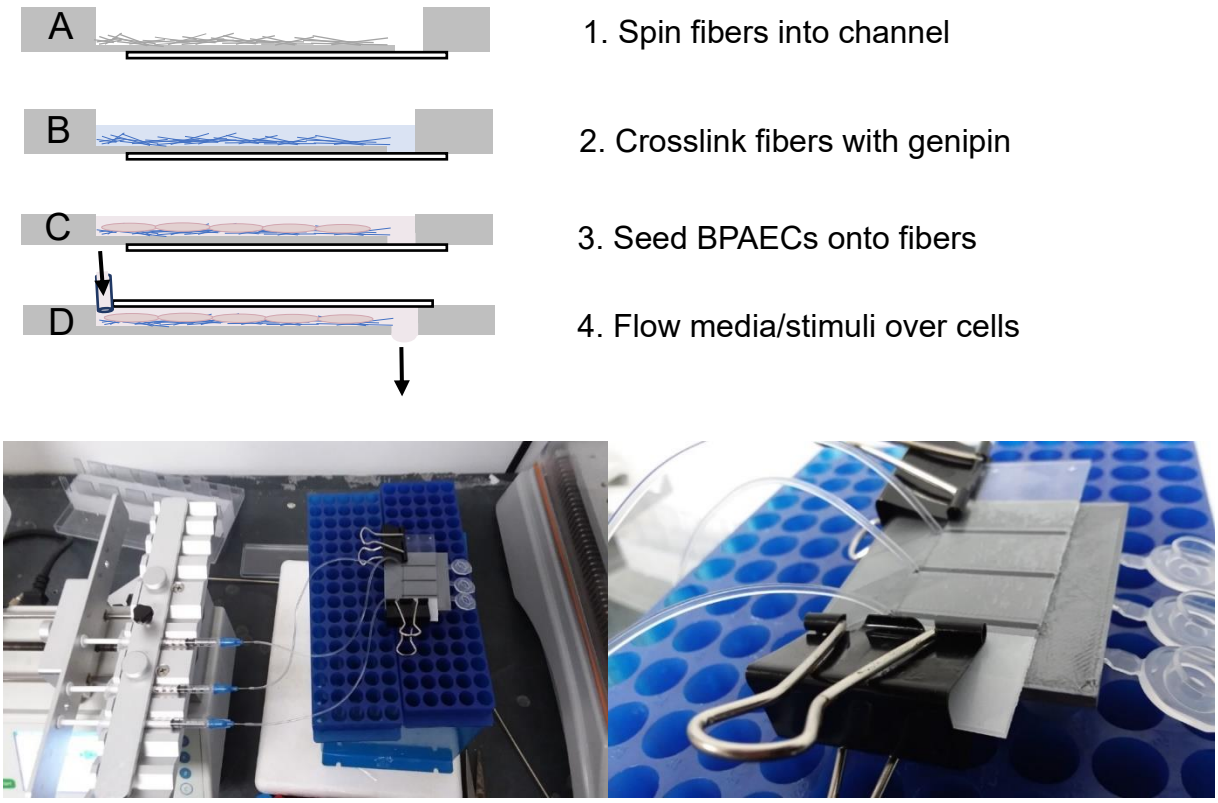

Figure 4.17: Flow based application of fiber device. Steps **A-C** were previously described in figure 4.15. **D.** A cover lip was bound to the device allowing for media to flow across the channel without overflowing the channels. A whole was integrated in the 3D sketch allowing drops of media to be collected into centrifuge tubes. A peristaltic pump with pre-loaded media in syringes were slowly extruded, creating a continuous flow-based system. The syringes can be loaded with a solution of the researchers desires, allowing this device to be a customizable detection mechanism.

Overall, 3D printing and additive manufacturing can be a powerful, cost-effective multidisciplinary tool for researchers. This chapter has summarized the history and types of 3D printing, and downstream applications. The future of 3D printing will trend more towards research applications, rather than prototyping seen historically. While technology advances, 3D printing technologies will continue to improve in material capabilities, resolution, and biological applications. To conclude, we have shown several potential

capabilities of 3D printing, applicable to industries such as health care, sciences, and medical devices.

REFERENCES

REFERENCES

1. B. C. Gross, J. L. Erkal, S. Y. Lockwood, C. Chen, D. M. Spence, Evaluation of 3D printing and its potential impact on biotechnology and the chemical sciences. *Anal Chem* **86**, 3240-3253 (2014).

2. G. M. Whitesides, The origins and the future of microfluidics. *Nature* **442**, 368-373 (2006).

3. F. P. Melchels, J. Feijen, D. W. Grijpma, A review on stereolithography and its applications in biomedical engineering. *Biomaterials* **31**, 6121-6130 (2010).

4. C. W. Hull. (UVP, Inc., United States, 1984).

5. ALL3DP. The Types of 3D Printing Technology of 2021. https://all3dp.com/1/types-of-3d-printers-3d-printing-technology/

6. J. R. Tumbleston *et al.*, Additive manufacturing. Continuous liquid interface production of 3D objects. *Science* **347**, 1349-1352 (2015).

7. J. W. Stansbury, M. J. Idacavage, 3D printing with polymers: Challenges among expanding options and opportunities. *Dent Mater* **32**, 54-64 (2016).

8. M. J. Beauchamp, G. P. Nordin, A. T. Woolley, Moving from millifluidic to truly microfluidic sub-100-μm cross-section 3D printed devices. *Anal Bioanal Chem* **409**, 4311-4319 (2017).

9. P. A. Webb, A review of rapid prototyping (RP) techniques in the medical and biomedical sector. *J Med Eng Technol* **24**, 149-153 (2000).

10. Z.-X. Low *et al.*, Perspective on 3D printing of separation membranes and comparison to related unconventional fabrication techniques. *Journal of Membrane Science* **523**, 596-613 (2017).

11. X. Wang, Y. Yan, R. Zhang, Rapid prototyping as a tool for manufacturing bioartificial livers. *Trends Biotechnol* **25**, 505-513 (2007).

12. S. Ko. All-inkjet-printed flexible electronics fabrication on a polymer substrate by low-temperature high-resolution selective laser sintering of metal nanoparticles (Nanotechnology, 2007), vol. 18.

13. H. N. Chia, B. M. Wu, Recent advances in 3D printing of biomaterials. *J Biol Eng* **9**, 4 (2015).

14. A. Razavykia, E. Brusa, C. Delprete, R. Yavari, An Overview of Additive Manufacturing Technologies-A Review to Technical Synthesis in Numerical Study of Selective Laser Melting. *Materials (Basel)* **13**, (2020).

15. D. Ibrahim *et al.*, Dimensional error of selective laser sintering, three-dimensional printing and PolyJet models in the reproduction of mandibular anatomy. *J Craniomaxillofac Surg* **37**, 167-173 (2009).

16. S. Vock, B. Klöden, A. Kirchner, Powders for powder bed fusion: a review. *Prog Addit Manuf*, 383-397 (2019).

17. A. S. Munshi, R. S. Martin, Microchip-based electrochemical detection using a 3-D printed wall-jet electrode device. *Analyst* **141**, 862-869 (2016).

18. C. Chen *et al.*, 3D-printed Microfluidic Devices: Fabrication, Advantages and Limitations-a Mini Review. *Anal Methods* **8**, 6005-6012 (2016).

19. A. D. Castiaux *et al.*, PolyJet 3D-Printed Enclosed Microfluidic Channels without Photocurable Supports. *Anal Chem* **91**, 6910-6917 (2019).

20. A. D. Castiaux *et al.*, PolyJet 3D-Printed Enclosed Microfluidic Channels without Photocurable Supports. *Analytical Chemistry* **91**, 6910-6917 (2019).

21. P. M. Crapo, T. W. Gilbert, S. F. Badylak, An overview of tissue and whole organ decellularization processes. *Biomaterials* **32**, 3233-3243 (2011).

22. J. Glowacki, S. Mizuno, Collagen scaffolds for tissue engineering. *Biopolymers* **89**, 338-344 (2008).

23. H.-W. Kang, Y. Tabata, Y. Ikada, Fabrication of porous gelatin scaffolds for tissue engineering. *Biomaterials* **20**, 1339-1344 (1999).

24. N. Farahani *et al.*, Three-dimensional Imaging and Scanning: Current and Future Applications for Pathology. *J Pathol Inform* **8**, 36 (2017).

25. S. Park, L. Pantanowitz, A. V. Parwani, Digital imaging in pathology. *Clin Lab Med* **32**, 557-584 (2012).

26. S. Hällgren, L. Pejryd, J. Ekengren. (Procedia CIRP, 2016), vol. 50, pp. 518-523.

27. A. Dolenc, I. Mäkelä, *Slicing procedures for layered manufacturing techniques*. (Computer-Aided Design, 1994), vol. Volume 26.

28. T. Fujii. (Microelectronic Engineering, 2002), vol. 61-62, pp. 907-914.

29. T. SC*,* J. JH, Ed. (IEEE, IEE Transactions on Electron Devices, 1979), vol. 26, pp. 1880-1886.

30. D. C. Duffy, J. C. McDonald, O. J. Schueller, G. M. Whitesides, Rapid Prototyping of Microfluidic Systems in Poly(dimethylsiloxane). *Anal Chem* **70**, 4974-4984 (1998).

31. J. Zhou, A. V. Ellis, N. H. Voelcker, Recent developments in PDMS surface modification for microfluidic devices. *Electrophoresis* **31**, 2-16 (2010).

32. A. D. Castiaux, C. W. Pinger, D. M. Spence, Ultrafiltration binding analyses of glycated albumin with a 3D-printed syringe attachment. *Anal Bioanal Chem* **410**, 7565-7573 (2018).

33. N. Ghonem *et al.*, Treprostinil, a prostacyclin analog, ameliorates ischemia-reperfusion injury in rat orthotopic liver transplantation. *Am J Transplant* **11**, 2508-2516 (2011).

34. M. Ding *et al.*, Treprostinil reduces mitochondrial injury during rat renal ischemia-reperfusion injury. *Biomed Pharmacother* **141**, 111912 (2021).

35. S. BOYDEN, The chemotactic effect of mixtures of antibody and antigen on polymorphonuclear leucocytes. *J Exp Med* **115**, 453-466 (1962).

36. S. H. Zigmond, Ability of polymorphonuclear leukocytes to orient in gradients of chemotactic factors. *J Cell Biol* **75**, 606-616 (1977).

37. B. Heit, P. Kubes, Measuring chemotaxis and chemokinesis: the under-agarose cell migration assay. *Sci STKE* **2003**, PL5 (2003).

38. B. Petri, M. J. Sanz, Neutrophil chemotaxis. *Cell Tissue Res*, (2018).

39. D. Zicha, G. Dunn, G. Jones, Analyzing chemotaxis using the Dunn direct-viewing chamber. *Methods Mol Biol* **75**, 449-457 (1997).

40. Organ Donations Statistics. Health Resources & Services Administration. https://www.organdonor.gov/learn/organ-donation-statistics#

41. D. Howard, L. D. Buttery, K. M. Shakesheff, S. J. Roberts, Tissue engineering: strategies, stem cells and scaffolds. *J Anat* **213**, 66-72 (2008).

42. A. V. Do, B. Khorsand, S. M. Geary, A. K. Salem, 3D Printing of Scaffolds for Tissue Regeneration Applications. *Adv Healthc Mater* **4**, 1742-1762 (2015).

43. S. Yang, K. F. Leong, Z. Du, C. K. Chua, The design of scaffolds for use in tissue engineering. Part I. Traditional factors. *Tissue Eng* **7**, 679-689 (2001).

44. E. Sachlos, J. T. Czernuszka, Making tissue engineering scaffolds work. Review: the application of solid freeform fabrication technology to the production of tissue engineering scaffolds. *Eur Cell Mater* **5**, 29-39; discussion 39-40 (2003).

45. S. Wüst, R. Müller, S. Hofmann, Controlled Positioning of Cells in Biomaterials-Approaches Towards 3D Tissue Printing. . *Journal of functional biomaterials*, 119–154 (2011).

46. M. Vural, A. M. Behrens, O. B. Ayyub, J. J. Ayoub, P. Kofinas, Sprayable elastic conductors based on block copolymer silver nanoparticle composites. *ACS Nano* **9**, 336-344 (2015).

47. K. Výborný *et al.*, Genipin and EDC crosslinking of extracellular matrix hydrogel derived from human umbilical cord for neural tissue repair. *Sci Rep* **9**, 10674 (2019).

48. M. J. Levesque, R. M. Nerem, The elongation and orientation of cultured endothelial cells in response to shear stress. *J Biomech Eng* **107**, 341-347 (1985).

Chapter 5 - Overall Conclusion and Future Directions

5.1 Overall Conclusion

The overall goal of the thesis is to further describe the role of immune cell homeostasis in autoimmune diseases. Immune cell function in individuals with type 1 diabetes (T1D), are hindered, showing slower reaction time to eradicate infections. We have shown the potential role of C-peptide administration increasing both activation and function on neutrophils. Previous Spence lab research identified similar characteristics in C-peptide and Zn^{2+} binding, as well as metabolic changes in red blood cells (RBC). RBCs only bind C-peptide in the presence of albumin, and observed increased Zn^{2+} uptake in the presence of C-peptide. Additionally, the Spence group observes no changes in RBC metabolism without the presence of Zn^{2+}. A commonality between immune cells and RBCs is the presence of glucose transporter 1 (GLUT1). Unlike insulin, which acts on GLUT4 containing cells (smooth muscle, adipose tissue), we have uncovered insulin like changes on GLUT1 containing cells via C-peptide, Zn^{2+}, and albumin stimulation.

Our early studies aimed to investigate similar C-peptide binding characteristics and metabolic changes seen in RBCs on immune cells. Interestingly, we only see C-peptide binding to neutrophils in the presence of albumin, and observe significantly more Zn^{2+} uptake in the presence of C-peptide. Further, we only see significant difference in downstream metabolic and functional changes in the presence of the entire complex, C-peptide, Zn^{2+}, and albumin. Initial changes in C-peptide concentration added to immune

cells were necessary to adjust to the smaller cell density of immune cells compared to RBCs. Here, we added 200 pM C-peptide to neutrophils and observed a bound concentration of ~$9x10^3$ per cell. In RBCs, ~ $2x10^3$ C-peptide molecules per cell were observed. We concluded the increase in the amount of C-peptide binding to the differences in size between the two cells. Red blood cells are ~ 7 µm in diameter with 1.7 to 2.2 µm in thickness, compared to the neutrophil that is ~ 15 µm in diameter.(*1, 2*) Further, cytosolic volume of a RBC is ~ 94 μm^3, while neutrophils have been identified having ~ 280 μm^3 cytosolic volume.(*2, 3*) With these distinguishing size characteristics, we conclude that the discrepancies between bound C-peptide concentrations is due to neutrophils being larger than RBCs.

Zn^{2+} homeostasis is important for several immune cell intracellular signaling pathways.(*4, 5*) Zn^{2+} homeostasis is controlled by Zn^{2+} transporters that regulate intracellular Zn^{2+} concentration, regulating mechanisms such as apoptosis, proliferation and differentiation, membrane rigidity, and receptor transmigration.(*4, 6*) To investigate Zn^{2+} binding, we utilized radiolabeled Zn^{2+} ($^{65}Zn^{2+}$). When 20 nM $^{65}Zn^{2+}$ was added to a solution of neutrophils, we observed an uptake of ~1.5 pM/10^6 cell. However, in the presence of C-peptide, we observed an increase in $^{65}Zn^{2+}$ uptake to ~2.9 pM/10^6 cell. The observed findings correlate with previous Spence lab research, in that more Zn^{2+} is taken up by GLUT1 containing cells in the presence of C-peptide. Interestingly, when the experiment was repeated with a different immune cell, T-cells, we observed significantly more uptake of $^{65}Zn^{2+}$ in the absence of C-peptide.

Key response in early immune factors increased in response to C-peptide, Zn^{2+} and albumin. Presented data described a significant increase in reactive oxygen species (ROS) via measurement of H_2O_2, a byproduct of several ROS synthesis.(*7, 8*). Compared to the control sample, we observed a 15% increase of ROS formation when neutrophils were exposed our C-peptide formulation. Increased ROS results in improvement in antimicrobial activity, regulated inflammatory response, and overall host immunity improvement.(*9*) Previous data collected in the Spence lab reports an increase in intracellular Ca^{2+} shown in figure 5.1. Intracellular Ca^{2+} is an important key factor in several immune cell signaling pathways, and subsequent immune cell activation.(*10-12*) Chapter 2 further described the administration of C-peptide, Zn^{2+} and albumin complex as a contributor to immune cell activation, with further evidence of C-peptide as a biologically relevant molecule post cleaving from insulin.

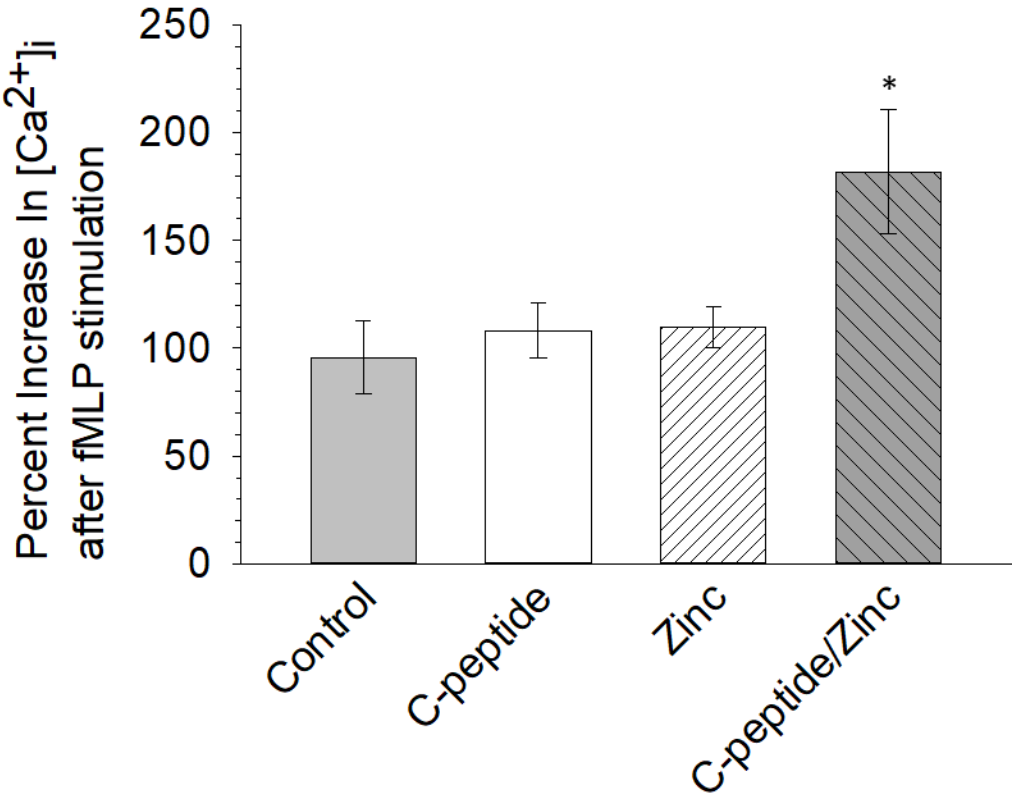

Figure 5.1: Intracellular Ca^{2+} increase in neutrophils. Neutrophils were stimulated with N-Formylmethionyl-leucyl-phenylalanine (fMLP), a peptide released from bacteria, to induce activation. Neutrophils were simultaneously exposed to three different conditions, C-peptide alone, Zn^{2+} alone, and the combination of C-peptide and Zn^{2+}. As measured by fura 2, a Ca^{2+} binding molecule with an excitation of 380 nm and emission of 510 when bound to Ca^{2+}, a significant increase in intracellular calcium was observed only in the presence of both C-peptide and Zn^{2+}. ($n \geq 4$, error=SEM, $*p < 0.005$)

5.1.1 Blood Circulating Components and NETosis

Novel investigations into the role of blood circulating components effecting neutrophil NETosis was reported in chapter 3. To describe NETosis dysregulation, upregulated circulating components (ATP, Zn^{2+}, albumin) present in individuals with Multiple Sclerosis (MS) were administered to human control and MS neutrophils. On control neutrophils, we observed a significant increase in NET formation when stimulated

by RBC derived (ATP). Interestingly, when ATP was derived from MS RBCs, we see heightened response in NET formation, concluding that MS RBCs may be a potential source for the observed blood circulating ATP levels in MS, that subsequently contributes to NETosis dysregulation. ATP acts through purinergic receptor signaling, thus for further confirmation ATP is specifically increasing NET formation, we chemically blocked purinergic receptors with PPADs, a purinergic receptor antagonist. Although not statistically different, we observed a decrease in NET formation as we increased the concentration of PPADs. We believe there are two future steps to see significant decreases in NET formation with PPADs administration. The PPAD concentration of 2-4 µM may be inadequate in competing with the administered concentration of ATP. Secondly, PPADs and ATP were administered simultaneously, since ATP is a natural agonist for purinergic receptors, ATP may bind at faster rates than PPADs. A short incubation of neutrophils with PPADs for ~ 2-3 minutes prior to ATP administration may give PPADs proper time to compete with ATP.

Further investigation of blood circulating components effect on NETosis, showed promising preliminary results of Zn^{2+}. It is reported that individuals with MS have increased circulatory levels of Zn^{2+}.(*13*) This dissertation provided the first evidence of Zn^{2+} having a direct effect on NET formation. This preliminary data shows an increase, although non-significant, in NET formation when neutrophils are exposed to exogenous Zn^{2+}. Additionally, we identified the highly abundant protein albumin, as a potential role in NETosis. When albumin was removed from the buffer, we measured a significant decrease in NET formation. Albumin is a known carrier protein, capable of carrying ions,

peptides, and molecules. It is important to note that abnormal albumin extravasation through the blood brain barrier is observed, allowing the protein to carrier factors that may contribute to NET formation.(*14*) We believe increasing the sample size of the experiment will decrease the error, as working with human immune cells poses discrepancies such as health conditions of the donor, sleep, and nutrition, altering immune cell function.

5.1.2 3D Printing Applications

As improvements to 3D printing technologies increase, devices and fabrication techniques presented in this dissertation further provide insight into future applications. Our novel modifications to print parameters allowed for the fabrication of innovative biological in vitro models. Previous fabrication methods to produce microfluidic devices often required lengthy hands-on methodology, leading to device variability lab to lab and subsequent inconsistency in data and device reproducibility. Our novel method of fabricating microfluidic devices is cost efficient, rapid, and requires fewer handling steps. Alterations of printer settings (carpet height, carpet protector Z, improve thickness of pedestal), allowed for printing without problematic support material clogging the channels. Further, segmenting the device into separate parts made it possible to integrate membranes over the channel. With our device we were able to sustain a continuous flow of a blood solution through 150 µm channels, and measure ATP release from RBCs, showing a fully functional microfluidic device is achievable using this method.

Commercially available cellular invasion assays are costly and lack customization. Using the same modifications to print settings as shown in the microfluidic device

fabrication methods, coupled with our novel print-pause-print technique, we were able to create a cell invasion device containing an integrated membrane. Our device enables researchers to integrate any type of membrane material and pore size, allowing full customization to the researchers needs. Using commercially available cell invasion assays, researchers would have to by an entire assay kit if different membrane parameters were to be investigated. For sterility of the entire device, a simple UV treatment allows for sterile cell culture if applicable. Additionally, our novel method of printing a channel device directly on a glass slide provides researchers with real time quantification of cell migration. Fluorescent staining the cell of choice and placing the device on the stage of a fluorescent microscope allows for real time quantification, as well as optimization for total assay time, improving efficiency.

5.2 Future Directions

5.2.1 C-peptide Binding and Downstream Effects on T1D Immune Cells

While we show that C-peptide binds to immune cells and elicits change in early key factors in immune cell function, more specific validation studies are needed to understand the mechanism of this increased activity. Previous Spence lab research reported an increase in measurable GLUT1 after C-peptide, Zn^{2+}, and albumin administration. GLUT1 facilitates glucose transport across the plasma membrane, providing energy to the cell. A subsequent increase of metabolism would follow this increased available energy source. Investigation of GLUT1 levels in response to C-peptide administration could confirm the reported increase in activation and

antipathogenic function of neutrophils. Several methods for quantifying membrane bound GLUT1 levels include western blot, flow cytometry, and fluorescent antibody detection via microscopy. Further validation through RT-qPCR, can provide evidence of synthesis of the GLUT1 protein at the DNA level. Additionally, the overall goal of the Spence lab is to determine the potential therapeutic action of C-peptide administration in T1D. It will be important to investigate how C-peptide binding effects immune cells isolated from individuals with T1D, since immune cell function in T1D is hindered. If C-peptide can prove effective restoration to T1D immune cell function, C-peptide can further be investigated as an effective co-therapeutic with insulin, as an innovative treatment.

5.2.2 NETosis effect on Blood Brain Barrier Permeability

In individuals with MS, a heightened circulating concentration of ATP is observed. Further, we show RBCs as a potential source of the increased ATP.(*15*) RBC release ATP due to shear stress and deformability while passing through micro vessels.(*16*) We have established ATP as a key promoter of neutrophil NETosis. A hallmark of MS is the loss of integrity of the blood brain barrier, that separates circulating blood components from passively crossing into the extracellular fluid of the central nervous system.(*17*)

To investigate the role of NETosis on the loss of integrity of the blood brain barrier, we will use a novel nanofiber/paper blood brain barrier model from a collaborator at Indiana University.(*18*) Using scanning ion conductance microscopy, we will determine integrity of the blood brain barrier model.(*19*) Neutrophils will be seeded directly on the

3D blood brain barrier, simultaneously, ATP derived from MS RBC or control RBC ATP will be added, inducing NETosis. The permeability will be measured using scanning ion conductance microscopy, the role of ATP from MS RBC inducing NET formation, and subsequent blood brain barrier breakdown.

5.2.3 In vitro Determination of Type 1 Diabetic Immune Cell Migration

The Spence lab has established a method in rapid fabrication of an immune cell migration device directly on a glass slide. The device will be used as an additional method to section 5.2.1. Migration has been identified as a function of immune cells hindered in T1D. It will be important to compare the rate of migration of immune cells from both control and isolated from individuals with T1D. Secondly, we will establish how C-peptide, Zn^{2+}, and albumin supplementation effects the rate of migration. As described in chapter 4, a microchannel with an integrated port for a transwell insert was printed directly on a glass slide. The glass will not suffice as an adequate surface for cell migration, to combat, after the device is printed, the bottom of the channel (glass) will be coated with fibronectin, a protein sufficient in cell attachment and migration.(*20*) Chemoattractant N-Formylmethionyl-leucyl-phenylalanine (fMLP) will be placed in the transwell insert, which sits in a port directly over the first well, allowing slow diffusion into the channel, mimicking a chemoattractant gradient seen in vivo. Opposite the transwell insert is a second well for seeding of a selected immune cell. In future studies, the cell membrane will be stained with CellLight^{TM}, for the real time determination of cell migration via fluorescent microscopy.

Preliminary studies have been conducted using the method described in the previous paragraph. A frequent problem the Spence lab have encountered is cell cytotoxicity. Human T- cell were added to a fibronectin coated well to adhere. We allowed the cells time to adhere with periodic supervision. After several attempts, we found excessive cell death that we attribute to several factors including, 3D printer material toxicity, cell density, and sterility. It will be important in future studies to identify the cause of cytotoxicity, and further optimize the device.

REFERENCES

REFERENCES

1. A. Tigner, S. Ibrahim, I. Murray, in *Histology, White Blood Cell*. (StatPearls, Treasure Island, FL, 2021).
2. M. Diez-Silva, M. Dao, J. Han, C. T. Lim, S. Suresh, Shape and Biomechanical Characteristics of Human Red Blood Cells in Health and Disease. *MRS Bull* **35**, 382-388 (2010).
3. H. P. Ting-Beall, D. Needham, R. M. Hochmuth, Volume and osmotic properties of human neutrophils. *Blood* **81**, 2774-2780 (1993).
4. M. Maywald, I. Wessels, L. Rink, Zinc Signals and Immunity. *Int J Mol Sci* **18**, (2017).
5. A. H. Shankar, A. S. Prasad, Zinc and immune function: the biological basis of altered resistance to infection. *Am J Clin Nutr* **68**, 447S-463S (1998).
6. H. Haase, L. Rink, Multiple impacts of zinc on immune function. *Metallomics* **6**, 1175-1180 (2014).
7. C. Lennicke, J. Rahn, R. Lichtenfels, L. A. Wessjohann, B. Seliger, Hydrogen peroxide - production, fate and role in redox signaling of tumor cells. *Cell Commun Signal* **13**, 39 (2015).
8. D. R. Gough, T. G. Cotter, Hydrogen peroxide: a Jekyll and Hyde signalling molecule. *Cell Death Dis* **2**, e213 (2011).
9. G. T. Nguyen, E. R. Green, J. Mecsas, Neutrophils to the ROScue: Mechanisms of NADPH Oxidase Activation and Bacterial Resistance. *Front Cell Infect Microbiol* **7**, 373 (2017).
10. P. W. Marks, F. R. Maxfield, Transient increases in cytosolic free calcium appear to be required for the migration of adherent human neutrophils. *J Cell Biol* **110**, 43-52 (1990).
11. K. Futosi, S. Fodor, A. Mócsai, Neutrophil cell surface receptors and their intracellular signal transduction pathways. *Int Immunopharmacol* **17**, 638-650 (2013).
12. M. Vig, J. P. Kinet, Calcium signaling in immune cells. *Nat Immunol* **10**, 21-27 (2009).
13. M. Bredholt, J. L. Frederiksen, Zinc in Multiple Sclerosis: A Systematic Review and Meta-Analysis. *ASN Neuro* **8**, (2016).
14. S. M. LeVine, Albumin and multiple sclerosis. *BMC Neurol* **16**, 47 (2016).

15. S. Letourneau, L. Hernandez, A. N. Faris, D. M. Spence, Evaluating the effects of estradiol on endothelial nitric oxide stimulated by erythrocyte-derived ATP using a microfluidic approach. *Anal Bioanal Chem* **397**, 3369-3375 (2010).

16. J. Wan, W. D. Ristenpart, H. A. Stone, Dynamics of shear-induced ATP release from red blood cells. *Proc Natl Acad Sci U S A* **105**, 16432-16437 (2008).

17. R. Daneman, A. Prat, The blood-brain barrier. *Cold Spring Harb Perspect Biol* **7**, a020412 (2015).

18. K. Huang *et al.*, A Hybrid Nanofiber/Paper Cell Culture Platform for Building a 3D Blood-brain Barrier Model. *Small Methods* **5**, (2021).

19. K. Huang, L. Zhou, K. Alanis, J. Hou, L. A. Baker, Imaging effects of hyperosmolality on individual tricellular junctions. *Chem Sci* **11**, 1307-1315 (2020).

20. A. J. Bergman, K. Zygourakis, Migration of lymphocytes on fibronectin-coated surfaces: temporal evolution of migratory parameters. *Biomaterials* **20**, 2235-2244 (1999).